Alma Mater Studiorum - Università di Bologna

Dipartimento di Elettronica, Informatica e Sistemistica

Sede Consorziata: Università di Roma "La Sapienza"

DOTTORATO DI RICERCA IN BIOINGEGNERIA
XIX CICLO
Settore Scientifico Disciplinare: ING-INF/06

Algoritmi e Parametri per la Valutazione Della Meccanica Cardiaca Tramite Catetere a Conduttanza

Parameters and Algorithms to Evaluate Cardiac Mechanics by Conductance Catheter

Coordinatore: Chiar.mo Prof. Angelo Cappello

Supervisore: Gent.ma Prof.ssa Serenella Salinari

Co-supervisore: Ing. Federica Censi

Controrelatore: Chiar.mo Prof. Gianni Gnudi

Tesi di Dottorato: Ing. Sergio Valsecchi

A. A. 2003 - 2006

Table of Contents

Section 2

Summary

This work is structured as follows:

In Section 1 we discuss the clinical problem of heart failure. In particular, we present the phenomenon known as ventricular mechanical dyssynchrony: its impact on cardiac function, the therapy for its treatment and the methods for its quantification. Specifically, we describe the conductance catheter and its use for the measurement of dyssynchrony. At the end of the Section 1, we propose a new set of indexes to quantify the dyssynchrony that are studied and validated thereafter.

In Section 2 we describe the studies carried out in this work: we report the experimental protocols, we present and discuss the results obtained.

Finally, we report the overall conclusions drawn from this work and we try to envisage future works and possible clinical applications of our results.

Ancillary studies that were carried out during this work mainly to investigate several aspects of cardiac resynchronization therapy (CRT) are mentioned in Appendix.

Ventricular mechanical dyssynchrony plays a regulating role already in normal physiology but is especially important in pathological conditions, such as hypertrophy, ischemia, infarction, or heart failure (Chapter 1,2.).

Several prospective randomized controlled trials supported the clinical efficacy and safety of cardiac resynchronization therapy (CRT) in patients with moderate or severe heart failure and ventricular dyssynchrony. CRT resynchronizes ventricular contraction by simultaneous pacing of both left and right ventricle (biventricular pacing) (Chapter 1.).

Currently, the conductance catheter method has been used extensively to assess global systolic and diastolic ventricular function and, more recently, the ability of this instrument to pick-up multiple segmental volume signals has been used to quantify mechanical ventricular dyssynchrony. Specifically, novel indexes based on volume signals acquired with the conductance catheter were introduced to quantify dyssynchrony (Chapter 3,4.).

Present work was aimed to describe the characteristics of the conductance-volume signals, to investigate the performance of the indexes of ventricular dyssynchrony described in literature and to introduce and validate improved dyssynchrony indexes. Morevoer, using the conductance catheter method and the new indexes, the clinical problem of the ventricular pacing site optimization was addressed and the measurement protocol to adopt for hemodynamic tests on cardiac pacing was investigated.

In accordance to the aims of the work, in addition to the classical time-domain parameters, a new set of indexes has been extracted, based on coherent averaging procedure and on spectral and cross-spectral analysis (Chapter 4.). Our analyses were carried out on patients with indications for electrophysiologic study or device implantation (Chapter 5.). For the first time, besides patients with heart failure, indexes of mechanical dyssynchrony based on conductance catheter were extracted and studied in a population of

patients with preserved ventricular function, providing information on the normal range of such a kind of values.

By performing a frequency domain analysis and by applying an optimized coherent averaging procedure (Chapter 6.a.), we were able to describe some characteristics of the conductance-volume signals (Chapter 6.b.).

We unmasked the presence of considerable beat-to-beat variations in dyssynchrony that seemed more frequent in patients with ventricular dysfunction and to play a role in discriminating patients. These non-recurrent mechanical ventricular non-uniformities are probably the expression of the substantial beat-to-beat hemodynamic variations, often associated with heart failure and due to cardiopulmonary interaction and conduction disturbances.

We investigated how the coherent averaging procedure may affect or refine the conductance based indexes; in addition, we proposed and tested a new set of indexes which quantify the non-periodic components of the volume signals.

Using the new set of indexes we studied the acute effects of the CRT and the right ventricular pacing, in patients with heart failure and patients with preserved ventricular function.

In the overall population we observed a correlation between the hemodynamic changes induced by the pacing and the indexes of dyssynchrony, and this may have practical implications for hemodynamic-guided device implantation.

The optimal ventricular pacing site for patients with conventional indications for pacing remains controversial. The majority of them do not meet current clinical indications for CRT pacing. Thus, we carried out an analysis to compare the impact of several ventricular pacing sites on global and regional ventricular function and dyssynchrony (Chapter 6.c.). We observed that right ventricular pacing worsens cardiac function in patients with and without ventricular dysfunction unless the pacing site is optimized. CRT preserves left ventricular function in patients with normal ejection fraction and improves function in patients with poor ejection fraction despite no clinical indication for CRT. Moreover, the analysis of the results obtained using new indexes of regional dyssynchrony, suggests that pacing site may influence overall global ventricular function depending on its relative effects on regional function and synchrony.

Another clinical problem that has been investigated in this work is the optimal right ventricular lead location for CRT (Chapter 6.d.). Similarly to the previous analysis, using novel parameters describing local synchrony and efficiency, we tested the hypothesis and we demonstrated that biventricular pacing with alternative right ventricular pacing sites produces acute improvement of ventricular systolic function and improves mechanical synchrony when compared to standard right ventricular pacing. Although no specific right ventricular location was shown to be superior during CRT, the right ventricular pacing site that produced the optimal acute hemodynamic response varied between patients.

Acute hemodynamic effects of cardiac pacing are conventionally evaluated after stabilization episodes. The applied duration of stabilization periods in most cardiac pacing studies varied considerably.

With an ad hoc protocol (Chapter 6.e.) and indexes of mechanical dyssynchrony derived by conductance catheter we demonstrated that the

usage of stabilization periods during evaluation of cardiac pacing may mask early changes in systolic and diastolic intra-ventricular dyssynchrony. In fact, at the onset of ventricular pacing, the main dyssynchrony and ventricular performance changes occur within a 10s time span, initiated by the changes in ventricular mechanical dyssynchrony induced by aberrant conduction and followed by a partial or even complete recovery.

It was already demonstrated in normal animals that ventricular mechanical dyssynchrony may act as a physiologic modulator of cardiac performance together with heart rate, contractile state, preload and afterload. The present observation, which shows the compensatory mechanism of mechanical dyssynchrony, suggests that ventricular dyssynchrony may be regarded as an intrinsic cardiac property, with baseline dyssynchrony at increased level in heart failure patients.

To make available an independent system for cardiac output estimation, in order to confirm the results obtained with conductance volume method, we developed and validated a novel technique to apply the Modelflow method (a method that derives an aortic flow waveform from arterial pressure by simulation of a non-linear three-element aortic input impedance model, Wesseling et al. 1993) to the left ventricular pressure signal, instead of the arterial pressure used in the classical approach (Chapter 7.).

The results confirmed that in patients without valve abnormalities, undergoing conductance catheter evaluations, the continuous monitoring of cardiac output using the intra-ventricular pressure signal is reliable. Thus, cardiac output can be monitored quantitatively and continuously with a simple and low-cost method.

During this work, additional studies were carried out to investigate several areas of uncertainty of CRT. The results of these studies are briefly presented in Appendix: the long-term survival in patients treated with CRT in clinical practice, the effects of CRT in patients with mild symptoms of heart failure and in very old patients, the limited thoracotomy as a second choice alternative to transvenous implant for CRT delivery, the evolution and prognostic significance of diastolic filling pattern in CRT, the selection of candidates to CRT with echocardiographic criteria and the prediction of response to the therapy.

Introduction

Ventricular contraction normally occurs in a highly coordinated manner. Mechanical activation of the ventricles depends on the rapid spread of electric signals via specialized fibers (His-Purkinje system) that arborize throughout the right ventricular and left ventricular endocardia. In patients with slowed-down or blocked His-Purkinje activation left ventricular activation and contraction become dyssynchronous.

Ventricular mechanical dyssynchrony is most commonly identified clinically by a prolonged QRS duration with left bundle-branch block morphology on surface electrocardiogram but can also be detected by echocardiographic imaging of contraction timing.

Ventricular mechanical dyssynchrony plays a regulating role already in normal physiology but is especially important in pathological conditions, such as hypertrophy, ischemia, infarction, or heart failure. Dyssynchrony exacerbates heart failure in a variety of ways, generating cardiac inefficiency as well as pathobiologic changes at the tissue, cellular, and molecular levels (Chapter 1.b.).

The abnormal activation sequence induced by spontaneous conduction defects or by right ventricular pacing generates changes in regional ventricular loading conditions, possibly redistributes myocardial blood flow, and creates a regional non-uniform myocardial metabolism. These effects of ventricular dyssynchrony might contribute to disease progression in left ventricle systolic dysfunction patients. Moreover, it is likely that these consequences of ventricular dyssynchrony lead to rearrangement of both contractile and non-contractile cellular elements and perhaps the extra-cellular matrix in the heart, thus stimulating the process of ventricular remodeling. Therefore, it is conceivable that dyssynchrony represents a newly appreciated patho-physiological process that directly depresses ventricular function and ultimately leads to ventricular dilatation and heart failure (Chapter 1.b.i.).

An overwhelming amount of evidence from prospective randomized controlled trials supports the clinical efficacy and safety of cardiac resynchronization therapy (CRT) in patients with moderate or severe heart failure and ventricular dyssynchrony.

In CRT, simultaneous pacing of both left and right ventricle (biventricular pacing) is delivered to resynchronize ventricular contraction. With biventricular pacing, separate pacing leads are placed to stimulate the ventricles. A third pacing lead is placed in the right atrium to permit the synchronization of the ventricular pacing to the atrial depolarization. CRT makes heart failure patients feel better, improves cardiac structure and function, and reduces all-cause as well as heart failure morbidity and mortality. Thus, there may be a clinical mandate for use of CRT in many patients with chronic heart failure (Chapter 1.b.ii.).

However, a number of key clinical research questions remain, perhaps most importantly the issue of why apparently suitable patients do not respond to CRT. Rates of non-response to CRT are quoted as 20–30%. These issues are also relevant to patients who do respond to CRT as potentially their response might be further increased.

The data indicates that the extent of mechanical dyssynchrony and left ventricular pacing site are likely to be important. In fact, as all patients with a ventricular conduction abnormality may not benefit from CRT and some patients with a normal QRS duration derive benefit from this therapy, it is logical to conclude that electrically measured ventricular dyssynchrony (by ECG) is a relatively crude reflection of mechanical ventricular dyssynchrony and it is reasonable to consider new techniques for quantifying the degree of mechanical dyssynchrony (Chapter 2.).

In this context, echocardiography-guided measurements of ventricular dyssynchrony are as yet not standardized, and none of the reported variables have been prospectively tested.

Acute hemodynamic studies have suggested that pacing site is crucial for improving ventricular mechanics. Thus, it can be postulated that non-responder patients are paced at a suboptimal site. Recent echocardiographic studies have shown that in a substantial proportion of patients, the anatomically selected pacing site does not always coincide with ventricular regions having large mechanical delay.

Whether MRI or echocardiography will help in identifying the most optimal pacing site is still under investigation.

In conclusion, it will be useful if additional methods can be developed that identify dyssynchrony in the human heart in a more sensitive and specific way, and potentially helpful if they are utilized to help place CRT leads in the future. Ensuring that dyssynchrony has been eliminated by careful selection of the ventricular locations for CRT may reduce the number of non-responders to this form of therapy.

Currently, the conductance catheter method has been used extensively to assess global systolic and diastolic ventricular function (Chapter 3.) and more recently the ability of this instrument to pick-up multiple segmental volume signals has been used to quantify mechanical ventricular dyssynchrony (Chapter 4.a.).

The aims of this work were:
- To describe the characteristics of the conductance-volume signals by means of the analysis in frequency domain and using coherent averaging, in order to investigate the performance and the potential limitations of the indexes of ventricular dyssynchrony introduced by Steendijk et al. (Am J Physiol 2004);
- To introduce new improved indexes to quantify the dyssynchrony, and to assess their ability to discriminate patients with and without ventricular dysfunction as well as describe the effects of cardiac pacing;
- To address the clinical problem of the ventricular pacing site optimization for CRT and for conventional right ventricular pacing, using the conductance catheter method and the new indexes that have been derived;
- To investigate the measurement protocol to adopt for hemodynamic tests on cardiac pacing.

The analyses included in this work were carried out on patients with indications for electrophysiologic study or device implantation. For the first time, besides patients with heart failure, indexes of mechanical dyssynchrony

based on conductance catheter were extracted and studied in a population of patients with preserved ventricular function, providing information on the normal range of such a kind of values.

In addition to the classical time-domain parameters, a new set of indexes has been extracted, based on coherent averaging procedure and on spectral and cross-spectral analysis. We performed a frequency domain analysis and we applied an optimized coherent averaging procedure in order to describe some characteristics of the conductance-volume signals.

We investigated how the coherent averaging procedure may affect or refine the conductance based indexes; in addition, we proposed and tested a new set of indexes which quantify the non-periodic components of the volume signals.

Using the new set of indexes we studied the acute effects of the CRT and the right ventricular pacing, in patients with heart failure and patients with preserved ventricular function.

Moreover, using conductance catheter technique and the new indexes of ventricular dyssynchrony we studied the impact of several ventricular pacing sites on global and regional ventricular function and dyssynchrony, and we investigated the optimal right ventricular lead location for CRT

A further protocol was carried out to assess how the stabilization periods that are usually applied to study the acute hemodynamic effects of cardiac pacing and that in most studies varied considerably, may affect the results of the analysis.

Finally, we developed and validated a novel technique to derive an aortic flow waveform from the left ventricular pressure signal to estimate the cardiac output, in order to confirm the results obtained with conductance volume method.

Section 1

1. The Clinical Problem

1.a. Heart Failure

1.a.i. Definition of Heart Failure

Heart failure (HF) is a complex clinical syndrome that can result from any structural or functional cardiac disorder that impairs the ability of the ventricle to fill with or eject blood (1).

The cardinal manifestations of HF are dyspnea and fatigue, which may limit exercise tolerance, and fluid retention, which may lead to pulmonary congestion and peripheral edema. Both abnormalities can impair the functional capacity and quality of life of affected individuals, but they do not necessarily dominate the clinical picture at the same time. Some patients have exercise intolerance but little evidence of fluid retention, whereas others complain primarily of edema and report few symptoms of dyspnea or fatigue.

The clinical syndrome of HF may result from disorders of the pericardium, myocardium, endocardium, or great vessels, but the majority of patients with HF has symptoms due to an impairment of left ventricle (LV) myocardial function. Heart failure may be associated with a wide spectrum of LV functional abnormalities, which may range from patients with normal LV size and preserved ejection fraction (EF) to those with severe dilatation and/or markedly reduced EF. In most patients, abnormalities of systolic and diastolic dysfunction coexist, regardless of EF. Patients with normal EF may have a different natural history and may require different treatment strategies than patients with reduced EF, although such differences remain controversial.

Coronary artery disease, hypertension, and dilated cardiomyopathy are the causes of HF in a substantial proportion of patients in the Western world. As many as 30% of patients with dilated cardiomyopathy may have a genetic cause (2). Valvular heart disease is still a common cause of HF. In fact, nearly any form of heart disease may ultimately lead to the HF syndrome.

1.a.ii. Heart Failure as a Symptomatic Disorder

The approach that is most commonly used to quantify the degree of functional limitation imposed by HF is one first developed by the New York Heart Association (NYHA). This system assigns patients to 1 of 4 functional classes, depending on the degree of effort needed to elicit symptoms: patients may have symptoms of HF at rest (class IV), on less-than-ordinary exertion (class III), on ordinary exertion (class II), or only at levels of exertion that would limit normal individuals (class I). Although the functional class tends to deteriorate over periods of time, most patients with HF do not typically show an uninterrupted and inexorable worsening of symptoms. Instead, the severity of symptoms characteristically fluctuates even in the absence of changes in medications, and changes in medications and diet can have either favorable or adverse effects on functional capacity in the absence of measurable changes in ventricular function. Some patients may demonstrate remarkable recovery, sometimes associated with improvement in structural and functional abnormalities. Usually, sustained improvement is associated with drug therapy, and that therapy should be continued indefinitely.

The mechanisms responsible for the exercise intolerance of patients with chronic HF have not been defined clearly. Although HF is generally regarded as a hemodynamic disorder, many studies have indicated that there is a poor relation between measures of cardiac performance and the symptoms produced by the disease. Patients with a very low EF may be asymptomatic, whereas patients with preserved EF may have severe disability. The apparent discordance between EF and the degree of functional impairment is not well understood but may be explained in part by alterations in ventricular distensibility, valvular regurgitation, pericardial restraint, cardiac rhythm, conduction abnormalities, and right ventricular function (2). In addition, in ambulatory patients, many noncardiac factors may contribute substantially to exercise intolerance. These factors include but are not limited to changes in peripheral vascular function, skeletal muscle physiology, pulmonary dynamics, neurohormonal and reflex autonomic activity, and renal sodium handling. The existence of these noncardiac factors may explain why the hemodynamic improvement produced by therapeutic agents in patients with chronic HF may not be immediately or necessarily translated into clinical improvement. Although pharmacological interventions may produce rapid changes in hemodynamic variables, signs and symptoms may improve slowly over weeks or months or not at all.

1.a.iii. Heart Failure as a Progressive Disorder

Left ventricular dysfunction begins with some injury to, or stress on, the myocardium and is generally a progressive process, even in the absence of a new identifiable insult to the heart. The principal manifestation of such progression is a change in the geometry and structure of the LV, such that the chamber dilates and/or hypertrophies and becomes more spherical — a process referred to as cardiac remodeling. This change in chamber size and structure not only increases the hemodynamic stresses on the walls of the failing heart and depresses its mechanical performance but may also increase regurgitant flow through the mitral valve. These effects, in turn, serve to sustain and exacerbate the remodeling process. Cardiac remodeling generally precedes the development of symptoms (occasionally by months or even years), continues after the appearance of symptoms, and contributes substantially to worsening of symptoms despite treatment.

Progression of coronary artery disease, diabetes mellitus, hypertension, or the onset of atrial fibrillation may also contribute to the progression of HF. The development of structural abnormalities can have 1 of 3 outcomes: patients die before developing symptoms, patients develop symptoms controlled by treatment, or patients die of progressive HF. Sudden death can interrupt this course at any time.

Although several factors can accelerate the process of LV remodeling, there is substantial evidence that the activation of endogenous neurohormonal systems plays an important role in cardiac remodeling and thereby in the progression of HF. Patients with HF have elevated circulating or tissue levels of norepinephrine, angiotensin II, aldosterone, endothelin, vasopressin, and cytokines, which can act (alone or in concert) to adversely affect the structure and function of the heart. These neurohormonal factors not only increase the hemodynamic stresses on the ventricle by causing sodium retention and

peripheral vasoconstriction but may also exert direct toxic effects on cardiac cells and stimulate myocardial fibrosis, which can further alter the architecture and impair the performance of the failing heart. Neurohormonal activation also has direct deleterious effects on the myocytes and interstitium, altering the performance and phenotype of these cells. The development of HF can be appropriately characterized by considering 4 stages of the disease. This staging system recognizes that HF, like coronary artery disease, has established risk factors and structural prerequisites; that the development of HF has asymptomatic and symptomatic phases; and that specific treatments targeted at each stage can reduce the morbidity and mortality of HF (Figure 1).
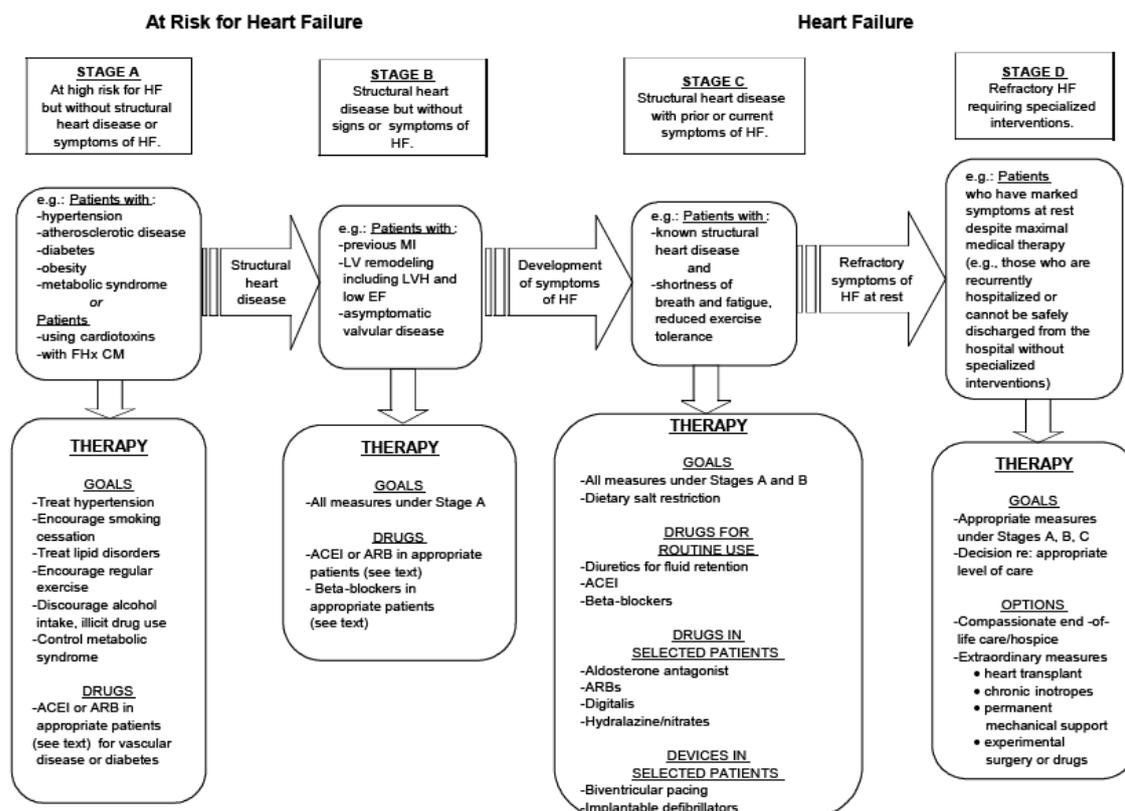
Figure 1. Stages in the development of HF/recommended therapy by stage. FHx CM indicates family history of cardiomyopathy; ACEI, angiotensin converting enzyme inhibitors; and ARB, angiotensin receptor blocker. *(From 1)*

1.a.iv. The Current Treatment

Most patients with HF should be routinely managed with a combination of 3 types of drugs: a diuretic, an Angiotensin Converting Enzyme Inhibitor (ACEI), and a beta-blocker (3). The value of these drugs has been established by the results of numerous large-scale clinical trials, and the evidence supporting a central role for their use is compelling and persuasive. Patients with evidence of fluid retention should take a diuretic until a euvolemic state is achieved, and

diuretic therapy should be continued to prevent the recurrence of fluid retention. Even if the patient has responded favorably to the diuretic, treatment with both an ACEI and a beta-blocker should be initiated and maintained in patients who can tolerate them because they have been shown to favorably influence the long-term prognosis of HF.

Therapy with digoxin as a fourth agent may be initiated at any time to reduce symptoms, prevent hospitalization, control rhythm, and enhance exercise tolerance.

Diuretics

Controlled trials have demonstrated the ability of diuretic drugs to increase urinary sodium excretion and decrease physical signs of fluid retention in patients with HF. In these short-term studies, diuretic therapy has led to a reduction in jugular venous pressures, pulmonary congestion, peripheral edema, and body weight, all of which were observed within days of initiation of therapy. In intermediate-term studies, diuretics have been shown to improve cardiac function, symptoms, and exercise tolerance in patients with HF. There have been no long-term studies of diuretic therapy in HF, and thus, their effects on morbidity and mortality are not known.

Angiotensin Converting Enzyme Inhibitors

Angiotensin converting enzyme inhibitors have been evaluated in more than 7000 patients with HF who participated in more than 30 placebo-controlled clinical trials.

Analysis of this collective experience indicates that ACEIs can alleviate symptoms, improve clinical status, and enhance the overall sense of well-being of patients with HF. In addition, ACEIs can reduce the risk of death and the combined risk of death or hospitalization. These benefits of ACE inhibition were seen in patients with mild, moderate, or severe symptoms and in patients with or without coronary artery disease.

Beta-adrenergic receptor blockers.

Beta-blockers act principally to inhibit the adverse effects of the sympathetic nervous system in patients with HF, and these effects far outweigh their well-known negative inotropic overeffects. Whereas cardiac adrenergic drive initially supports the performance of the failing heart, long-term activation of the sympathetic nervous system exerts deleterious effects that can be antagonized by the use of beta-blockers. Sympathetic activation can increase ventricular volumes and pressure by causing peripheral vasoconstriction and by impairing sodium excretion by the kidneys. Norepinephrine can also induce cardiac hypertrophy but restrict the ability of the coronary arteries to supply blood to the thickened ventricular wall, leading to myocardial ischemia. Activation of the sympathetic nervous system can also provoke arrhythmias by increasing the automaticity of cardiac cells, increasing triggered activity in the heart, and promoting the development of hypokalemia. Norepinephrine can also increase heart rate and potentiate the activity and actions of other neurohormonal systems. Finally, by stimulating growth and oxidative stress in terminally differentiated cells, norepinephrine can trigger programmed cell death or apoptosis. These deleterious effects are mediated through actions on alpha-1–, beta-1–, and beta-2–adrenergic receptors.

Betablockers have now been evaluated in more than 20 000 patients with HF who participated in more than 20 published placebo-controlled clinical trials. This collective experience indicates that long-term treatment with beta-blockers can lessen the symptoms of HF, improve the clinical status of patients, and enhance the patient's overall sense of well-being. In addition, like ACEIs, beta-blockers can reduce the risk of death and the combined risk of death or hospitalization.

Non pharmacological treatment of HF – Implantable Cardioverter Defibrillators
Patients with LV dilation and reduced EF frequently manifest ventricular tachyarrhythmias, both nonsustained ventricular tachycardia (VT) and sustained VT. The cardiac mortality of patients with all types of ventricular tachyarrhythmias is high.
Patients with previous cardiac arrest or documented sustained ventricular arrhythmias have a high risk of recurrent events. Implantation of an implantable cardioverter defibrillator (ICD) has been shown to reduce mortality in cardiac arrest survivors. An ICD is indicated for secondary prevention of death from ventricular tachyarrhythmias in patients with otherwise good clinical function and prognosis, for whom prolongation of survival is a goal. Patients with chronic HF and a low EF who experience syncope of unclear origin have a high rate of subsequent sudden death and should also be considered for placement of an ICD (4).
Patients with low EF without prior history of cardiac arrest, spontaneous VT, or inducible VT (positive programmed electrical stimulation study) have a risk of sudden death that is lower than for those who have experienced previous events, but it remains significant.
The role of ICDs in the primary prevention of sudden death in patients without prior history of symptomatic arrhythmias has been explored recently in a number of trials. If sustained ventricular tachyarrhythmias can be induced in the electrophysiology laboratory in patients with previous myocardial infarction or chronic ischemic heart disease, the risk of sudden death in these patients is in the range of 5% to 6% per year and can be improved by ICD implantation (5). The role of ICD implantation for the primary prevention of sudden death in patients with HF and low EF and no history of spontaneous or inducible VT has been addressed by several large trials. The first of these demonstrated that ICDs, compared with standard medical therapy, decreased the occurrence of total mortality for patients with EF less than or equal to 30% after remote myocardial infarction (6). Absolute mortality was decreased in the ICD arm by 5.6%, a relative decrease of 31% over 20 months. A second trial examining the benefit of ICD implantation for patients with EF less than 35% and NYHA class II to III symptoms of HF included both ischemic and nonischemic causes of HF; absolute mortality was decreased by 7.2% over a 5-year period in the arm that received an ICD. This represented a relative mortality decrease of 23%, which was a survival increase of 11% (7).

1.a.v. Epidemiology and Economic Impact of Chronic Heart Failure

Heart failure is a major and growing public health problem.
Heart failure is diagnosed in 1–2% of the general population in developed countries (8). Approximately 5 million patients in the United States have HF,

and over 550 000 patients are diagnosed with HF for the first time each year (9). The disorder is the primary reason for 12 to 15 million office visits and 6.5 million hospital days each year (10). From 1990 to 1999, the annual number of hospitalizations has increased from approximately 810 000 to over 1 million for HF as a primary diagnosis and from 2.4 to 3.6 million for HF as a primary or secondary diagnosis (11). In 2001, nearly 53 000 patients died of HF as a primary cause. The number of HF deaths has increased steadily despite advances in treatment, in part because of increasing numbers of patients with HF due to better treatment and "salvage" of patients with acute myocardial infarctions earlier in life (9).

Heart failure is primarily a condition of the elderly (12), and thus the widely recognized "aging of the population" also contributes to the increasing incidence of HF. The incidence of HF approaches 10 per 1000 population after age 65 (9), and approximately 80% of patients hospitalized with HF are more than 65 years old (13).

Direct costs due to HF were (in one million per one million population) 26 in the UK, 37 in Germany, 39 in France and 70 in the US, respectively. In the US $ 38 billion have been spent for patients with chronic HF in 1991 and the expenditures for HF were higher than that for the treatment of cancer and myocardial infarction (10).

Overall, chronic HF consumes 1–2% of the total healthcare resources in the developed countries. The economic burden of HF may become unmanageable in the setting of an ageing population indicating the need for cost-effective treatment options and preventive strategies.

Repeated hospitalizations are not only a powerful marker of poor prognosis and of poor life quality but also for increased costs for the health care system.

The direct costs are mainly attributed to hospitalizations (approximately 75%), with an average cost of approximately 10,000 per patient per hospitalization (10). In the EuroHeart Failure survey programme 24% of patients had been readmitted to hospital within 12 weeks of discharge (14). The three main causes of hospitalizations due to chronic heart failure are sodium retention (55% of cases), angina or myocardial infarction (25%) and arrhythmia (15%) (15).

1.b. Ventricular Dyssynchrony

Recently, poorly synchronized activation of the LV itself has been shown to compromise global systolic function and has been linked to increased morbidity, arrhythmia susceptibility, and mortality in patients with HF (16-18). Ventricular contraction normally occurs in a highly coordinated manner. Mechanical activation of the ventricles depends on the rapid spread of electric signals via specialized fibers (His-Purkinje system) that arborize throughout the right ventricular (RV) and LV endocardia (19). Normal activation occurs from the endocardium to the epicardium (20) as well as from the apex to the base (21) and is nearly coincident in all regions of the LV. In patients with slowed-down or blocked His-Purkinje activation (a circumstance frequently compounded by sluggish intramyocardial conduction) (22), LV activation and contraction become dyssynchronous.

Dyssynchrony plays a regulating role already in normal physiology (23) but is especially important in pathological conditions, such as hypertrophy (24), ischemia (25), infarction (26), or HF (27).

This is most commonly identified clinically by a prolonged QRS duration with left bundle-branch block (LBBB) morphology on surface electrocardiogram but can also be detected by echocardiographic imaging of contraction timing. Dyssynchrony exacerbates HF in a variety of ways, generating cardiac inefficiency as well as pathobiologic changes at the tissue, cellular, and molecular levels. Established predictors of HF mortality include age, degree of LV systolic impairment, and NYHA functional class. Recently, intraventricular LV dyssynchrony (identified either indirectly through QRS prolongation on surface electrocardiogram or directly by tissue Doppler echocardiography) has been identified as an independent powerful predictor of mortality in patients with HF (16,17).

Iuliano et al (16) investigated the prognostic significance of QRS duration in the CHF-STAT patient cohort, retrospectively analyzing mortality trends in 669 patients with HF. Over a period of 45 months, 272 deaths occurred (41% mortality rate), with sudden death accounting for roughly half of those events. The mortality rate was significantly higher in patients with a QRS duration longer than 120 milliseconds (49.3%) as compared with patients with a QRS duration shorter than 120 milliseconds (34%).

Independent predictors of mortality (after controlling for EF, age, NYHA class, etiology of dilated cardiomyopathy, LBBB, and medical therapy) included QRS duration, EF, and NYHA class. Although LBBB morphology on electrocardiogram was associated with increased mortality rates, right bundle-branch block (RBBB) morphology was not.

In a similar study, Baldasseroni et al (17) investigated 1-year mortality in 5517 patients enrolled in the Italian Network on Congestive Heart Failure Registry. Complete LBBB (QRS duration >140ms) was present in 25%, complete RBBB was in 6%, and other intraventricular delays were in 6% of the patients. Overall mortality was 11.9%, with sudden death accounting for 46% of total deaths. Mortality in patients with LBBB was 16% (vs that of 11% in patients with RBBB and that of 8% in patients with other forms of bundle-branch block). After controlling for multiple covariates (age, etiology of disease, EF, NYHA class, medical therapy with beta-blockers and angiotensin-converting enzyme inhibitors, third heart sound, atrial fibrillation, ventricular tachycardia),

LBBB was found to be an independent predictor of both overall mortality and mortality from sudden cardiac death.

Dyssynchrony can also be induced by an artificial pacemaker, and evidence suggests that this can itself lead to LV systolic failure (see Appendix.a.).

1.b.i. Impact of Ventricular Dyssynchrony on Chamber Function

Left ventricular dyssynchrony typically results from delay in the activation of the lateral LV free wall and is manifest frequently (but not necessarily) as LBBB on surface electrocardiogram. Contraction of the septum and anterior LV in early systole results in pre-stretch of the still-quiescent lateral wall, delaying intracavitary pressure rise and mitral valve closure. Late systolic activation of the LV lateral free wall leads to a corresponding stretch of the anteroseptal region, thereby competing with aortic ejection and reducing net cardiac output. The result is mechanical inefficiency, with transmission of the ventricular blood pool between 2 intracavitary sinks (the stretched lateral wall in early systole and the anteroseptal region in late systole). Functional mitral regurgitation, caused by delay in both the rise in LV intracavitary pressure and discoordinate papillary muscle contraction, can exacerbate this inefficiency further.

The immediate effects of LV dyssynchrony on global systolic function have been demonstrated quantitatively through pacing studies on both ex vivo whole organ preparations and in vivo models. Compared with atrial pacing and activation of the LV through the His-Purkinje network, RV pacing causes reductions in net generated LV pressure (28, 29), dP/dtmax (30), stroke volume (29), and the slope of the end-systolic pressure-volume relationship (ESPVR) (28). Right ventricular pacing–induced dyssynchrony also shifts the ESPVR to the right (29), demonstrating a load-independent compromise of LV mechanical function. Many of the deleterious effects of pacing-induced dyssynchrony are best appreciated in ventricular pressure-volume loop tracings (Figure 2B).

In addition to a rightward shift in the ESPVR, stroke volume in paced dyssynchronous ventricles is decreased (29), leading to increased LV end-systolic volume and, in turn, increased LV end-systolic wall stress. Recent investigations of regional myocardial work by tagged magnetic resonance imaging of dyssynchronous hearts have further defined the mechanical inefficiency generated by LV discoordination.

Prinzen et al (31) paced the hearts of anesthetized dogs from the right atrium, right ventricle, or left ventricle. Regional myocardial work, represented by the stress-strain loop area for a given region, was markedly heterogeneous between early-activated and late-activated myocardial segments (Figure 2A). In early-activated territories, myocardial work was essentially zero. In contrast, late-activated zones underwent increased fiber strain (distension) as well as stress and consequently performed a disproportionate amount of net myocardial work.
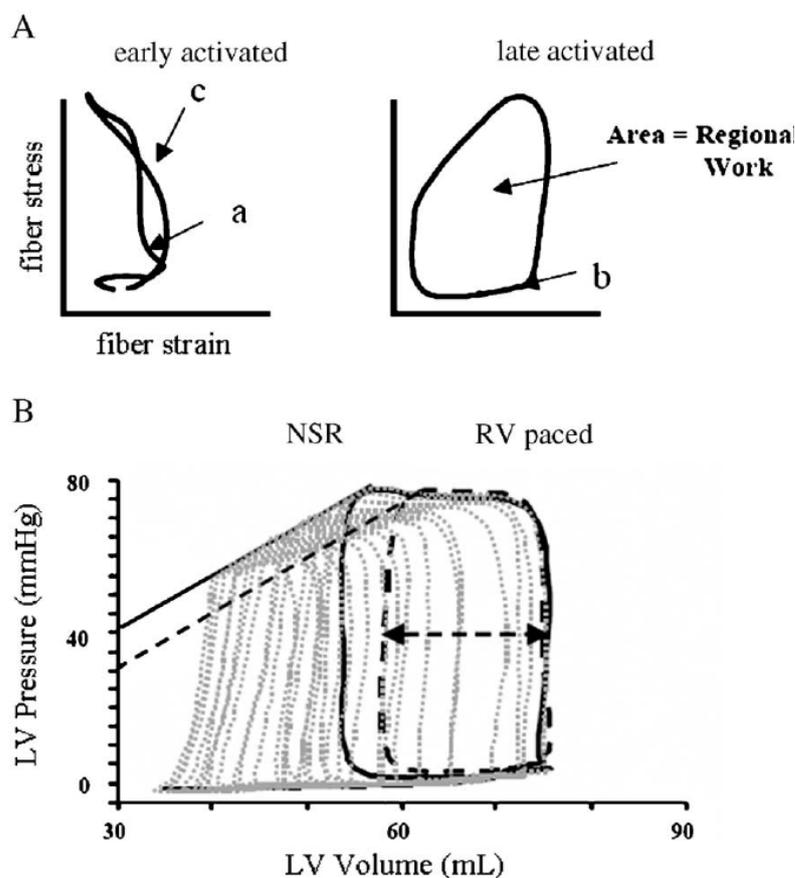
Figure 2. A, Stress-strain loops from early-activated and late-activated myocardial regions in dyssynchronous hearts. In early-activated regions, contraction initially occurs at low stress levels (a) as quiescent late-activated regions undergo passive stretch. Subsequently in systole, early-activated regions undergo reciprocal deformation as the late-activated territories contract (c). The small net area of the stress-strain loop in early-activated regions reflects reduced regional work performed. In late-activated territories, passive stretch in early systole generates increased stress before contraction (b). The increased stress-strain loop area reflects increased work performed by late-activated territories. B, Pressure-volume loops showing the effect of LV dyssynchrony induced by RV pacing. Stroke volume is reduced, the LV ESPVR is shifted to the right, and end-systolic volume and stress are increased. *(From 29 and 31)*

In both regions, work is wasted: anteroseptal contraction results primarily in distension of the lateral free wall and may occur early enough relative to mitral valve closure to result in functional mitral regurgitation; lateral LV contraction in late systole ejects blood into the systemic vasculature but also generates distension of the anteroseptal LV. The net impact of mechanical dyssynchrony on myocardial energetics has been reported. Although external work by the heart on the body declines with acute dyssynchrony, the oxygen consumption required remains similar, thus confirming mechanical inefficiency (32,33).

In the context of established LV dysfunction, mechanical dyssynchrony has clear additive deleterious effects. However, chronic dyssynchrony can itself result in abnormal chamber function. This was recently reported by Vernooy et al (34), who assessed cardiac structure and function for 16 weeks after ablation of the LBBB. They observed a gradual decline in the ejection fraction of 23% and an increase in chamber dimensions of 25%. The mechanisms underlying dyssynchrony-induced changes in LV systolic function and architecture are as yet unknown.

1.b.ii. Cardiac Resynchronization Therapy

Approximately one third of patients with low EF and class III to IV symptoms of HF manifest a QRS duration greater than 120 ms (35-37).

It has been hypothesized that simultaneous pacing of both the LV and RV (biventricular pacing) to resynchronize ventricular contraction (cardiac-resynchronization therapy, or CRT) might be beneficial in patients with HF and ventricular dyssynchrony. With biventricular pacing, separate pacing leads are placed to stimulate the RV and LV, with pacing through each lead timed to coordinate electrical activation (Figure 3). A third pacing lead is placed in the right atrium to permit the synchronization of the ventricular pacing to the atrial depolarization.

Although biventricular pacing does not restore the physiologic conduction pattern, it eliminates the delay in electrical activation of the left ventricular free wall (38).

1.b.ii.1. Cardiac Mechanoenergetics of Resynchronization Therapy

The mechanical and energetic consequences of intraventricular dyssynchrony can be mitigated by biventricular (BiV) pacing. Early stimulation of the lateral LV free wall results in recoordination of ventricular contraction (39). The effects of ventricular resynchronization on LV mechanical work are instantaneous, with appreciable increases in dP/dtmax, aortic systolic pressure, and cardiac output occurring within one beat of LV pacing onset. Stroke volume increases immediately and with a decline in end-systolic stress. Underlying these laudatory effects on global LV systolic function is the elimination of early systolic stretch and late systolic stretch in the lateral and anteroseptal LV walls, respectively; instead, both territories contract throughout systole.

The beneficial effects of mechanical LV resynchronization appear independent of whether electric synchrony is concomitantly achieved.

Long-term ventricular resynchronization with BiV pacing results in further improvement of LV function and induces reverse remodeling in patients with dilated cardiomyopathy. In a study on 25 patients with class III or IV HF and QRS widths longer than 140ms, Yu et al. (40) demonstrated reductions in both end-systolic and end-diastolic volumes after 3 months of long-term BiV pacing.
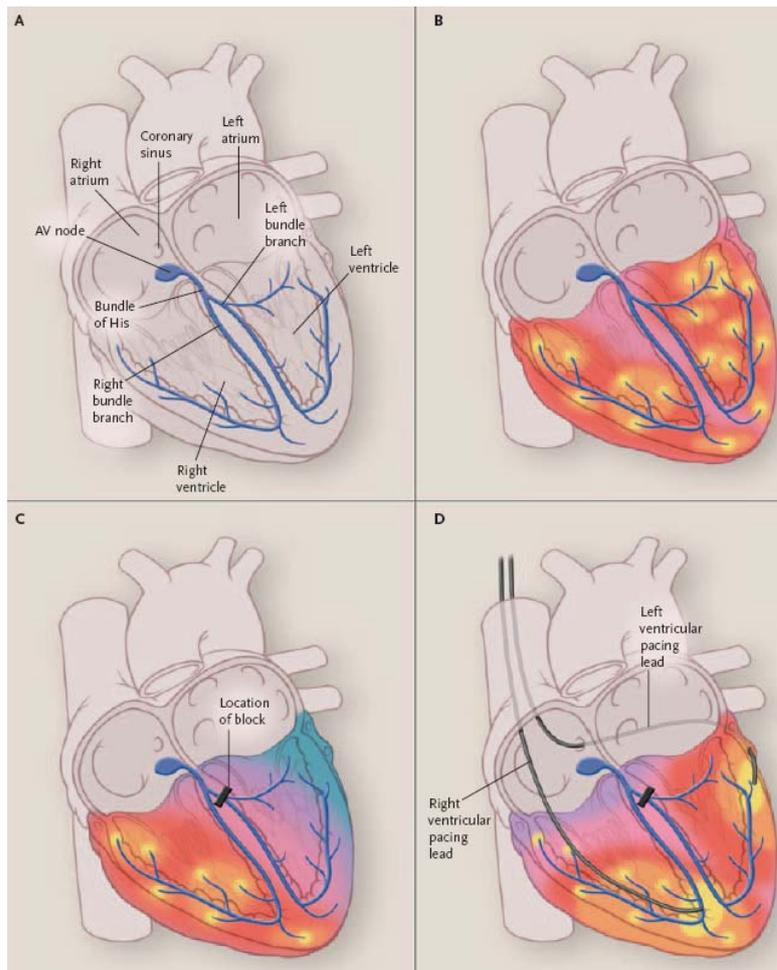
Figure 3. The cardiac conduction system is designed to initiate depolarization of the cardiac ventricles widely and synchronously. **Panel A** shows the anatomy of the system, with the locations of the atrioventricular (AV) node, the bundle of His, and the right and left bundle branches. With normal conduction, the LV and RV are depolarized simultaneously, with consequent simultaneous contraction (**Panel B**). In Panel B, yellow areas are the sites of earliest depolarization (at the terminal ramifications of the conduction system), with successive regions of depolarization shown in orange, red, and pink. In the setting of LBBB, the RV free wall and the interventricular septum are depolarized rapidly (**Panel C**). There is a clinically significant delay in the depolarization of the LV free wall. As a result, LV contraction is dyssynchronous. In Panel C, the sites of earliest depolarization are yellow and are all in the RV; successive regions of depolarization are shown in orange, red, pink, purple, and blue. With CRT, pacemaker leads are situated to stimulate both ventricles, thus bypassing the conduction block in the left bundle branch (**Panel D**). Simultaneous depolarization and simultaneous contraction of the ventricles is restored. In Panel D, the sites of early depolarizations are yellow and are near the tip of both pacemaker leads as well as in the branches of the normally conducting right bundle-branch system. Successive regions of depolarization are shown in orange, red, pink, and purple.

Importantly, at this time point, they stopped pacing and found that although dP/dtmax immediately declined (immediate CRT effect), chamber volumes were not immediately altered. This supports a remodeling effect rather than an active effect of CRT itself on long-term chamber volumes. Subsequent studies such as the MIRACLE trial (41) and Vigor-CHF (42) have reported approximately 10% reductions of both end-systolic and end-diastolic volumes with 6-month CRT.

In contrast to therapy with positive inotropes, the increase in systolic function obtained from CRT in dyssynchronous failing hearts does not increase (and may actually reduce) myocardial oxygen consumption. Nelson et al. (43) first reported on the energetics of a traditional inotropic treatment (dobutamine) vs CRT in dyssynchronous LV failure. They found that equivalent increases in dP/dtmax triggered marked differences in oxygen consumption, with consumption (per beat) rising nearly 20% with dobutamine but falling by 10%

with CRT. It remains unknown whether CRT reverses the electrophysiologic changes reported to occur with chronic dyssynchrony, and it is equally unclear what the net effects of CRT are on arrhythmia susceptibility in patients with HF. In theory, CRT could have antiarrhythmic effects caused by salutary changes in LV systolic function and geometry or by reversal of dyssynchrony-coupled pathologic changes in electrophysiology and molecular expression. Conversely, some have expressed concern that the use of an epicardial pacemaker (LV lead in the CRT system) is arrhythmogenic because of differences in transmural conduction and repolarization (44). Studies on the effect of CRT on the incidence of ventricular arrhythmias have provided mixed results. Cardiac resynchronization therapy neither reduced nor increased the incidence of ventricular tachycardia (polymorphic or monomorphic) in patients from the Contak-CD and InSync-ICD studies, (45) whereas some smaller studies found lower rates of appropriate ICD firings in patients with ICD-CRT systems (46-48). In the recent and larger CARE-HF trial, mortality from both pump failure and sudden death declined with CRT only, arguing against a proarrhythmic CRT effect and perhaps favoring an antiarrhythmic effect (49). Very little is still known about the molecular changes induced by chronic dyssynchrony or on what can be reversed by CRT, but this is presently under study. In a recent study on tumor necrosis factor a expression, apoptotic index, and myocardial fibrosis in patients with cardiomyopathy before CRT and after CRT, resynchronization therapy appeared to reduce interstitial myocardial collagen volume, tumor necrosis factor a levels, and apoptosis (50). Clearly, more human and animal studies are needed to address the effects of CRT at the molecular level.

1.b.ii.2. Clinical Evidence

The initial randomized trials of CRT involved no more than 500 patients and lasted less than one year (51-55). These trials enrolled patients with NYHA class III or IV HF, with other requirements typically including sinus rhythm, an EF of 35 percent or less, and a QRS interval of at least 120ms. These trials confirmed that the physiological effects of CRT were associated with increases in functional capacity and improvements in the quality of life. Such changes could be demonstrated as early as one month after the device was implanted (54). Two subsequent trials, Comparison of Medical Therapy, Pacing, and Defibrillation in Heart Failure (COMPANION) and Cardiac Resynchronization–Heart Failure (CARE-HF), evaluated the effect of CRT on survival (49, 56). As in most of the earlier trials, enrollment criteria included sinus rhythm, an NYHA class of III or IV, an EF of 35 percent or less, and a QRS interval of at least 120ms. In both trials, the risk of death from any cause was reduced by CRT as compared with no pacing; this difference was not significant in the COMPANION trial (hazard ratio, 0.76; P=0.06), but it was significant in the CARE-HF study (hazard ratio, 0.64; P<0.002).

1.b.ii.3. Clinical Use

Current indications for CRT include dilated cardiomyopathy (ischemic or nonischemic), an LVEF of 35 percent or less, a QRS interval of at least 120ms, and NYHA class III or IV HF despite optimal medical therapy (49,56).

Increased risks of bleeding or infection are relative contraindications, as is the presence of any other major life-limiting medical condition, such as advanced cancer. It has been suggested that patients whose HF is severe enough to require parenteral inotropic therapy should not receive a biventricular pacemaker (57). Candidates for CRT may need a device with both cardiac-resynchronization and cardioverter–defibrillator functions; most candidates for BiV pacing are also candidates for an ICD (7).

1.b.ii.4. Implant

The implantation of a BiV pacemaker requires a method for pacing the LV. In the standard approach, a specifically designed pacing lead is inserted into the mouth of the coronary sinus (in the right atrium) and advanced posteriorly around the atrioventricular-valve ring.
The lead is then passed into a venous branch running along the free wall of the LV (58). In some patients, the LV electrode cannot be properly positioned through the coronary sinus; minimally invasive thoracic surgical techniques have been used for lead placement in such patients (59).
No specific preparation is required before the implantation of a biventricular pacemaker. Implantation is performed by a cardiologist or cardiac surgeon with the patient under local anesthesia. After the pacemaker has been implanted, some patients report symptomatic improvement almost immediately, although it is unclear how much of this effect is psychological. As noted above, in clinical trials, objective evidence of functional improvement has been documented as early as one month after implantation (54). An electrocardiogram is obtained to document the new baseline appearance with pacing. Care of the incision site used for the implant is similar to that for other pacemakers. Patients who receive a BiV pacemaker must undergo periodic clinical evaluation as well as have the device evaluated. Lead impedance, device programming, and battery life are all checked on a regular basis.

1.b.ii.5. Areas of Uncertainty

Several areas of uncertainty remain.

Long-term survival in patients treated with CRT in clinical practice. The characteristics of patients enrolled in randomized controlled trials are strictly defined and frequently different from those of "real world" patients. Currently, apart from single-center observations, studies reporting the long-term survival of patients treated with CRT outside the realm of randomized controlled trials are still lacking, and so are analyses concerning the persistence of CRT benefit following the first year of treatment (see Appendix.b.).

Effects of CRT in patients with mild symptoms of HF. It has not been established whether CRT is beneficial in patients with mild HF (NYHA class II), since only two small trials have included such patients (53, 60). In these analyses, CRT did not significantly improve functional status or the quality of life, although it did increase LV volumes and, in one trial, EF. The Multicenter Automatic Defibrillator Implantation Trial–Cardiac Resynchronization Therapy (MADIT-CRT) and the Resynchronization Reverses Remodeling in Systolic

Left Ventricular Dysfunction (REVERSE) trial will evaluate the role of ICD with or without CRT in large cohorts of patients with NYHA class I or II HF (see Appendix.c.).

Efficacy of CRT in very old patients. Generally, resynchronization trials have excluded very old patients (>80 years old), and little data exists on the outcomes after CRT in the elderly. This represents an important limitation, since almost half of the patients evaluated in community studies are over 80 years old (see Appendix.d.).

The site of left ventricle stimulation. Butter et al. (61) studied 30 patients undergoing CRT. Benefit from CRT was significantly greater when the lateral wall was paced as compared to the anterior wall.
Gold et al. (62) showed that pacing from different sites within a given vein could have a substantial impact on acute hemodynamic benefits and that there was a major inter-individual variation in optimal pacing site. Dekker et al. (63) produced similar data in 11 patients using an epicardial approach.
Rosillo et al. (64) evaluated 233 CRT patients and compared two groups based on anatomic lead position. After implant, EF improved significantly only in subjects with leads in the lateral and postero-lateral branches.
However, in a similar retrospective analysis of 158 patients Gasparini et al. (65) did not find a difference in EF benefit between septal and lateral pacing sites.
Ansalone et al. (66) investigated 31 patients by tissue Doppler imaging (TDI) to identify the most delayed site of LV contraction before CRT. They found that the lack of concordance between the site of delay and the site of pacing is likely to reduce the improvement in LV performance due to BIV.
The sum of these data suggests that pacing at late activated LV free wall sites produces the best results and that there is considerable and important inter-patient variation in the location of these sites.
However, in patients receiving BIV, the LV lead positioning varies randomly for several anatomical and technical reasons so that LV pacing cannot be applied at the optimal site in all patients.

LV lead implantation technique. The LV lead is implanted with a transvenous approach in the majority of the cases. Unfortunately, LV pacing via transvenous procedure has an overall success rate ranging from 88% to 92% according to different experiences. Moreover, limited availability of suitable coronary sinus tributary veins often increases difficulties in achieving the optimal hemodynamic response. Alternative approaches to CRT were not consistently studied, although some experiences have been recently reported (see Appendix.e.).

The effects of CRT on diastolic function. Advanced stage of HF is characterized by a heterogeneous picture, where signs and symptoms of diastolic and systolic dysfunction coexist. In dilated cardiomyopathy the abnormalities of diastolic function occur early, often preceding dysfunction of contraction phase, and have a major role in producing symptoms. Several trials showed the mechanisms of action and the effects of CRT on systolic

function, while the effects on diastolic function are controversial and conflicting data have been published so far (see Appendix.f.).

Ventricular dyssynchrony and the selection of candidates for CRT. CRT does not result in significant clinical improvement in 20 to 30 percent of patients (54). Although there may be various explanations for this observation, it has been suggested that an increased QRS interval may not be the best criterion for benefit from CRT and that guidelines for the selection of candidates for CRT should suggest the use of echocardiography to identify dyssynchrony (67).

However, none of the major clinical trials of CRT used echocardiographic measures of dyssynchrony as the principal criteria for enrollment. Furthermore, it is not clear which echocardiographic variables should be used to select candidates for CRT (see Appendix.g. and h.).

2. Non-Invasive Evaluation and Quantification of Ventricular Dyssynchrony

Quantification of non-uniform mechanical function and dyssynchrony may lead to a more complete diagnosis of ventricular dysfunction. Moreover, it may guide therapy, because patients with extensive dyssynchrony are likely to benefit from resynchronization therapy.

2.a. QRS Duration to Assess Dyssynchrony and to Predict Response to CRT

The response to CRT was initially considered to result in part from resynchronization of interventricular dyssynchrony (dyssynchrony between the left and right ventricle). Thus, patients with interventricular dyssynchrony were selected for CRT. This selection was based on the QRS duration, because this parameter is considered to reflect interventricular dyssynchrony. Indeed, Rouleau et al. (68) demonstrated a good relation between interventricular dyssynchrony (assessed by tissue Doppler imaging [TDI]) and QRS duration. Accordingly, patients with wide QRS were considered candidates for CRT. In general, studies used QRS duration >120 to 130 ms as a selection criterion. The initial studies required the presence of a left bundle branch block pattern on the electrocardiogram, whereas more recent studies also included patients with non-specific interventricular conduction delay (a poorly defined entity) or even right bundle branch block pattern. The beneficial effect of CRT on symptoms, exercise capacity, systolic LV function, and hospitalization rate was demonstrated in these patients with wide QRS complex. In addition, data from the Pacing Therapies in Congestive Heart Failure (PATH-CHF) II trial demonstrated that the benefit of CRT was most pronounced in patients with QRS duration >150 ms (as compared to patients with QRS duration 120 to 150 ms) (69). These observations tend to support the use of the QRS duration for patient selection. However, careful analysis of the individual patients in many CRT studies demonstrated that 20% to 30% of the patients failed to respond to CRT, despite prolonged QRS duration. These observations prompted Molhoek et al. (70) to analyze the precise value of the QRS duration to predict response to CRT. Their study included 61 patients, and 45 (74%) responded to CRT. The QRS duration at baseline before pacing was similar between the responders and non-responders (179 $\pm$ 30 ms vs. 171 $\pm$ 32 ms; p = NS). However, a significant shortening in QRS duration after six months of CRT was observed only in responders. Receiver operating characteristic curve analysis showed that a reduction in QRS duration >10 ms had a high sensitivity (73%) with low specificity (44%) in prediction of responders. Conversely, a reduction in QRS duration >50 ms was highly specific (88%) but not sensitive (18%) to predict response to CRT. It has subsequently been suggested that intraventricular dyssynchrony may predict response to CRT more accurately (67). In this respect, studies using TDI demonstrated that patients with intraventricular dyssynchrony had a high likelihood of a positive response to CRT (67). Bleeker et al. (71) evaluated the relation between QRS duration and LV dyssynchrony (assessed by TDI) in 90 patients with severe HF; EF <35%; and narrow (<120 ms), intermediate (120 to 150 ms), or wide (>150 ms) QRS complexes. Substantial LV dyssynchrony

on TDI was present in 27%, 60%, and 70% of patients, respectively. When QRS duration was considered as a continuous variable, no relation between QRS duration and LV dyssynchrony could be demonstrated. Ghio et al. (72) confirmed the absence of LV dyssynchrony in 48% of patients with an intermediate (120 to 150 ms) QRS complex and in 28% of patients with a wide (>150 ms) QRS complex. These observations indicate that patients with a wider QRS complex have a higher likelihood of LV dyssynchrony, although 30% of patients with wide (>150 ms) QRS complex lack LV dyssynchrony. This 30% may partially explain a similar percentage of non-responders in the large trials. These observations have resulted in many echocardiographic studies evaluating different echocardiographic parameters to detect LV dyssynchrony and predict response to CRT.

2.b. Echocardiographic Quantification of Ventricular Dyssynchrony and Selection of Responders to CRT

A variety of echocardiographic techniques have been suggested for the assessment of LV dyssynchrony and prediction of response to CRT. These techniques include M-mode assessment, two-dimensional echocardiography using phase imaging or intravenous contrast, TDI, and potentially three-dimensional echocardiography (67). Tissue Doppler imaging is the most extensively tested technique, and different methods have been proposed, including pulsed-wave TDI, color-coded TDI, tissue tracking, displacement mapping, strain and strain rate imaging, and, most recently, tissue synchronization imaging (TSI). A comprehensive summary of the merits of the different techniques to predict response to CRT is provided in Table 1.

M-Mode Echocardiography
Using an M-mode recording from the parasternal short-axis view (at the level of the papillary muscles), the septal-to-posterior wall motion delay can be obtained, and a cutoff value of 130 ms or more was proposed as a marker of intraventricular dyssynchrony. Pitzalis et al. (73) evaluated 20 patients and reported a sensitivity and specificity of 100% and 63%, respectively, to predict response to CRT. In addition, the authors recently demonstrated the prognostic value of the septal-to-posterior wall motion delay (74). However, this parameter is often difficult to obtain. Marcus et al. (75) evaluated the feasibility of obtaining this parameter in the patients of the CONTAK-CD database. A clear definition of the systolic deflection of both the septal and posterior wall was possible in only 45% of 79 patients. Moreover, the septal-to-posterior wall motion delay did not correlate with LV reverse remodeling. Most importantly, the sensitivity and specificity to predict response (both clinical and echocardiographic) were 24% and 66%. These findings were similar in patients with ischemic and dilated cardiomyopathy.

Two-Dimensional Echocardiography
The first use of two-dimensional echocardiography was that of a semiautomatic method for endocardial border delineation (76). The degree of LV dyssynchrony was quantified in two-dimensional echocardiographic sequences from the apical four-chamber view, focusing on the septal-lateral relationships. Computer-generated regional wall movement curves were

compared by a mathematical phase analysis, based on Fourier transformation. The resulting septal-lateral phase angle difference is a quantitative measure for intraventricular (dys)synchrony. Using this approach, patients with extensive LV dyssynchrony between the septum and lateral wall exhibited an immediate improvement in hemodynamics after CRT. The second approach utilized echo contrast (Optison, Mallinckrodt, Hazelwood, Missouri) to optimize LV border detection (77). With the improved LV border detection, regional fractional area changes were determined and plotted versus time, yielding displacement maps. From these maps, the LV dyssynchrony between the septum and lateral wall was determined. The authors observed an acute reduction in LV dyssynchrony after biventricular pacing, which correlated with an acute increase in EF. No studies on the two-dimensional techniques for prediction of long-term outcome have been published.

TDI, Strain, and Strain Rate Imaging
Tissue Doppler imaging measures the velocity of longitudinal cardiac motion and allows comparison of timing of motion in relation to electrical activity (QRS complex). Different parameters can be derived, and the most frequently used include the peak systolic velocity, the time to onset of systolic velocity, and the time to peak systolic velocity. The TDI measurements can be obtained directly using pulsed-wave TDI and using color-coded TDI, which needs post-processing. With pulsed-wave TDI, only one region can be interrogated at a time making the procedure time-consuming and precludes comparison of segments simultaneously. Because measurements are influenced by differences in heart rate, loading conditions and respiration measurements that are not simultaneous may be less meaningful. In addition, the timing of peak systolic velocity is often difficult to identify, resulting in imprecise information on LV dyssynchrony. There is limited evidence of pulsed-wave TDI to predict response to CRT. Two studies have demonstrated a relation between LV dyssynchrony on pulsed-wave TDI and improvement in symptoms and/or EF after CRT (78, 79), but prediction of response was not addressed.

Several studies have used color-coded TDI to assess LV dyssynchrony and predict outcome (Table 1) (80-85). From these color-coded images, TDI tracings can be obtained by post-processing, and the majority of studies have used time to peak systolic velocity to assess LV dyssynchrony. Initially, investigators focused on the four-chamber view to identify LV dyssynchrony by color-coded TDI. Velocity tracings were derived from the basal septal and lateral segments, and the septal-to-lateral delay was measured. It was shown that a delay >60 ms was predictive of acute response to CRT (81). Subsequently, a four-segment model was applied, which included four basal segments (septal, lateral, inferior, and anterior) (86). It was shown that a delay >65 ms allowed prediction of response to CRT. Using this cutoff value, sensitivity/specificity for prediction of clinical improvement (defined by an improvement in NYHA functional class and 6-min walking distance) were both 80% whereas sensitivity/specificity for LV reverse remodeling (defined as a >15% reduction in LV end-systolic volume) were both 92%. In addition, patients with LV dyssynchrony >65 ms had a favorable prognosis after CRT.

The extensive studies by Yu et al. (87, 80, 81) have used a 12-segment model. Tracings were derived from 12 segments, and an LV dyssynchrony index was derived from the standard deviation of all 12 time intervals demonstrating that a dyssynchrony index >31 ms yielded a sensitivity and specificity of 96% and 78% to predict LV reverse remodeling (87). In general, prediction of response to CRT based on time to peak systolic velocity (using a varying number of segments) yields a high sensitivity (ranging from 76% to 97%) and specificity (ranging from 55% to 92%) (Table 1). Seven studies have used tissue tracking, strain, and/or strain rate imaging (84, 85,87-91). Tissue tracking (GE Vingmed, Horten, Norway) provides a color-coded display of myocardial displacement, allowing for easy visualization LV dyssynchrony and the region of latest activation. Sogaard et al. (85) pioneered this approach and demonstrated that the number of segments with delayed longitudinal contraction was related to the improvement in EF during CRT. Strain and strain rate analysis is performed by off-line analysis of the color-coded tissue Doppler images. Strain analysis allows direct assessment of the extent and timing of myocardial deformation during systole and is expressed as the percentage of segmental shortening or lengthening in relation to its original length (67). The main advantage over TDI is that strain analysis allows differentiation between active systolic contraction and passive motion. This is important in patients with ischemic cardiomyopathy with the presence of scar tissue. Breithardt et al. (88) showed that CRT reversed the pathologic septal-lateral strain relationships and reduced the incidence of early systolic pre-stretch in the late activated wall and of post-systolic shortening. However, no study with strain or strain rate imaging has so far reported on the actual prediction of response to CRT (Table 1), except for Yu et al. (87), who demonstrated that strain rate imaging could not predict LV reverse remodeling. Despite the technical advantages of the strain imaging, the technique has not become routine practice in the evaluation of patients considered for CRT. The main limitations are the time-consuming aspect of the technique, the high operator dependency, and the moderate reproducibility. Only one direct comparison between TDI and strain rate imaging has been reported in 54 patients undergoing CRT (87). Left ventricular dyssynchrony on TDI was predictive of LV reverse remodeling, but strain rate imaging failed to predict response to CRT (87).

TSI to Assess LV Dyssynchrony
A recent addition to the tissue Doppler approach to quantify LV dyssynchrony has been the automated color-coding of time to peak longitudinal velocities. This color-coding of temporal velocity data is superimposed on the routine two-dimensional echocardiographic images to provide visual mechanical information on the anatomical regions. Tissue synchronization imaging (GE Vingmed) (90-93) is a signal-processing algorithm of the tissue Doppler data to automatically detect peak positive velocity and then color-code the time to peak velocities in green for normal timing, yellow-orange for moderate delay, and red for severe delays in peak longitudinal velocity.

Three-Dimensional Echocardiography to Assess LV Dyssynchrony
Three-dimensional echocardiography has evolved from a technique based on reconstruction of multiple two-dimensional scan planes to an almost real-time

methodology. Left ventricular volumes and EF can be assessed with high accuracy (94). In the context of LV dyssynchrony, analysis of regional function in the time-domain is important (67), and a series of plots is obtained representing the change in volume for each segment (usually 16 or 17 segments) throughout the cycle. With synchronous contraction of all segments, each segment would be expected to achieve the minimum volume at almost the same point in the cardiac cycle. In LV dyssynchrony, dispersion exists in the timing of the point of minimum volume for each of the segments. The degree of dispersion reflects the severity of LV dyssynchrony (95). Parametric "polar-map" displays (of the three-dimensional data) of the timing of LV contraction have been developed to facilitate interpretation of data. This methodology examines regional LV contraction at approximately 3,000 points over the endocardial surface rather than in 16 or 17 segments. Color-coding is used to identify the region/site of latest activation, and this is potentially useful for electrophysiologists to select the optimal LV lead position. Zhang et al. (96) used three-dimensional echocardiography in 13 patients who had previously received CRT; when CRT was withheld, significant LV dyssynchrony occurred, associated with a decrease in EF. Currently, no extensive data are available on the prediction of response to CRT using three-dimensional echocardiography.

Table 1. Echocardiographic Studies on LV Dyssynchrony to Predict Response to CRT.

Authors	Patients (n)	Follow-Up Period (month)	Echo Technique	Methodology for LV Dyssynchrony	Main Findings	Sensitivity (%)	Specificity (%)
Pitzalis et al. 2002	20	1	M-mode	Septal-to-posterior wall motion delay	Septal-to-posterior delay ≥130 ms predicted LV reverse remodeling	100	63
Pitzalis et al.2005	60	14	M-mode	Septal-to-posterior wall motion delay	Septal-to-posterior delay ≥130 ms predicted event-free survival	NA	NA
Marcus et al. 2005	79	6	M-mode	Septal-to-posterior wall motion delay	Septal-to-posterior delay ≥130 ms insufficient to predict LV reverse remodeling	24	66
Breithardt et al. 2002	34	Acute	2D phase imaging	Difference between the lateral and septal wall motion phase angles	Delayed lateral wall motion predicted acute hemodynamic improvement	NA	NA
Kawaguchi et al. 2002	10	9	Contrast echo	Septal and lateral fractional area changes	↑ Septal inward motion, ↓ spatial and temporal LV dyssynchrony by 40%, and correlated with ↑ LVEF	NA	NA
Penicka et al. 2004	49	6	Pulsed-wave TDI	Ts(onset) of 3 basal LV and 1 basal RV segments	Summation of inter- and intra(LV)-ventricular delay >102 ms predicted ↑ LVEF	96	71
Ansalone et al. 2001	21	1	Pulsed-wave TDI	Systolic dyssynchrony among 5 basal segments	Extensive LV dyssynchrony resulted in ↑ in symptoms, and ↑ LVEF	NA	NA
Garrigue et al. 2001	12	12	Pulsed-wave TDI	Ts(onset) between septum and lateral wall	Post-CRT reduction in LV dyssynchrony and improvement in symptoms	NA	NA
Bordachar et al. 2004	41	3	Pulsed-wave TDI, M-mode, Pulsed-wave Doppler	Maximal difference in 12 LV segments for Ts, Ts(onset), Ts-SD, and DLC	Maximal difference in 12 LV segments for Ts, T(onset), Ts-SD closely correlated with improvement of MR and CO, but not interventricular delay by pulsed-wave Doppler echo	NA	NA
Yu et al. 2002	25	3	Color-coded TDI	Ts of 12 LV segments in ejection phase	Improve LV dyssynchrony by delaying Ts in 12 LV segments globally resulting in homogenous Ts	NA	NA
Bax et al. 2003	25	Acute	Color-coded TDI	Septal-to-lateral delay of Ts in ejection phase	Septal-to-lateral delay of Ts ≥60 ms predicted ↑ LVEF	76	88
Yu et al. 2003	30	3	Color-coded TDI	Ts-SD of 12 LV segments in ejection phase	Ts-SD of 12 LV segments >33 ms predicted LV reverse remodeling	NA	NA
Bax et al. 2004	85	12	Color-coded TDI	Septal-to-lateral delay of Ts in ejection Phase	Septal-to-lateral delay of Ts ≥65 ms predicted LV reverse remodeling; and associated with lower event rate	92	92

Authors	Patients (n)	Follow-Up Period (month)	Echo Technique	Methodology for LV Dyssynchrony	Main Findings	Sensitivity (%)	Specificity (%)
Notabartolo et al. 2004	49	3	Color-coded TDI	Maximal difference in Ts in 6 basal segments (both ejection phase and post-systolic shortening)	Maximal difference in Ts in 6 basal segments >110 ms predicted reverse remodeling	97	55
Yu et al. 2004	54	3	Color-coded TDI, SRI	Ts-SD of 12 LV segments in ejection phase (and 17 other parameters)	Ts-SD of 12 LV segments >31 ms predicted LV reverse remodeling	96	78
Sogaard et al. 2002	20	12	Color-coded TDI, SRI	DLC	Number of basal segments with DLC predicted ↑ LVEF	NA	NA
Sogaard et al. 2002	20	Acute	Color-coded TDI, TT, SRI	TT and DLC	Optimization of V-V timing by TT resulted in ↓ DLC and ↑ LVEF	NA	NA
Breithardt et al. 2003	18	Acute	Strain, SRI	Strain and SRI at septal and lateral walls	Baseline: lateral wall strain and strain rate higher than septal; CRT: septal wall strain and strain rate higher than lateral	NA	NA
Sun et al. 2004	34	Acute	Displacement, strain, and SRI	Strain, SRI, and displacement at septal and lateral walls	↑ LVEF and ↑ peak strain rate at lateral wall by CRT; ↑ Septal and inferior wall displacement by LV pacing	NA	NA
Popovic et al. 2002	22	1-12	Displacement and strain	Strain at septal and lateral walls	↑ Global LV peak strain, ↓ coefficient of change in LV strain, no change in septal or lateral wall displacement	NA	NA
Dohi et al. 2005	38	Acute	TSI and strain	Peak radial strain septum versus posterior wall	Delay in septal-posterior strain ≥130 ms, predicted ↑ stroke volume	95	88
Gorcsan III et al. 2004	29	Acute	TSI	Septal-posterior delay (both ejection phase and post-systolic shortening)	Septal-posterior delay ≥65 ms predicted 1 stroke volume	87	100
Yu et al. 2005	56	3	TSI	Ts-SD of 12 LV segments in ejection phase (inclusion of post-systolic shortening)	Ts-SD of 12 LV segments in ejection phase >34 ms predicted reverse LV remodeling	87	81
Zhang et al. 2005	13	3	3D echo	Time to minimal systolic volume (Tmsv) in 6, 12, and 16 LV segments	Improvement of Tmsv parameters during CRT Tmsv of 16 LV segments by 3D echo correlated closely with Ts-SD of 12 LV segments by TDI	NA	NA

CO = cardiac output; DLC = delayed longitudinal contraction; MR = mitral regurgitation; SRI = strain rate imaging; TMSV = time to minimal systolic volume; Ts = time to peak myocardial systolic velocity; TSI = tissue synchronization imaging; Ts(onset) = time to onset of myocardial systolic velocity; Ts-SD = standard deviation of time to peak myocardial systolic velocity; TT = tissue tracking; V-V interventricular.

2.c. MRI Quantification of Ventricular Dyssynchrony and Selection of Responders to CRT

Most mechanical dyssynchrony analysis is based on echo-Doppler methods, which in turn are largely derived from only two-dimensional longitudinal motion data. This choice of orientation is mainly based on practical grounds given available windows for transducer placement. However, cardiac contraction is principally circumferential, and thus echo-based Doppler methods may not provide the most accurate and comprehensive assessment of global dyssynchrony in HF. Further, the variance of repeated echocardiographic measures is fairly high owing to dependence on operator experience, machine settings, available acoustic windows, and angle of incidence effects. This can introduce noise when applying such approaches to the routine clinical setting. Quantitative magnetic resonance imaging (MRI)-based strain analysis provides highly reproducible, high-resolution three-dimensional circumferential and longitudinal myocardial activation data that are largely operator- and patient-independent and thus may be better suited to characterize dyssynchronous HF and identify appropriate candidates for CRT.

Cine mode MRI is an excellent imaging modality for the assessment of global and regional myocardial function in patients with contractile dysfunction (97). This method captures multiple slices and phases of the heart to generate what appears to be a real-time representation of cardiac contraction. Global function is measured by simple volumetric analysis of the LV, whereas regional myocardial function is most commonly derived from qualitative wall motion assessment and/or quantitative methods that track myocardial deformation over the cardiac cycle.

The evolution of advanced MRI quantitative strain pulse sequence algorithms designed to work with traditional cine-MRI, as well as new methods to analyze their output, have opened new avenues for assessment of cardiac dysfunction.

Cine Myocardial Tagging
Magnetic resonance imaging myocardial tagging is a technique that places non-physical markers (stripes or grids) inside the myocardium by manipulating the magnetization of the tissue using special encoding pulses (98,99). These markers, called tags, appear in the acquired images as dark lines and serve as fiducial myocardial markers that move and bend with the myocardium to which they are linked. In addition to simplifying the visual/qualitative assessment of cardiac wall motion abnormalities, analysis of the relative movement of these tags over the cardiac cycle is used to calculate local myocardial motion or strain (relative shortening). There are three primary strains for three-dimensional deformation— circumferential, radial, and longitudinal —and each can be computed. Techniques for such analysis were developed by O'Dell et al. (100) to generate detailed four-dimensional mechano-anatomic activation maps from MRI tagged data sets. The analytic algorithm (FINTAGS) has been used to characterize mechanical dyssynchrony in animal models (101,102) and in humans with HF and intraventricular conduction delay (103,104). Although the information

generated by this approach is comprehensive, processing and analysis time is extensive, limiting its clinical utility.

Harmonic Phase Analysis of Tagged MRI

To enhance the clinical utility of myocardial tagging data acquisitions, a rapid analysis method called harmonic phase (HARP) has recently been developed (105) and commercialized (Diagnosoft, Inc., Palo Alto, California). This approach shortens the analysis time to generate regional dynamic color stain maps/data from 1 week to under 2 min for three to four myocardial slices. The HARP method measures the motion from tagged magnetic resonance images by filtering harmonic peaks in the frequency domain of the images (106,107). The resulting image is then decomposed into a harmonic magnitude and harmonic phase, which are related to the underlying anatomy of the heart and tag deformation, respectively. The HARP method measures the local strain of tissue by measuring the frequency of the tag lines. If the tissue contracts, the tag lines become closer to each other and the tag frequency increases in proportion to that contraction, and vice versa. Circumferential strain in a given angular sector of each slice is then plotted during the cardiac cycle.

Strain-Encoded MRI

Although faster, HARP analysis still requires some post-processing. A more automatic alternative is strain-encoded (SENC) MRI, a new method for direct imaging of regional strain that does not require complex image processing (108-110). The SENC imaging is derived from a standard myocardial tagging sequence that tags the tissue at end-diastole with a sinusoidal tag pattern designed to modulate the longitudinal magnetization orthogonal to the imaging plane. Deformations of tissue during systole will change the local frequency of the pattern in proportion to the through-plane strain component. The distribution of regional contraction (circumferential shortening in long-axis views or longitudinal compression in short-axis views) is then displayed as contrast in the images. The SENC technique has several features that make it especially well suited for assessing dyssynchronous HF and CRT, in that it provides: 1) instantaneous real-time quantitative strain measurements without the need for user intervention; 2) higher spatial resolution over standard tagging as a result of reduced tag spacing; 3) allows acquisition of both circumferential and longitudinal myocardial stain information; and 4) application to assessment of regional function of the right as well as the LV.

CRT and MRI Device Compatibility

Although new methods have substantially improved the practicality of MRI CRT assessment, there remain a number of concerns, including cost, longer examination times, need for complex imaging/data processing infrastructure, and, perhaps most importantly, inability to image patients with implanted devices.

3. An Invasive Method of Evaluation of Left Ventricle Mechanics: the Conductance Catheter

Assessment of cardiac function is of vital importance in clinical cardiology for diagnosis, monitoring, and treatment. A prerequisite for quantification of cardiac function is a reliable estimation of pressure–volume relationships of the LV.

Besides pressure, that can only be obtained invasively using a transducer mounted on a catheter, absolute ventricular volume should be determined continuously. However, it must be considered that the volume of the LV is not easy to define, due to the displacement of the atrio-ventricular plane and, if defined, that volume is not easy to measure.

As for spatial resolution, volume is best measured using for example MRI or computed tomography, but the temporal resolution of these techniques is still limited. Thus, they do not meet the requirements for on-line registration or high temporal resolution. Ultrasound can be used for estimation of LV volume, but it is not suitable for obtaining absolute volumes, unless temporal resolution is decreased.

There are alternatives, e.g. metallic radiopaque markers and sonomicrometry, but they are not used in clinical practice because of their invasiveness (111, 112).

In 1981, Baan and co-workers presented a new volume measurement technique, which was based on conductance measurement (113, 114).

The principle used to obtain intraventricular volume, i.e. the time-varying volume of blood contained within the cavity, was by measuring electrical conductance of the blood employing a multi-pole catheter (Figure 4). The catheter was placed within the ventricle along its long axis in such a way that the electrode at the tip was situated within the apex and the proximal one just above the aortic valve.

A weak alternating current (0.4 mA peak-to-peak, 20 kHz) was induced between these electrodes in order to set up an electrical field within the ventricular cavity. The induced voltage was then measured with six electrodes in between, yielding 5 segmental voltages.

Since the conductance of the blood itself is constant (neglecting long term changes in haematocrite) the measured voltage will be proportional to blood resistivity, and thus inversely proportional to the conductance or amount of blood between the measuring (voltage) electrodes.

$$V_{segment}(t) = \frac{1}{\alpha} \times \frac{L^2}{\sigma_b} \left[G_{segment}(t) - G_{p,segment} \right]$$

$V_{segment}(t)$ = Time-varying (intraventricular) segmental volume
α = Slope factor
L = Inter-electrode distance
σ_b = Specific conductivity of blood
$G_{segment}(t)$ = Time-varying segmental conductance
$G_{p,segment}$ = Parallel conductance; conductance of structures surrounding the intraventricular blood

The segmental volumes are then summed to form total volume.

This method has several advantages over other methods which determine intra- ventricular volumes. The results are obtained immediately, i.e. on-line, and precise geometric assumptions regarding the ventricle or labor-intensive analyses are not required.
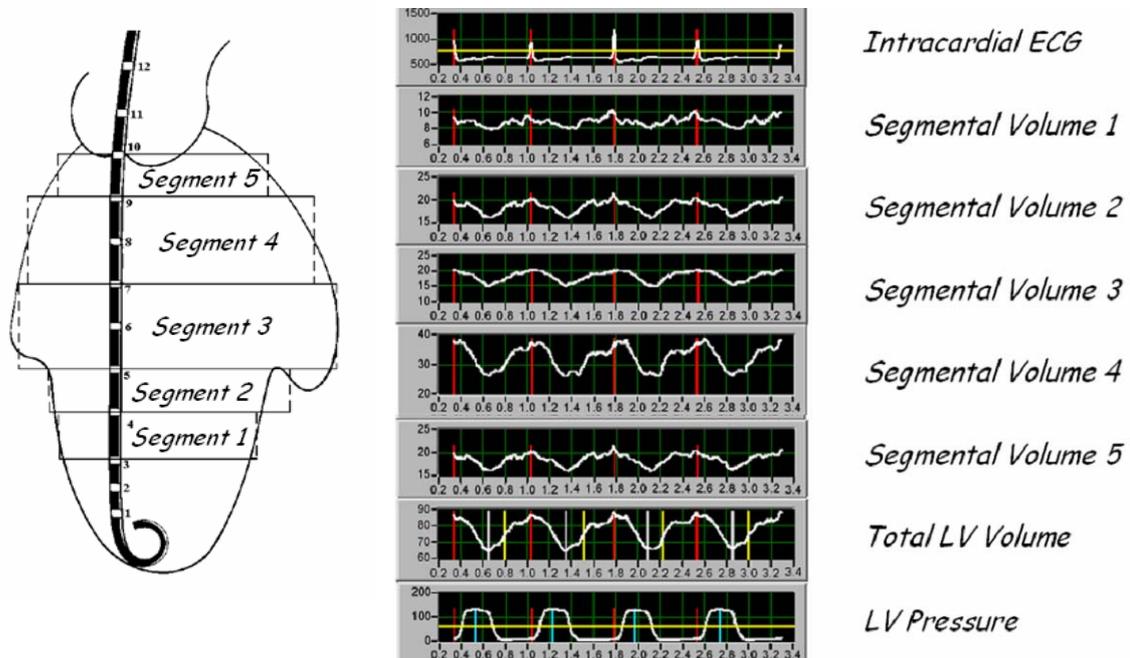
Figure 4. The catheter has 12 electrodes and should be positioned along the long axis of the LV. The two most distal and two most proximal electrodes are employed to generate the electrical field. This dual pair of current electrodes enables the use of a dual excitation mode. Other 6 electrodes are used pairwise to measure segmental conductance signals. Two electrodes are used to record the intracardial ECG. A micromanometer measures real-time LV pressure.

Dual Field Catheters
Implicit in the volume calculation from conductance data, an assumption is made that the electrical field is homogenous. Since this is not the case, especially in larger LV, a dual-field catheter was introduced (115, 116). Proximal and distal to the existing pair of current electrodes, another pair was positioned. This pair of electrodes also generates current with the same frequency, but with opposite polarity. This was suggested to give a more homogenous field, and thus a more linear relation between true volume and volume estimate from the conductance method (115). This was also reported to be true although results were not perfect, especially, as mentioned, for larger ventricles (116, 117).

3.a. Calibration

The conductivity of blood (σ_b) is determined in practice by taking a small arterial sample and transferring it to a measuring cell.
The slope factor (α) is a correction factor accounting for the fact that the ventricle is not a regular cylinder. Alpha is determined through an independent cardiac output measurement, such as thermo-dilution: the dynamic range of

the conductance signal has to be multiplied with a calibration factor (α) to reflect the amount of blood ejected into aorta during a minute.

The conductive tissues and fluids surrounding the ventricle contribute to the measured electrical conductance of the blood inside the ventricle, causing an offset in the relation between measured conductance and true intra-ventricular volume (114). This offset is called parallel conductance. When parallel conductance is not quantified, only changes in conductance as a measure of changes in volume can be presented (113, 118-120).

To extend the conductance method to absolute volume measurements, a method to determine tissue conductance has been introduced by Baan et al. (114). They determined conductance of the tissues surrounding the blood in the ventricular cavity, by changing the specific conductivity (σ_b) of blood by injecting hypertonic saline into the pulmonary artery (Figure 5). The conductance signal was recorded and the successive conductance values at end-diastole (G_{dias}) were plotted versus the corresponding values at end-systole (G_{sys}).
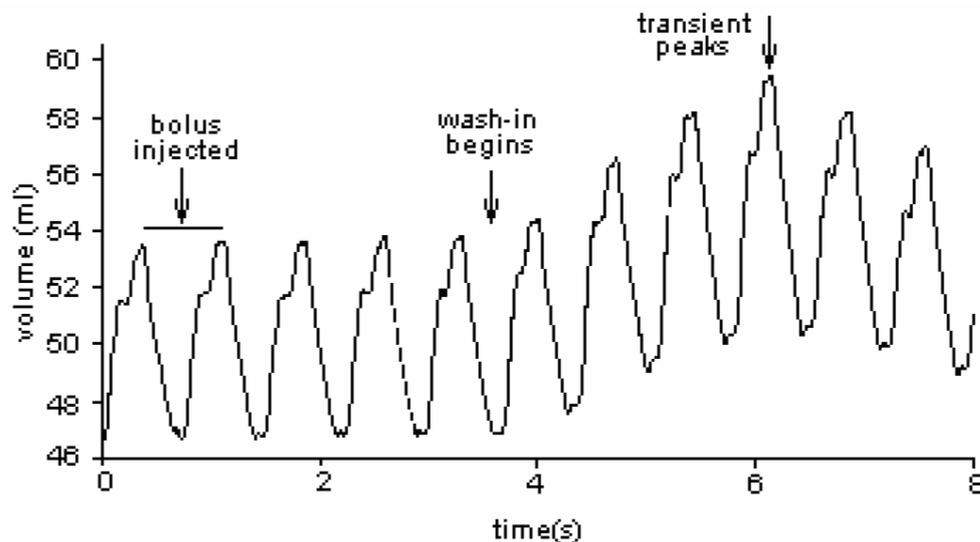
Figure 5. The method to determine the correction volume Gp is a dilution technique, which relies on the analysis of the conductance signal during an induced transient change in blood conductivity. In order for this method to work properly, the heart must be in a relatively steady state, with no beat-to-beat changes in end-diastolic and end-systolic volume. A small bolus of hypertonic saline is injected into the pulmonary artery, allowing good mixing with the blood before it enters the LV. As the mixture enters the LV, a temporary, gradual change in the conductance signal will occur over several beats. The increase in the conductance signal is then analyzed to extrapolate the effects of decreasing conductivity.

A linear regression line was fitted through G_{sys} – G_{dias} points and extrapolated to the identity line. The intersection point between the lines corresponds to a zero value of conductivity of blood (σ_b), and therefore, yields parallel conductance (G_p). A disadvantage of this extrapolation method is that a small variation in the determined G_{dias} and G_{sys} values will result in a large error in the extrapolated value of parallel conductance.

Since introduction in the early 1980s, other calibration techniques have been described. Three different techniques are presented: 1) the dual frequency

method, 2) development of the dilution technique, and 3) the volume reduction technique.

The dual frequency technique was first described by Gawne et al., indicating that surrounding structures have different frequency characteristics compared to blood: a dual frequency catheter system could then separate the two (blood from tissue), and thus calculate G_p (121). This concept has later been contradicted by another study (122). Theoretically, this technique is very elegant, since Gp can be estimated without any further manipulation that might be harmful to the patient.

The dilution technique still uses a bolus of hypertonic saline, but instead of extrapolating to the point where blood conductivity is zero, the area below the dilution curve is analysed (123). A better reproducibility is achieved, and fewer injections are needed.

The third technique described is a development of the suction technique, where the left ventricle is emptied – the conductance thus measured is equal to G_p (114, 124).

This method is for understandable reasons not applicable in clinical use. Instead the inflow of blood from vena cava inferior or superior is reduced, and the volume curve is extrapolated to zero (125). Thus, G_p can be calculated.

Calibration Discussion

The parallel conductance Gp has been under severe investigation, probably due to the fact that it is difficult to measure accurately. For example, the saline bolus itself is reported to effect the measured variable, as well as bolus temperature (126). Other investigated variables possibly affecting parallel conductance are lung insufflation, and LV ventricular volume (127-130). Further, different studies propose that parallel conductance does or does not vary during the cardiac cycle, and slope factor alpha is reported to vary during a heart beat (131,132). The most recent study, though, implies that Gp does vary during the cardiac cycle, and that it must be corrected for (133).

There is definitely a need for more studies in this matter, at least to confirm the latest results (see Chapter 7).

3.b. Clinical Application

This method has gained a wide interest, with literary hundreds of articles published since the introduction.

Only one year after introducing the conductance technique in 1981, Baan et al. reported of use of this catheter in humans, for obtaining relative volumes (i.e. without calibration) (134). Two years later, they introduced all of the technique to measure true volume, including calibration methods to determine the gain factor (α) and the parallel conductance (G_p) (114).

Kass et al. were the first to report the use of the same technique in humans (135).

Currently, the conductance catheter is used mainly to assess global systolic and diastolic function to investigate pathologies, the outcome of drug treatment and surgical procedures, and the effects of ventricular pacing therapies (136-144).

Recently, new methods were introduced to estimate mechanical dyssynchrony, using the segmental volume signals obtained with the conductance catheter.

4. Quantification of Left Ventricular Dyssynchrony by Conductance Catheter

Conductance method has been used extensively to assess global systolic and diastolic ventricular function and more recently the ability of this instrument to pick-up multiple segmental volume signals has been used to quantify mechanical ventricular dyssynchrony (145, 146).

The use of conductance method may offer several technical advantages. After catheter placement, the signals are obtained continuously without operator interaction. Real-time display of dyssynchrony indexes is technically feasible and should enable immediate quantification of the effects of interventions, and, e.g., the effects of changes in pacemaker settings. The method is invasive, but positioning of the catheter in the LV largely eliminates problems with through-plane motion inherent in most imaging methods. Heart failure is often associated with substantial beat-to-beat hemodynamic variations due to changes in cycle length, cardiopulmonary interaction and conduction disturbances. Thus techniques (like magnetic resonance imaging) that require hemodynamic steady-state and beat averaging to increase signal-to-noise may filter out important components of dyssynchrony. Furthermore, the temporal resolution of the conductance signals (4 ms) is relatively high.

To quantify dyssynchrony, novel indexes based on volume signals acquired with the conductance catheter were introduced. The conductance catheter was validated previously (114), and the segmental signals reflect instantaneous volume slices perpendicular to the LV long axis as obtained by cine-computerized tomography (147).

Nonuniform LV performance was determined from the segmental LV conductance signals and characterized by the following indexes.

4.a. Classical Parameters in the Time-Domain

Mechanical dyssynchrony. At each time point, a segmental signal is defined as dyssynchronous if its change (i.e., dSV/dt) is opposite to the simultaneous change in the total LV volume (dTV/dt). Segmental dyssynchrony is quantified by calculating the percentage of time within the cardiac cycle that a segment is dyssynchronous.

Overall LV dyssynchrony (DYS) is calculated as the mean of the segmental dyssynchronies (140). DYS may be calculated within each specified time interval, i.e. during systole and diastole, with systole defined as the period between the moments of dP/d$t$max and dP/d$t$min (Figure 6).

Internal flow. Nonuniform contraction and filling is associated with ineffective shifting of blood volume within the LV. This internal flow (IF) is quantified by calculating the sum of the absolute volume changes of all segments and subtracting the absolute total volume change:

$$IF(t) = \left[\sum \left| dSVi(t)/dt \right| - \left| dTV(t)/dt \right| \right] / 2$$

Note that dTV(t)/dt represents the effective flow into or out of the LV. Thus IF measures the segment-to-segment blood volume shifts, which do not result in effective filling or ejection. Division by two takes into account that any non-effective segmental volume change is balanced by an equal but opposite

volume change in the remaining segments. IF fraction (IFF) is calculated by integrating IF(t) over the full cardiac cycle and dividing by the integrated absolute effective flow (145) (Figure 6).
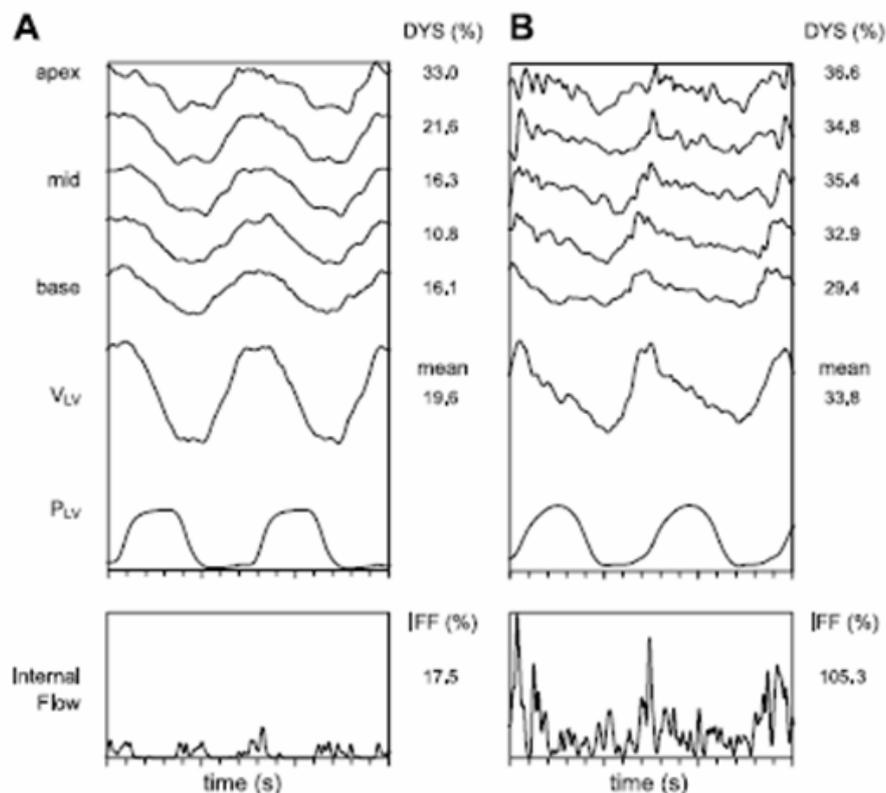
Figure 6. Panel a: Example of patient with low values of DYS and IFF both in systolic and diastolic phase. **Panel b:** Marked DYS and IFF are evident in all segmental signals: changes of segmental volumes (dVseg/dt) are opposite to the simultaneous change in the total LV volume (dVLV/dt).

Mechanical dispersion. In the HF patients, a substantial dispersion is present in the onset of contraction between the segments.

This dispersion is assessed by segmental lag times which are determined by calculating the cross correlations between TV(t) and SV(t) for all systolic time points (i.e., between dP/dtmax and dP/dtmin). For each segment the lag which produces the highest linear correlation is determined. Mechanical dispersion (DISP) is defined as 2 × standard deviation of the segmental lag times (145) (Figure 7).
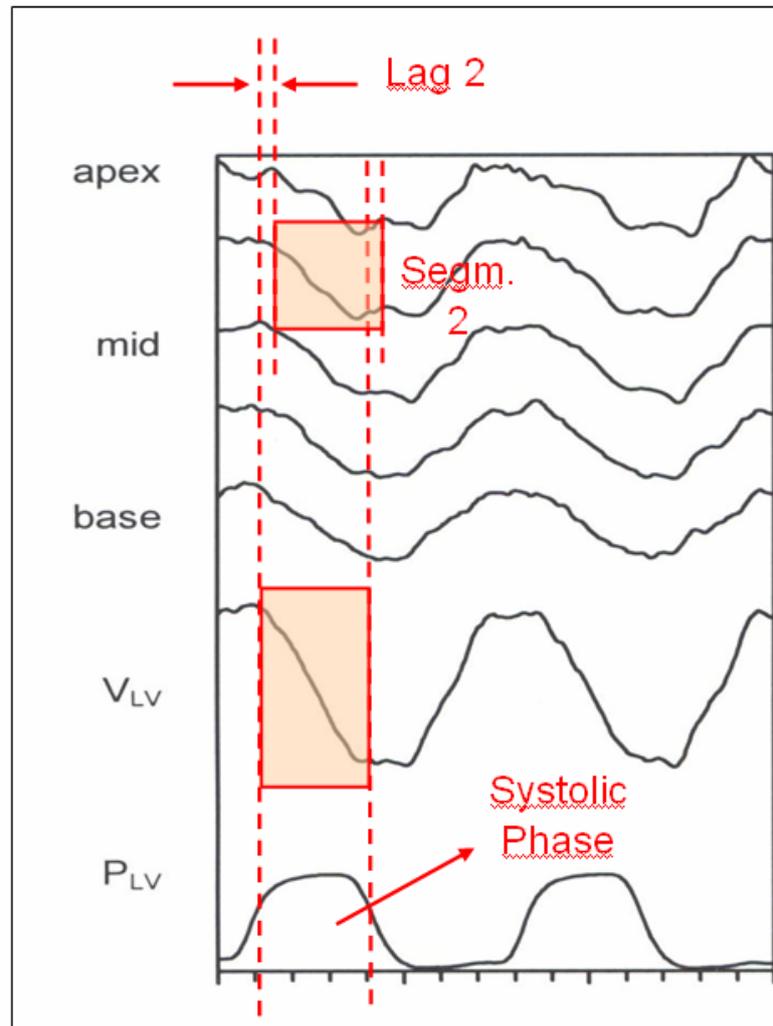
Figure 7. DISP is assessed by segmental lag times between Vlv(t) and Vi(t) for all systolic time points. DISP is defined as $2 \times$ standard deviation of the segmental lag times.

In HF patients, the conductance-derived dyssynchrony indexes were compared with the delay in timing of peak systolic velocity between the septal and lateral wall as obtained by tissue-Doppler echocardiography. Septal-to-lateral delay has recently been introduced as an index of mechanical dyssynchrony (81). A significant correlation was found for both DYS and IFF, but DISP did not reach a statistically significant correlation. Apparently, patients with a larger septal-to-lateral delay also show more segmental dyssynchrony, as reflected by DISP and IFF. The lack of correlation with DISP was unclear.

Discussion and Limitations
Determination of absolute LV volume from the conductance catheter requires careful calibration, however the dyssynchrony indexes can be calculated from the raw segmental conductance signals and do not require calibration. Correction for parallel conductance is not required because the calculations are based on volume changes, and correction for slope factor is not required because segmental volume changes are judged relative to the global LV

volume changes. The latter, however, implicitly assumes that the segmental slope factors are all the same (and thus equal to the slope factor for global volume). This assumption may be a concern because theoretical studies indicate that volume in the segments closest to the current electrodes may be relatively underestimated due to electric field inhomogeneity, especially in enlarged hearts (148-150).

However, recent analysis showed that the influence of a potential underestimation of the outer segments on the dyssynchrony indexes is relatively small (145).

Optimally, the conductance catheter is placed in a straight position from the aortic valve to the LV apex. The distance from the pigtail to the first measurement electrode is about 2 cm. Thus volume changes in the most apical part of the LV are not measured. If this region is highly dyssynchronous, as might be the case in patients with apical infarcts, underestimation of dyssynchrony may be expected.

Furthermore, the segmental conductance catheter signals do not provide an anatomic view but represent the total volume of slices perpendicular to the LV long axis. Thus, e.g., in CAD patients, abnormal regional wall motion might be obscured by compensatory wall motions within the same circumferential segment. The proposed dyssynchrony indexes therefore reflect intersegmental differences in contraction and filling and may underestimate phase changes obtained by comparing regional lateral and septal wall motions, e.g., using tissue Doppler imaging.

Finally, up to now normal subjects were not studied and thus normal ranges for the dyssynchrony indexes are not established yet.

Similarly the prognostic value of the dyssynchrony indexes was not investigated.

4.b. New Parameters in the Time-Domain Derived from Echocardiography

Recently, new parameters have been introduced to quantify LV dyssynchrony with echocardiographic techniques. These indices can be directly applied to conductance method:

Cycle Efficiency. Calculated as previously described (151) by the formula: CE=SW/[ΔLVP*ΔLV volume], with SW = stroke work, ΔLVP = end-systolic – end-diastolic LV pressure. This index quantifies distortions in the shape of the pressure-volume diagram. The calculation assumes that the optimal contraction would have CE value near 1.0, corresponding to a rectangular pressure volume diagram. Decreases in cycle efficiency may be caused by multiple factors including isovolumic volume shifts as well as changes in afterload and ventricular stiffness (Figure 8). Similarly, regional cycle efficiency can be calculated from the most basal to the most apical segmental volume signal plotted against LV pressure. Differences in regional cycle efficiency during isovolumic filling or emptying may indicate inefficient patterns contraction or relaxation due to dyssynchrony.
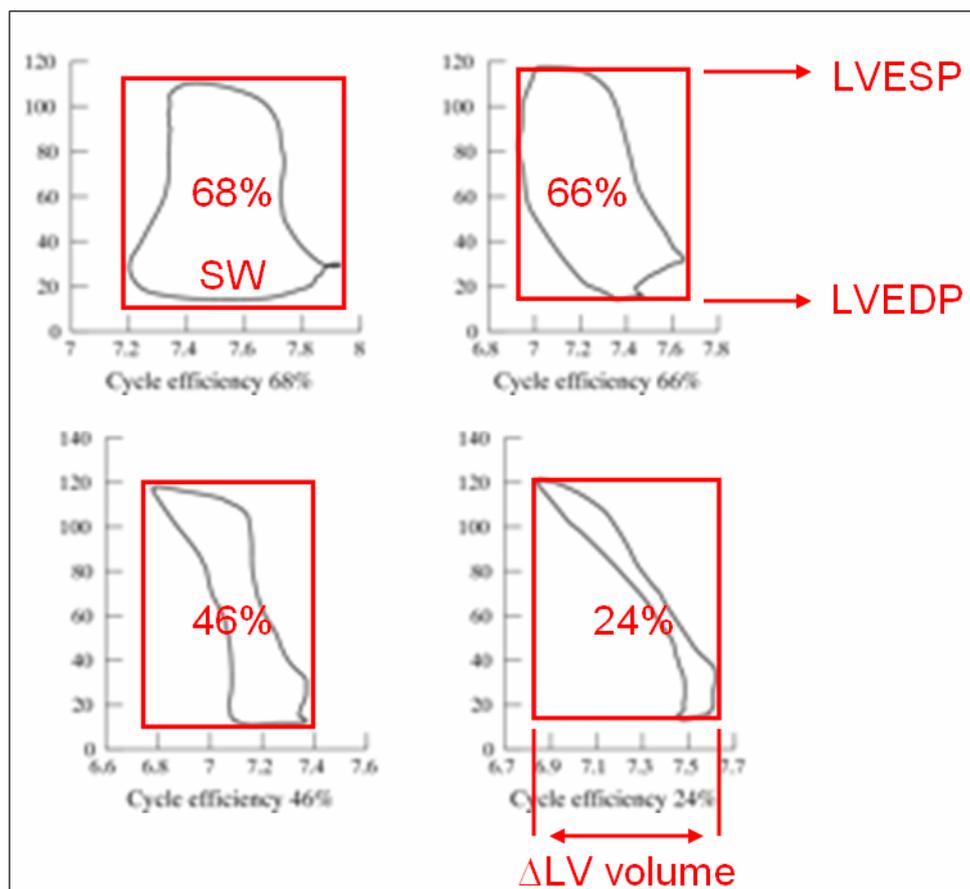

Figure 8. Four pressure-volume loops. In the upper panels mild incoordination is shown. In the lower panels incoordination is greater — note the increase in cavity size while the ventricular pressure generated is still relatively high, and the reduction of volume when the ventricular pressure is low.

Time exceeding aortic closure. In order to measure diastolic dyssynchrony and specifically to quantify LV contraction in diastolic phase, a new index was proposed, quantitatively reflecting the whole temporal amount spent by 12 LV segments in contracting after aortic valve closure (152).

Using strain imaging that reflects myocardial deformation, the time of strain tracing exceeding aortic valve closure (ExcT) was measured in each segment as the interval between the marker of aortic closure and the nadir of the strain tracing. ExcT was considered 0 when the nadir of strain curve did not exceed aortic valve closure. The overall time of strain exceeding aortic valve closure (oExcT) was computed as the sum of the 12 segmental ExcTs.

The index may be implemented in conductance method by considering each segment presenting a systolic phase (negative dSVi/dt) persisting during the phase of global diastole (positive dTV/dt). oExcT is estimated as the sum of these delays for all segments (Figure 9).
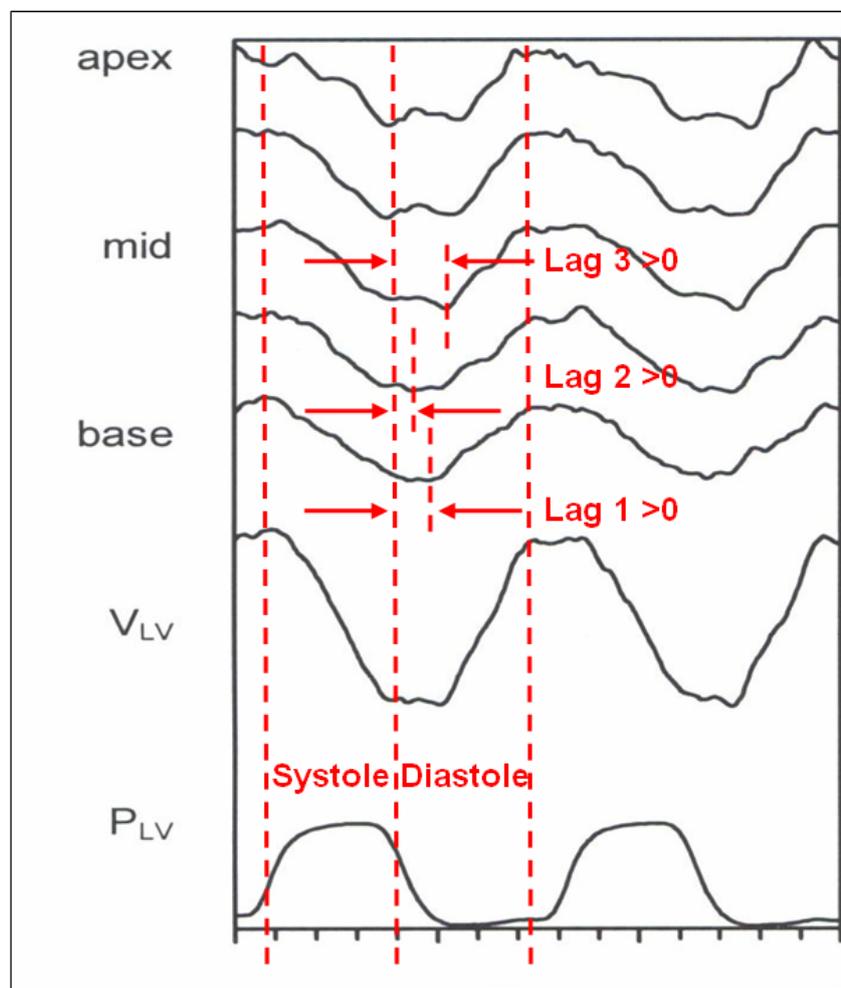
Figure 9. The segments 1, 2 and 3 present a systolic phase (negative dSVi/dt) persisting during the phase of global diastole. oExcT is estimated as the sum of the lags for these segments.

4.c. The Coherent Averaging

Following the original approach, each dyssynchrony index is extracted for each cardiac cycle and then averaged over consecutive beats.

Coherent averaging is used to recover the response to repetitively applied stimuli when that response is embedded in random noise (153,154). The coherent averaging method is based on the principle that each segment of the signal contains an invariant component x(t), plus a noise component n(t).
In coherent averaging, all x(t) are systematically added, whereas the random noise components are summed and tend toward zero, in the following hypotheses: n(t) is additive, uncorrelated with x(t), stationary and normally distributed with zero mean.

The presence of a noise component may influence the estimation of mechanical dyssynchrony performed over single cardiac cycles. In particular, noise components may alter the measure of repetitive mechanical inhomogenities. The impact of signal processing procedures such as coherent averaging on mechanical LV dyssynchrony estimation has never been evaluated.

The use of coherent averaging permits to investigate the characteristics of the volume signals and to introduce new improved indexes of ventricular dyssynchrony.

4.d. Parameters in the Time-Domain by Coherent Averaging

Instead of calculating the indexes from the original signals, the coherent averaging is performed to extract a template of cardiac cycle for each segmental volume signal (Figure 10), and for the total volume. In this work, three new indexes have been derived from the templates with the standard method:

- *Mechanical dyssynchrony of averaged signal* (DYSCoh),
- *Internal flow fraction of averaged signal* (IFFCoh),
- *Mechanical dispersion of averaged signal* (DISPCoh).

These indexes of dyssynchrony permit to quantify the repetitive component of the mechanical inhomogenities.

The procedure of coherent averaging permits to derive the residual signal, that is the difference between the segmental volume signal SVi and its estimated template. This signal represents the sum of all non-repetitive components of ventricular mechanics. The percentage power of this signal with respect to the total power of SVi (Res_i, i.e. segmental residual powers), permits to quantify the amount of non-repetitive components in the volume signal.

- *Segmental residual power* (Res1, Res2, Res3, Res4, Res5),
- *Total residual power* (ResTotAvg): the average of segmental values.

In addition, the total residual power has been estimated in 4 frequency bands (the bandwidth of the volume signals is 125Hz), thus deriving 4 new indexes:

- *from 0 to 1 Hz* (ResTotAvg0-1),
- *from 1 to 5 Hz* (ResTotAvg1-5),
- *from 5 to 20 Hz* (ResTotAvg5-20),
- *from 20 to 125 Hz* (ResTotAvg>20).
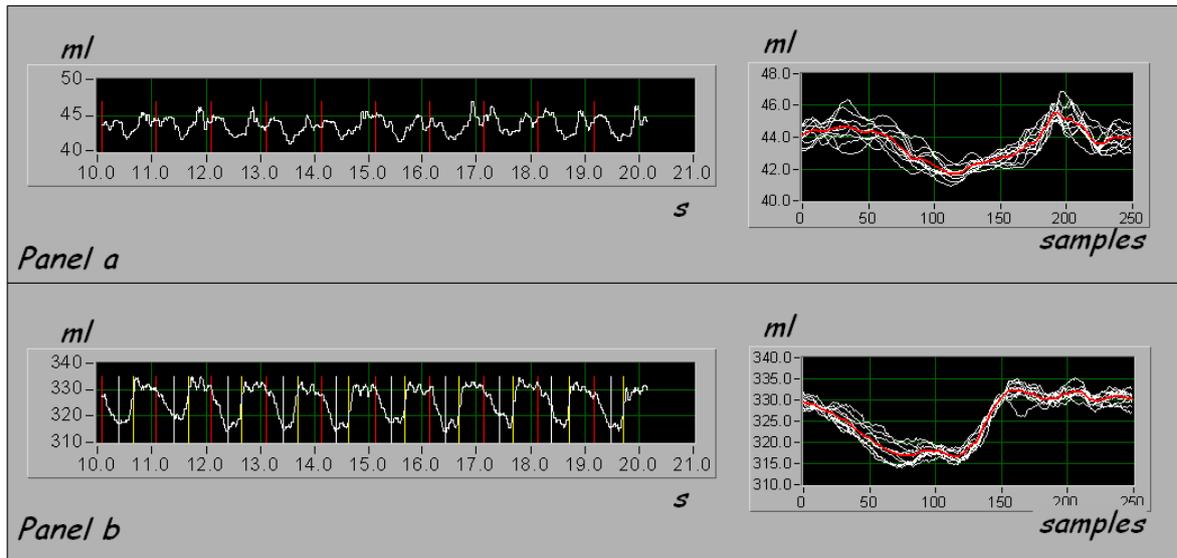
Figure 10. Segmental volume signal [Panel a] and total volume [Panel b]. The graphs on the right show the signal templates (red curves) obtained from several cardiac cycles using the coherent averaging.

4.e. Parameters in the Frequency Domain

The continually changing temporal or phase relationship between two time series may be quantified in the frequency domain by magnitude-squared coherence (155). Magnitude-squared coherence (C(f)) between two recordings is defined as

$$C(f) = \frac{\left|S_{xy}(f)\right|^2}{S_{xx}(f)S_{yy}(f)}$$

Where x(t) and y(t) are two simultaneous recordings, Sxy is the cross power spectrum between signals x and y, and Sxx and Syy are the individual power spectra for signals x and y, respectively. C(f) is a measure of the linear relation between signals as a function of frequency, f, and is a real quantity with value between zero and one. In other terms, C(f) measures the constancy of the time delay (phase) at a specific frequency between signals x and y. Two linearly related signals (in the absence of noise) will have an C(f) function equal to one at all frequencies present in both signals, while two

random, uncorrelated signals will have an C(f) equal to zero at all frequencies. Any linear operation (multiplication by a constant or addition of a constant) on one or both of the signals will not alter the C(f) between x and y. However, additive, uncorrelated noise and system nonlinearities will reduce C(f) for two similar signals.

C(f) may be estimated for sampled data using a method of overlapped and averaged FFT spectral estimates (156). Basically, estimates of Sxx, Syy and Sxy are determined using a periodogram technique, and their estimates are then used in the definition of C(f).

The C(f) functions between each segmental volume SVi and the TV have been estimated over the band 0-125 Hz. A Total Coherence function has been defined over the band 0-125 Hz by averaging the 5 C(f) functions. From the Total Coherence function, 5 new frequency domain indexes have been extracted:

- mean value of the Total Coherence over the band 0-125 Hz (CohTot)
- mean value of the Total Coherence from 0 to 1 Hz (Coh0-1),
- mean value of the Total Coherence from 1 to 5 Hz (Coh1-5),
- mean value of the Total Coherence from 5 to 20 Hz (Coh5-20),
- mean value of the Total Coherence from 20 to 125 Hz (Coh>20).

Section 2

5. Experimental Protocols

The Institutional Review Boards at the Careggi Hospital (Florence), the Detroit Medical Center (Detroit) and the Istituto Auxologico Ospedale S. Luca (Milan) approved the experimental design and all subjects provided written informed consent.

Patients with indications for electrophysiologic study or device implantation were included. Patients with a previously implanted device, valvular insufficiency or stenosis were excluded from participation.

5.a. Ventricular Pressure and Volume Measurements

LV pressure and volume were measured using a 7F, 12-electrode combination high fidelity micromanometer-conductance catheter (CD Leycom, Zoetermeer, The Netherlands) inserted through a femoral artery and advanced into the LV apex over an 0.025 flexible guide wire using fluoroscopic guidance. The catheter was connected to a cardiac function analyzer (CFL 512, CD Leycom) that automatically recorded (sample rate: 250 Hz, accuracy: 12 bit) and displayed pressure and up to 7 segmental volumes delineated by the electrodes.

The signal analysis was performed off-line with a custom-made software.

The pigtail of the conductance catheter was accurately positioned in the apex, and the interelectrode spacing was adjusted to the long heart axis. Segmental volumes originating from the proximal ascending aorta were discarded.

5.b. Pacing Protocol

Temporary pacing electrodes were positioned in the right ventricular apex, right ventricular outflow tract free wall and septum, and LV free wall.

Experimental interventions were performed after electrophysiologic study and before device implant. Constant atrial overdrive pacing (AAI) was maintained throughout the protocol at a rate of 10 bpm greater than the sinus rate. Baseline data were recorded during AAI pacing. Each patient was randomly assigned to receive dual chamber pacing from the sites to test using a Latin square design. AV delay was programmed to the measured p to His interval minus 10 ms in order to limit the potential effects of atrial contraction and partial intrinsic conduction through the AV node. Data were collected under steady-state hemodynamic conditions after a minimum of 2 minutes of stabilization at each pacing configuration. The transitions from atrial pacing to dual chamber pacing and back to atrial pacing were recorded continuously.

5.c. Data Analysis

When required by the specific experimental protocol, hemodynamic status was evaluated using multiple parameters. Indices of LV pressure, volume, and function were calculated and averaged over 8 to 10 beats at end expiration from the raw LV pressure and conductance volume data including LV systolic (LVSP) and end-diastolic (LVEDP) pressure, +dP/dtMAX and −dP/dtMIN, LV end-systolic (LVESV) and end-diastolic volume (LVEDV), LV stroke volume (SV) defined as the difference between conductance volumes

at the times of +dP/dtMAX and –dP/dtMIN, stroke work (SW) calculated as the area of the pressure-volume diagram, cardiac output (CO), ejection fraction (EF), and the time constant of isovolumic relaxation (τ). End-diastole was identified immediately before the isovolumic increase in LV dP/dt and end-systole was defined as the maximum ratio of LV pressure to volume.

7.d. Off-Line Signal Analysis System

The system for off-line data analysis was developed in LabVIEW 5.1 (National Instrument, Houston, TX, USA). (Figure 11)
The acquired signals are shown and the user is allowed to select the cardiac cycles to analyze and the segmental volume signals to consider in the estimation of the total volume curve. Specific cardiac cycles can be indicated and removed from the analysis to exclude ectopic beats.
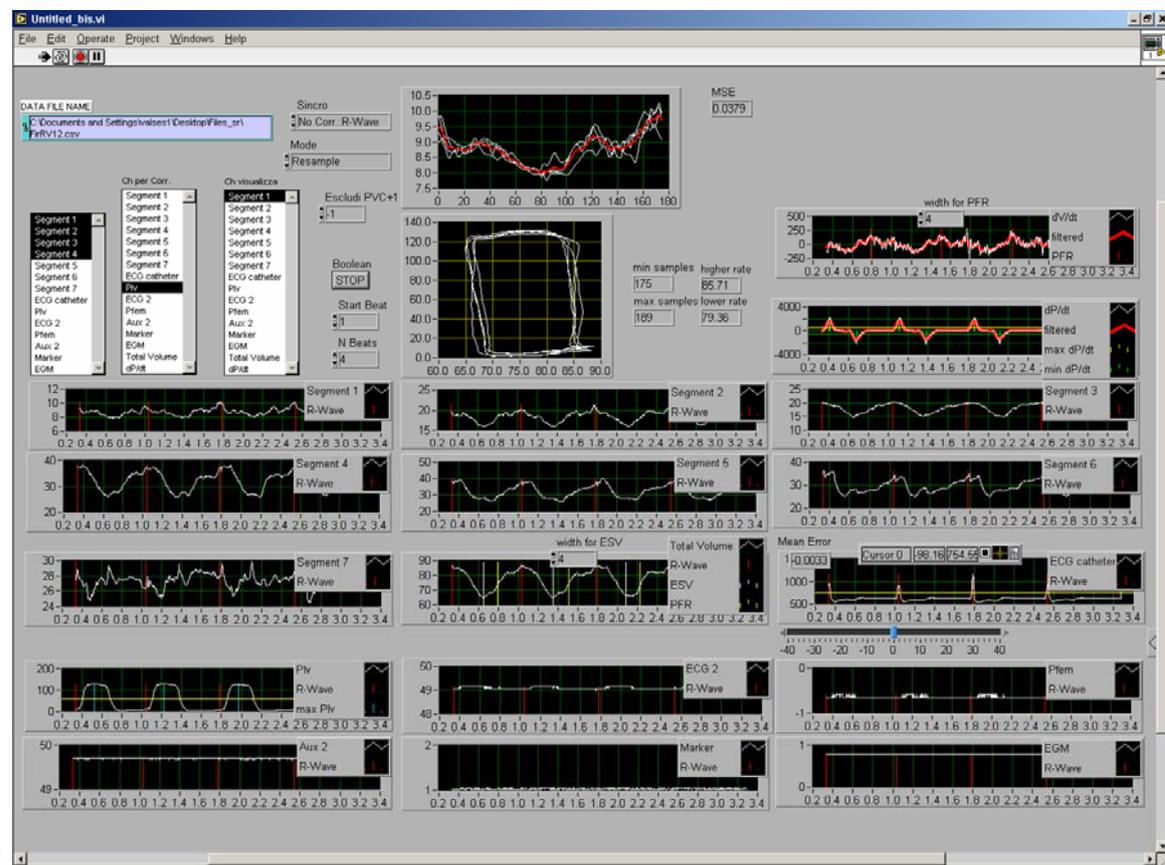
Figure 11. Panel of the analysis system. It includes the indicators representing the acquired signals, the controls to select the cardiac cycles to analyze and the signals to include in the total volume estimation.

Moreover, the system permits to show the signal on the pressure-volume plane and to extract all relevant hemodynamic indexes.
The dP/dt signal is calculated from the ventricular pressure signal. The noise in the original signal is amplified when the derivative is taken: digital low-pass filtering was used to remove the noise. A digital low-pass filter model was implemented using the cascaded form of infinite impulse response (IIR) filtering technique (Butterworth filter of order four and a cut-off frequency of 10

Hz). The Butterworth filter model was used because of its smooth response at passband frequencies.

The time shift caused by the digital filtering was cancelled out by the following equalization technique. The discrete filtered signal (dP/dt) is first reversed before being filtered again using the same filter. The resultant signal is reversed to give a filtered dP/dt which is free of time lag. (Figure 12 Panel i – filtered segnal: red curve)

Similarly, the dVol/dt signal is obtained from the ventricular volume signal. (Figure 12 Panel g – filtered signal: red curve)

Timing points

The system estimates the end diastolic point from the intra-cardiac electrogram (maximum of R-wave, identified with parabolic interpolation of the signal in order to minimize the jitter error). (Figure 12 Panel a – red markers)

The maximum and minimum of dP/dt signal are identified to define the start and the end systole. (Figure 12 Panel i – white markers)

The minimum of volume signal during systolic phase is extracted. (Figure 12 Panel f – white markers).

The point of peak filling rate is identified by the maximum of dVol/dt signal and distinguishes the early and late-diastolic phases. (Figure 12 Panel g – red markers)

Indexes of dyssynchrony

According to the methods described before, the system permits the estimation of following dyssynchrony indexes:

- *Mechanical dyssynchrony* (DYS),
- *Internal flow fraction* (IFF),
- *Mechanical dispersion* (DISP),
- *Cycle Efficiency* (CE),
- *Time exceeding aortic closure* (oExcT),
- *Mechanical dyssynchrony of averaged signal* (DYSCoh),
- *Internal flow fraction of averaged signal* (IFFCoh),
- *Mechanical dispersion of averaged signal* (DISPCoh),
- *Segmental residual power* (Res1, Res2, Res3, Res4, Res5),
- *Total residual power* (ResTotAvg),
    - *from 0 to 1 Hz* (ResTotAvg0-1),
    - *from 1 to 5 Hz* (ResTotAvg1-5),
    - *from 5 to 20 Hz* (ResTotAvg5-20),
    - *from 20 to 125 Hz* (ResTotAvg>20),
- *Total Coherence* (CohTot),
    - *from 0 to 1 Hz* (Coh0-1),
    - *from 1 to 5 Hz* (Coh1-5),
    - *from 5 to 20 Hz* (Coh5-20),
    - *from 20 to 125 Hz* (Coh>20).
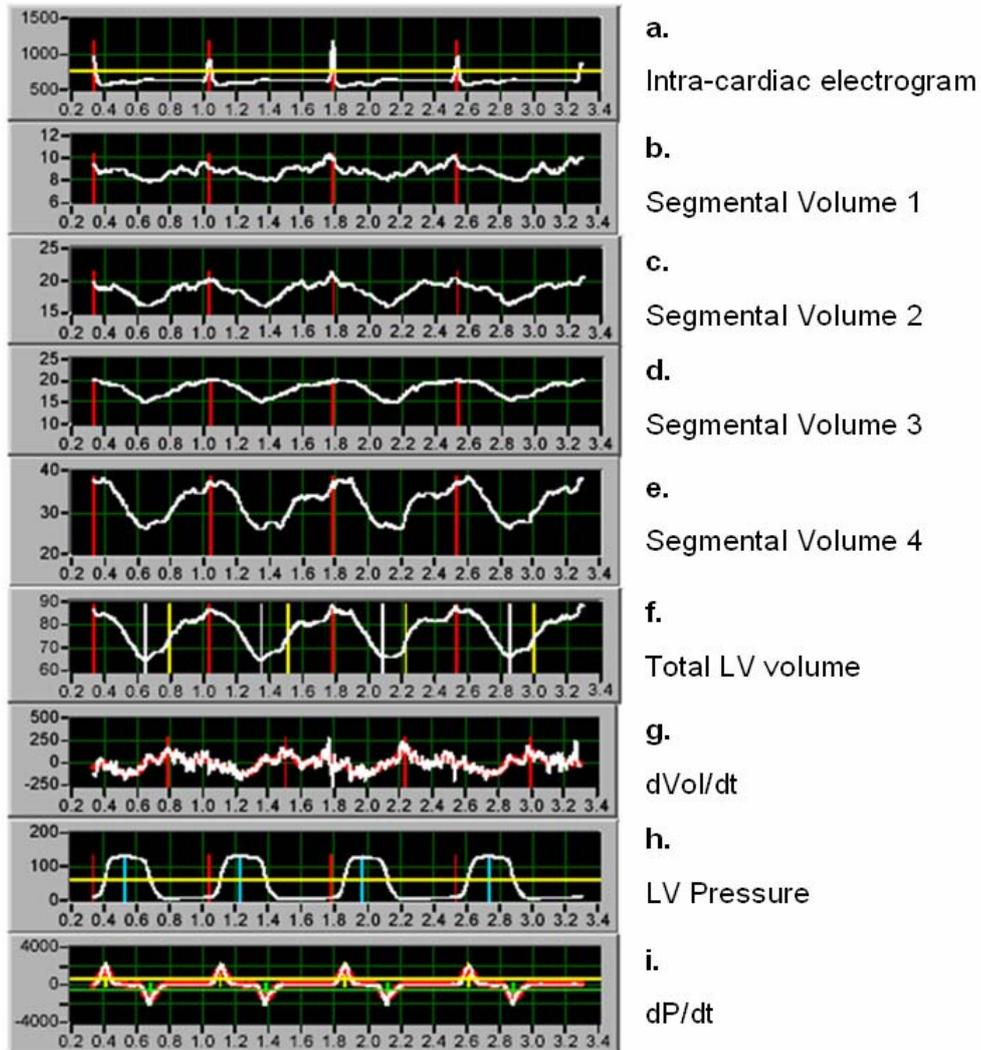
Figure 12. Acquired and estimated signals with the calculated timing points.

Coherent averaging and alignment algorithms
In order to implement the coherent averaging, the system permits to apply 3 algorithms for alignment of the cardiac cycles:
Use of single fiducial point:
1. Maximum of ECG R-wave,
2. Zero of first derivative of LV pressure signal (157),
Maximization of cross correlation function of:
3. Consecutive beats signals,
4. Systolic phase of consecutive beats signals (from the point of max dP/dt to min dP/dt).

6. Experimental Results

6.a. Optimal Algorithm to Implement Coherent Averaging of the Ventricular Volume Signals

Introduction

Four alignment algorithms have been considered to perform coherent averaging for total and segmental volume template extraction.
Aim of this analysis was to identify the optimal algorithm of cardiac cycle alignment.

Methods

Patients with indications for electrophysiologic study or device implantation were studied. Subjects with a previously implanted device, valvular insufficiency or stenosis were excluded from analysis. For a detailed description of methods see Chapter 5. For this analysis we considered the conductance catheter recordings collected with the patient in sinus rhythm in the absence of ventricular pacing.

Data Analysis
Sequences of 20 consecutive cardiac cycles were considered, all ectopic beats were excluded from the analysis. The analysis was performed on the total volume signal, estimated as the sum of 4 segmental volumes.
We identified the method resulting in the minimum mean square error (MSE) between the original signal and the resulting template.
Statistical analysis was performed with paired Student's t-test for comparisons between MSE values. Statistical significance was assumed at $p < 0.05$. Results are presented as mean±SD.

Results

A total of 12 patients were studied (7 males, 67±14 years, 71±11Kg, 171±8cm).
The MSE associated to the alignment algorithms under test (All.1: Max R-wave; All.2: dP/dt=0; All.3: Max correlation function; All.4: Max correlation function of systolic phase signals) is reported in Table 2 for each subject.

Table 2. MSE associated to the four alignment algorithms.

Patient	MSE All.1 [ml^2]	MSE All.2 [ml^2]	MSE All.3 [ml^2]	MSE All.4 [ml^2]
1	2.003	10.576	2.099	2.055
2	2.496	4.660	2.785	2.617
3	0.554	5.453	1.293	0.586
4	2.221	1.931	3.086	2.375
5	0.978	4.460	1.167	1.012
6	2.198	4.560	7.519	2.364
7	0.716	0.766	0.874	0.767
8	0.932	0.984	1.248	1.082
9	3.214	9.552	8.083	3.22
10	1.409	10.331	1.925	1.501
11	0.839	0.818	0.98	0.918
12	0.587	0.632	1.093	0.642
mean	1.512	4.560	2.679	1.595
stddev	0.883	3.799	2.498	0.893
p-value Vs.All.1		0.01	0.05	0.00

Conclusions

In our population, the alignment method using R-wave identification resulted in the best performance.

6.b. Indexes for the Quantification of Left Ventricular Mechanical Dyssynchrony by Conductance Catheter

Introduction

Analysis 1
Background noise could affect the estimation of mechanical dyssynchrony when performed on each cardiac cycle. Random noise components could alter the estimation of dyssynchrony due only to recurrent mechanical LV nonuniformities. The impact of signal processing procedures such as coherent averaging and signal alignment on mechanical LV dyssynchrony estimation has never been evaluated.

We characterized conductance-volume singals with an analysis in frequency domain and using coherent averaging.

We evaluated new methods for LV dyssynchrony estimation, using coherent averaging with alignment algorithm before averaging. Moreover, new improved indexes were introduced to quantify non-recurrent components of volume signals.

To test our approach we compared data from congestive heart failure (HF) patients with left bundle branch block (LBBB) with those from patients with preserved LV function.

Analysis 2
CRT was demonstrated to mitigate the mechanical and energetic consequences of intraventricular dyssynchrony in HF patients with LBBB.

Moreover, in patients with preserved LV function dyssynchrony can be induced by right ventricular apical pacing and evidence suggests that this can itself lead to LV systolic failure.

We studied the acute effects of CRT in patients with HF and the effects of right ventricular apical pacing in healthy subjects. Moreover, we assessed the ability of the indexes of mechanical dyssynchrony to describe the changes in LV activation induced by different pacing modalities.

Methods

Sequences of 30 s, i.e. 40-50 consecutive non-arrhythmic cardiac cycles at fixed heart rate induced by atrial pacing (at 10 bpm above the sinus rate) and steady-state conditions were selected for off-line analysis using custom-designed software.

The system for coherent averaging estimation uses an algorithm for cadiac cycles alignment based on single fiducial point, i.e. maximum of R-wave, that demonstrated to minimize the mean square error with respect other methods.

For the spectral analysis, the periodogram of the signals was estimated.

To reduce spectral leakage a Hamming window was applied after removal of the mean value. The length of segments was 1000 samples and a segment-overlap of 30% was used.

As reported in Chapter 4.e., the spectral coherence was estimated as the mean value of the coherence function between each segmental volume and the total volume over the band considered. The values obtained for all segments were averaged to obtain the total value.

Analysis 1

For this analysis, we used the recordings obtained during atrial pacing and spontaneous ventricular activation. The spectral characteristics were extracted and compared between the two groups of patients. The classical indexes in the time-domain were compared with the ones obtained with coherent averaging. Finally, a head-to-head comparison of all indexes was performed to estimate the ability to discriminate the patient groups.

Analysis 2

In this analysis the recordings obtained during atrial pacing and during ventricular pacing (CRT and right ventricular apical pacing) were considered. Intra-patient comparisons were performed between pacing modes.

The data analysis is described in Chapter 5.. In particular, the hemodynamic variables analyzed were: LV systolic and end-diastolic pressure, positive (dP/dt) and negative (n dP/dt) maximum of first derivative pressure, LV end-systolic and end-diastolic volume, stroke volume (SV), stroke work (SW), cardiac output (CO), and the time constant of isovolumic relaxation (Tau).

Classical and new indexes of dyssynchrony were estimated and compared between pacing modes.

Regression analysis was performed to identify variables associated to the changes of LV function.

Statistical Analysis

All data are presented as means±SD.

Differences between distributions were compared by a t-test for Gaussian variables, and by Mann-Whitney nonparametric test for nongaussian variables. Statistical correlations between variables were tested by least-squares linear regression. A P value < 0.01 was considered significant. We performed receiver-operating characteristic (ROC) curve analysis to test the diagnostic performance of the indexes to discriminate the patient groups. Sensitivities and specificities at the optimal cut-off point were determined.

Results

The study population consisted of 27 consecutive patients.
- 15 HF patients with left bundle branch block (HF Group):

11 males, 68±6 years, 7 with ischemic etiology, NYHA class 3.1±0.5, ejection fraction 26±6%, QRS duration 167±24 ms.

- 12 patients with preserved LV function (no-HF Group):

7 males, 67±14 years, ejection fraction 57±9%, QRS duration 88±21 ms.

Analysis 1

Characterization of conductance-volume signals
The frequency analysis, performed to extract dyssynchrony indexes, permitted to characterize conductance-volume SVi and TV singals.
Some characteristics of the power spectrum of TV signal are reported in Table 3 (similar results were obtained for SVi signals, but were not reported): power and frequency peaks in different bands.
The majority of the signal power is in the band from 1 to 5 Hz (programmed heart rate during acquisition from 70 to 100 bpm). The components above 20Hz are associated to less than 1% of the total signal power. The frequency peak in the 0 – 1 Hz band matches with the respiratory rate and the power in this band seems higher in HF group.

Table 3. Characteristics of the power spectrum of TV signal.

	no-HF	**HF**	**p-values**
Power 0-1Hz, %	4.34±6.26	9.12±12.00	0.071
Peak 0-1Hz, Hz	0.41±0.17	0.45±0.12	
Power 1-5Hz, %	93.24±6.45	88.44±11.85	0.194
Peak 1-5Hz, Hz	1.52±0.20	1.44±0.13	
Power 5-20Hz, %	2.16±1.84	2.21±1.34	0.946
Peak 5-20Hz, Hz	8.37±0.88	7.63±0.80	
Power >20Hz, %	0.25±0.25	0.23±0.15	0.814
Peak >20Hz, Hz	37.59±5.12	44.14±7.59	

Parameters in the time domain and the coherent averaging
DYSCoh resulted significantly lower than DYS in HF patients (25.8±4.8% Vs. 32.6±3.9%, p=0.000) and in no-HF patients (19.6±9.3% Vs. 26.0±7.2%, p=0.000). Both indexes were significantly higher in HF group (even if non-significantly for DYSCoh).
Similar results were obtained for IFF: IFF was higher than IFFCoh (estimated on the template) (25.8±18.8% Vs. 17.3±18.7% in no-HF group and 40.8±13.6% Vs. 20.8±11.1% in HF group, both p=0.000). Also in this case, IFF and IFFCoh were higher for HF group (significance level reached only for IFF).
No differences resulted between DISP and DISPCoh in no.HF patients (23.4±16.4ms Vs. 23.2±16.9ms, p=0.870).While, DISPCoh was significantly higher than DISP in HF patients (48.3±19.8ms vs. 35.6±13.2ms, p=0.006).
Differences were not observed in DISP values between no-HF and HF. However, DISPCoh was higher for HF patients.

Performance of parameters under test
Table 4 summarizes the results of the comparison between groups for all indexes considered in the analysis, represented as mean ± standard deviation.
Overall, 7 parameters permitted to discriminate the two groups (p<0.01): DISPCoh, Coh1-5, Coh5-20, ResTotAvg, Res2, ResTotAvg1-5, CE.

Table 5 shows the results of the ROC curve analysis. Optimal cut-off with sensitivity and specificity values are reported for the 7 variables obtained from previous comparison. In Figure 13 the ROC curves are shown.

Table 4. Indexes of mechanical dyssynchrony in no-HF and HF groups.

	no-HF	HF	p-values	Test
DYS, %	26.0±7.2	32.6±3.9	0.012	t-test
DYSCoh, %	19.6±9.3	25.8±4.8	0.054	t-test
IFF, %	25.8±18.8	40.8±13.6	0.033	t-test
IFFCoh, %	17.3±18.7	20.8±11.1	0.139	Mann-Whitney
DISP, ms	23.4±16.4	35.6±13.2	0.068	t-test
DISPCoh, ms	23.2±16.9	48.3±19.8	0.003*	t-test
CohTot	0.44±0.07	0.37±0.10	0.016	Mann-Whitney
Coh0-1	0.63±0.19	0.51±0.18	0.099	t-test
Coh1-5	0.69±0.10	0.57±0.10	0.004*	t-test
Coh5-20	0.47±0.07	0.32±0.04	0.000*	t-test
Coh>20	0.43±0.08	0.37±0.12	0.041	Mann-Whitney
ResTotAvg, %	11.1±9.9	25.7±13.1	0.006*	Mann-Whitney
Res1, %	17.5±19.1	34.1±21.7	0.028	Mann-Whitney
Res2, %	9.8±8.5	28.9±19.9	0.004*	t-test
Res3, %	7.2±6.6	20.7±20.2	0.019	Mann-Whitney
Res4, %	10.1±10.7	23.3±12.7	0.021	Mann-Whitney
Res5, %	17.3±17.2	21.5±12.6	0.213	Mann-Whitney
ResTotAvg0-1, %	80.1±39.0	64.9±36.0	0.323	Mann-Whitney
ResTotAvg1-5, %	6.4±8.4	16.6±9.3	0.005*	Mann-Whitney
ResTotAvg5-20, %	45.2±17.8	59.5±21.4	0.070	t-test
ResTotAvg>20, %	78.0±26.0	89.9±18.3	0.252	Mann-Whitney
CE	0.78±0.12	0.58±0.16	0.000*	Mann-Whitney
oExcT, ms	6.9±8.8	15.7±10.5	0.016	Mann-Whitney

* p<0.01

Table 5. ROC curve analysis of the tested variables.

	Area Under Curve (95% CI)	p-value	Cut-off	Sensitivity	Specificity
DISPCoh, ms	0.83 (0.66-1.00)	0.007	41.71	0.64	0.90
Coh1-5	0.81 (0.65-0.98)	0.006	0.57	0.67	0.92
Coh5-20	0.98 (0.94-1.02)	0.000	0.40	1.00	0.92
Res2, %	0.82 (0.65-0.99)	0.006	24.26	0.64	1.00
ResTotAvg, %	0.81 (0.64-0.98)	0.007	19.69	0.71	0.83
ResTotAvg1-5, %	0.81 (0.63-0.99)	0.006	10.25	0.80	0.83
CE	0.88 (0.75-1.00)	0.001	0.70	0.80	0.83
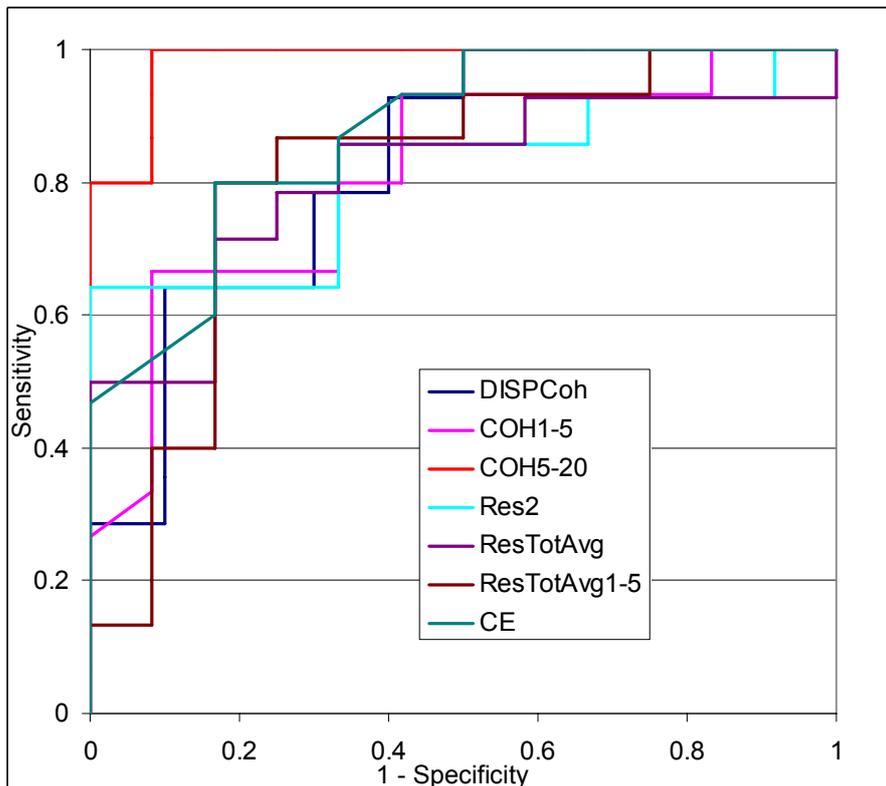
Figure 13. The ROC curve analysis demonstrated a sensitivity of 100% and a specificity of 92% for Coh5-20, with a cut-off = 0.40.

Analysis 2

The results of the analysis are reported in Table 6. Among subjects of HF group, the biventricular pacing resulted in a marked improvement of cardiac function (significant increase of maximum dP/dt and a trend toward an increase of cardiac output, stroke volume and stroke work as well as a reduction in end-systolic volume) associated to a significant reduction of dyssynchrony, as evidenced by IFF, CE, CohTot, Coh>20, and a trend for DISPCoh, oExcT, Coh5-20, ResTotAvg, ResTotAvg1-5, ResTotAvg>20.

Among subjects of the no-HF group, the right ventricular pacing impaired cardiac function, as shown by an increase of Tau and a trend to a reduction of maximum dP/dt, demonstrating a compromised diastolic and systolic function. In this case, indexes of dyssynchrony did not present significant differences.

In the overall population, we observed a significant correlation between changes in stroke volume and following indexes: IFF (r=-0.68, p=0.000), CE (r=0.85, p=0.000), CohTot (r=0.51, p=0.017), Coh>20 (r=0.53, p=0.004).

Table 6. Acute effects of CRT in the HF group and right ventricular pacing in no-HF group.

	HF		no-HF	
	Baseline	**CRT**	**Baseline**	**Right V. Pacing**
CO, l/min	2.4±1.1	4.2±3.6*	4.2±1.4	3.9±1.7
EDVolume, ml	246.6±69.3	232.0±63.0	137.9±39.1	135.2±38.8
ESVolume, ml	215.8±65.6	198.9±81.3*	102.9±38.6	104.1±39.1
EDPressure, mmHg	16.1±8.6	14.6±8.0	10.0±5.4	11.2±2.2
ESPressure, mmHg	102.9±19.7	103.8±17.5	128.3±16.7	123.3±22.9
dP/dt, mmHg/s	750.0±169.6	813.3±153.0**	1659.1±319.1	1559.7±283.6*
n dP/dt, mmHg/s	-765.0±134.3	-788.9±113.9	-1782.3±437.6	-1628.8±489.7
Tau, ms	43.8±9.6	42.7±9.0	33.7±5.6	37.5±6.7**
SV, ml	22.5±16.6	35.9±38.0*	38.3±28.7	33.5±26.0
SW, l*mmHg	2.0±1.6	3.3±3.5*	4.4±3.2	3.7±2.6
DYS, %	28.4±5.5	27.5±4.6	24.5±9.4	25.1±8.2
IFF, %	38.4±15.1	31.1±12.9**	29.8±19.1	29.7±17.8
DISPCoh, ms	55.7±25.4	44.5±28.3*	39.4±28.8	40.4±27.2
CE	0.5±0.2	0.7±0.2**	0.8±0.1	0.8±0.2
oExcT, ms	14.4±11.8	9.0±9.0*	6.9±8.8	5.4±6.3
CohTot	0.40±0.12	0.52±0.12**	0.41±0.05	0.45±0.10
Coh0-1	0.53±0.17	0.50±0.17	0.60±0.14	2.77±6.13
Coh1-5	0.58±0.11	0.57±0.11	0.65±0.10	0.65±0.06
Coh5-20	0.36±0.12	0.38±0.12*	0.45±0.06	0.44±0.07
Coh>20	0.40±0.13	0.53±0.13**	0.40±0.06	0.44±0.11
ResTotAvg, %	30.9±18.8	28.9±16.7*	14.9±10.3	20.1±15.9
Res1, %	40.0±24.7	40.1±22.3	23.9±20.8	28.1±16.8
Res2, %	30.7±21.0	27.2±17.4	13.5±8.1	16.1±13.3
Res3, %	27.6±25.8	24.2±19.5	9.0±7.6	12.7±15.0
Res4, %	29.6±20.3	25.2±17.1	10.7±11.3	20.1±23.9
Res5, %	25.0±16.7	26.6±19.2	17.3±17.2	23.4±23.0
ResTotAvg0-1, %	81.6±57.0	106.1±62.7	90.9±35.5	125.8±36.4
ResTotAvg1-5, %	21.3±15.9	18.0±13.1*	9.0±9.3	10.0±8.0
ResTotAvg5-20, %	62.9±20.1	58.6±21.0	45.3±20.1	36.2±16.6
ResTotAvg>20, %	95.7±19.4	79.7±26.9*	75.4±28.6	191.1±427.4

p-values: * < 0.05; ** <0.01

Discussion and Conclusions

Dyssynchrony plays a regulating role already in normal physiology (23) but is especially important in pathological conditions, such as hypertrophy (24), ischemia (25), infarction (26), or heart failure (27). Quantification of nonuniform mechanical function and dyssynchrony may lead to a more complete diagnosis of ventricular dysfunction (140,142). Moreover, it may guide therapy, because patients with extensive dyssynchrony are likely to benefit from resynchronization therapy (158).
Currently, cardiac resynchronization by biventricular pacing is emerging as an important therapy for heart failure (158,159). Recently, magnetic resonance imaging (27,109) and echocardiography (66,76,77,80,85) have been used to visualize mechanical dyssynchrony, further emphasizing the important role of mechanical dyssynchrony in cardiac dysfunction. However, these methods are laborious and require substantial operator interaction and expertise.

Recently, novel indexes were introduce to quantify dyssynchrony based on volume signals acquired with the conductance catheter during cardiac catheterization.

Quantification of nonuniform mechanical function and dyssynchrony may lead to a more complete diagnosis of ventricular dysfunction (140,142). Moreover, it may guide therapy, because patients with extensive dyssynchrony are likely to benefit from resynchronization therapy (158).

Analysis 1

To test the performance of the indexes we compared data obtained in the same conditions, from HF patients with left bundle branch block undergoing CRT implantation and from patients with preserved LV function. To the best of our knowledge, this is the first time that indexes of mechanical dyssynchrony based on volume signals acquired with the conductance catheter are studied in a population of normal patients. In fact, previous work used as control group a population with coronary artery disease and relatively preserved LV function before undergoing coronary artery bypass grafting (145). However, in such a kind of population the presence of dyssynchrony can not be excluded, due to akinetic ischemic areas. Moreover, in that study the two groups were studied in different conditions: the HF group in the catheterization laboratory, while the control group in the operating room during anesthesia and after sternotomy.

Similarly, for the first time coherent averaging technique is applied either to extract new indexes to quantify ventricular dyssynchrony and to characterize the signals obtained with conductance catheter, differentiating repetitive and non-recurrent components. In fact, volumetry by conductance catheter permits to acquire, with high temporal resolution, real-time signals. This may allow to overcome the limitations of techniques like MRI or echocardiography that require beat averaging to derive indexes of dyssynchrony, masking all possible components associated with beat-to-beat hemodynamic variations.

Present analysis permitted to describe some characteristics of the conductance-volume signals. The frequency analysis evidenced the absence of relevant components above 20 Hz: this result corroborate the validation of segmental signals acquisition obtained by comparison with cine-computerized tomography (147), whose sampling rate has approximately the same value.

The amplitude of the components in the range 0-1 Hz, attributable to the respiratory artifact, resulted markedly higher in HF patients, this may be due to the higher (mechanical) cardio-pulmonary interaction or to an altered vasovagal activity.

When extracting indexes to quantify synchronism between signals, random, spurious or non-synchronous components of the signals may play an important role. We hereby investigated how the coherent averaging procedure may affect or refine the conductance based indexes proposed by Steendijk et al. (145); in addition, we proposed a new set of indexes which quantify the non-periodic components of the volume signals different from the white acquisition noise.

The implementation of coherent averaging unmasked the presence of considerable beat-to-beat variations in dyssynchrony that seem more frequent in patients with LV dysfunction and seem to play a role in discriminating

patients. These non-recurrent mechanical LV non-uniformities are probably the expression of the substantial beat-to-beat hemodynamic variations, often associated with HF and due to cardiopulmonary interaction and conduction disturbances

This result is confirmed by the findings obtained by the new indexes based on residual percentage power that quantify the contribution of non-periodic components of the volume signals. In fact, ResTotAvg, Res2 and ResTotAvg1-5 resulted higher in HF group.

When estimated on SV and TV templates, DYSCoh and IFFCoh resulted to be significantly lower than their counterparts estimated on each cardiac cycle; also, sensitivity and specificity associated to these new indexes were lower. These results suggest that the non-periodic components of the volume signals determine the random left ventricle activations reflecting cardiac dyssynchrony.

The estimation of the mechanical dispersion (DISP) is instead improved by the coherent averaging: when estimated on SV and TV templates DISPCoh resulted significantly higher than when estimated for each cardiac cycle in HF patients. Coherent averaging optimizes the estimation of time delays when it is corrupted by spurious components.

In the no-HF patients no significant differences have been found between DISP and DISPCoh because when the volume signals are less corrupted by non-periodic components, time lag estimations by cross-correlation are less affected by coherent averaging.

This result may contribute to explain the lack of correlation noticed between DISP and the delay in timing of peak systolic velocity between the septal and lateral wall as obtained by tissue-Doppler echocardiography (16). Indeed, the extraction of that index from tissue-Doppler images requires the estimation of the average peak systolic velocity time over consecutive beats, a procedure equivalent to the coherent averaging method.

Among new indexes in the frequency domain, Coh1-5 and especially Coh5-20 demonstrated high values of sensitivity and specificity in discriminating groups.

Among the indexes in the time-domain derived from echocardiography, CE demonstrated best performance in discriminating groups. In fact, this parameter is mainly affected by volume shifts during isovolumic phases that, as known from echo-TDI studies, characterize patients with heart failure and intra-ventricular conduction disorders. Moreover, this index offers the advantage to quantify regional efficiency, when estimated from segmental signals. However, the oExcT index, even if different between groups, did not emerge among the best parameters, probably because it quantifies only the diastolic component of the mechanical dyssynchrony.

Analysis 2

For the first time a complete set of conductance catheter based indexes of dyssynchrony were used to describe the acute effects of of the CRT and the right ventricular pacing.

The results of this analysis are in agreement with the literature, describing a marked improvement of the cardiac function following CRT, in patients with ventricular dysfunction.

Among the indexes considered in this analysis, the ones that demonstrated higher sensitivity to the effects of CRT were IFF, CE, CohTot, Coh>20. This demonstrates that they are able to detect the reduction of internal ineffective flows, the inhomogeneity during isovolumic contraction and relaxation as well as the recovered coherence among segments that, as shown by previous analysis, is more accurately described by cross-spectral parameters.

Moreover, the analysis confirms the impairment induced by right ventricular pacing in patients with preserved ventricular function, specifically on the diastolic function.

In this group, the indexes of dyssynchrony did not demonstrate a significant increase following ventricular pacing. This result may be explained by the presence of the compensation mechanisms that, especially in healthy subjects, take place early after the onset of pacing and lead to a partial recovery of the cardiac function and the normalization of dyssynchrony indexes (see Chapter 6.e.).

Moreover, as clearly shown in Chapter 6.c., in healthy subjects regional dysfunction may not be revealed by the assessment of the global ventricular function.

In the overall population we observed a correlation between the changes in stroke volume induced by the pacing and the indexes of dyssynchrony. This result may have practical implications for pacing therapy delivery.

In fact, some authors advocated the need to perform a patient tailoring of LV pacing site, due to the considerable inter-patient variation in the hemodynamic response to pacing (63,160). The identification of parameters associated to the hemodynamic improvement may help in guiding the implant optimization.

Whether these acute results are associated to an improved long-term prognosis has to be defined.

6.c. Ventricular Pacing Lead Location: an Acute Evaluation of Global and Regional Left Ventricular Function and Dyssynchrony Using Conductance Catheter Indexes

Introduction

The optimal right ventricular (RV) pacing lead location for patients with a standard indication for ventricular pacing remains controversial. Clinical studies comparing atrial and ventricular-based pacing have demonstrated that atrial pacing modes delay the development of atrial tachyarrhythmias and reduce hospitalization for congestive heart failure compared to ventricular pacing modes (161-163). These results suggested that right ventricular apex (RVA) pacing might be detrimental to left ventricular (LV) function, presumably because bypass of the His-Purkinje system produces dysynchronous LV contraction. Indeed, several clinical and experimental studies examining the consequences of RVA pacing observed that this technique caused prolonged QRS duration, LV asymmetrical hypertrophy, dilatation, remodeling, mitral valve regurgitation, altered myocyte histology, reduced exercise capacity and coronary perfusion abnormalities (164-167). The DAVID clinical trial also suggested that RVA pacing was associated with an increased risk of death and hospitalization for heart failure in patients with an implantable defibrillator (168). The RV outflow tract (RVOT) was initially suggested as a potentially favorable alternative to RVA pacing. However, most investigations that compared RVOT to RVA pacing yielded equivocal results. This may be due to the heterogeneous populations and methodology of the trials as well as the short follow-up durations (169-172). Other recent clinical trials examined the utility of LV or biventricular (BiV) pacing to avoid the adverse hemodynamic consequences associated with RVA pacing (38,173,174). The results of these studies were encouraging, and emphasized an important relationship between ventricular pacing site(s), hemodynamics and LV dyssynchrony. However, many patients indicated for right ventricular pacing do not meet clinical requirements for BiV pacing. Thus, proper ventricular lead positioning may have important clinical ramifications on this broad device population. We compared systemic hemodynamics and LV systolic and diastolic function during acute RV, LV and BiV pacing in patients with and without preexisting LV dysfunction who did not meet current clinical indications for cardiac resynchronization therapy.

Methods

Patients with indications for electrophysiologic study or device implantation were prospectively stratified into two groups based on LV ejection fraction (EF) ≥40% or <40%. EF was determined before electrophysiologic study using standard echocardiographic techniques. Patients with QRS duration > 120 ms were excluded from participation.

For LV pressure and volume measurements see Chapter 5.a..

A fluid-filled Swan-Ganz catheter was placed via a femoral vein and advanced into the proximal pulmonary artery for the determination of pulmonary artery pressure and stroke volume (thermodilution) and parallel conductance for conductance volume calibration. Parallel conductance was assessed by injection of 10ml hypertonic saline (6%) into the pulmonary artery (114).

Absolute LV volumes were calculated by matching effective conductance stroke volume (SV) with simultaneously measured thermodilution SV and by subtracting parallel conductance from total volume.

Temporary pacing electrodes were positioned in the right atrial appendage (RAA), RVA, RVOT free wall (RVF), RVOT septum (RVS) and LV free wall (LVF).

Lead location was confirmed using standard criteria (175). High septal position was determined using right anterior oblique fluoroscopic view. RVS position was confirmed by negative QRS morphology in lead I. RVF was confirmed by positive morphology in lead I.

For more details on the applied pacing protocol see Chapter 5.b..

Data Analysis

The data analysis is described in Chapter 5.c.. In particular, the hemodynamic variables analyzed were: LV systolic (LVSP) and end-diastolic (LVEDP) pressure, +dP/dtMAX and –dP/dtMIN, LV end-systolic (LVESV) and end-diastolic volume (LVEDV), SV, stroke work (SW), cardiac output (CO), EF, and the time constant of isovolumic relaxation (τ). Effective arterial elastance (EA), an index of LV afterload, was calculated by: (LVESP)/SV (176).

In this analysis, following parameters were considered to quantify mechanical dyssynchrony.

Mechanical dyssynchrony (DYS), estimated on each cardiac cycle according to the classical approach. In fact, it demonstrated a better performance in detecting dyssynchrony with respect to its counterpart estimated with coherent averaging (see Chapter 6.b.). This parameter was preferred because it permits to quantify ventricular dyssynchrony for specific segments of the cardiac cycle: systolic (DYSS) and diastolic (DYSD) dyssynchrony (145).

Global cycle efficiency (CE), calculated as previously described (Chapter 4.b. and (151)). This parameter was demonstrated to detect ventricular dyssynchrony with high sensitivity and specificity (Chapter 6.b.), moreover it permits to quantify the dyssynchrony associated to each volume segment by means of its regional value: regional cycle efficiency (RCE).

In order to evaluate whether the optimal RV pacing site varied between patients, the RV pacing sites resulting in the maximum or minimum SW and dP/dtMAX were compared to AAI. QRS duration was determined from the 12 lead ECG.

Statistical Analysis

Hemodynamic data collected during dual-chamber pacing were compared based on ventricular pacing site and normal and depressed EF groups using 2-way ANOVA for repeated measures. A Student-Neuman-Keuls test was used for post hoc comparisons. Dual chamber pacing interventions were compared to AAI pacing using one-way repeated measure ANOVA with

Dunnet's test. Demographic data between groups were compared using t-test or Fischer's exact test. A probability (p) value less than 0.05 was considered significant. All data are reported as mean±SD unless indicated.

Results

A total of 31 patients were enrolled (n=17 EF≥40%; n=14 EF<40%). Age, sex and QRS duration were similar between groups (Table 7). Patients with reduced EF had a greater incidence of cardiomyopathy, congestive heart failure, coronary artery disease, myocardial infarction, and previous coronary bypass surgery than patients with normal EF. No differences in the incidence of bradycardia and atrial and ventricular tachyarrhythmias were observed between groups.

Table 7. Patient Demographics.

	EF≥40% (n=17)	EF<40% (n=14)
Sex (M)	7 (41%)	6 (43%)
Age (yrs)	61 ± 13	62 ± 10
QRS (ms)	91 ± 18	106 ± 25
Cardiomyopathy	2	13*
CHF	2	11*
CAD	5	10*
Hypertension	3	6
MI	3	10*
Valve disease	1	0
CABG	1	9*
Atrial Tachyarrhythmias	1	3
Ventricular Tachyarrhythmias	4	4
Bradycardia	4	2
LBBB	0	1

*p<0.05 vs. EF<40%

Representative pressure-volume diagrams for one patient from each group are shown in Figure 14. Patients with preexisting LV dysfunction demonstrated reduced EF and LV +dP/dtMAX, -dP/dtMIN, decreased basal cycle efficiency, elevated LVEDV, and impaired diastolic relaxation compared to patients with EF≥40%. Pacing rate for experimental interventions was higher in patients with normal as compared to reduced EF. Programmed AV delay was similar during dual chamber pacing (103±31 vs. 110±23 ms) between groups. All pacing locations resulted in increased QRS duration relative to control. However, QRS duration was typically shorter during BiV pacing, compared to the other pacing sites (Tables 8&9).

In patients with EF≥40%, one or more RV pacing sites, but not LVF or BiV pacing, reduced stroke work, cardiac output, stroke volume, EF, and impaired diastolic relaxation (Table 8, Figures 15&16). RV pacing sites also resulted in reduced LV systolic pressure, stroke volume and +dP/dtMAX, -dP/dtMIN and pulse pressure in patients with EF<40%.
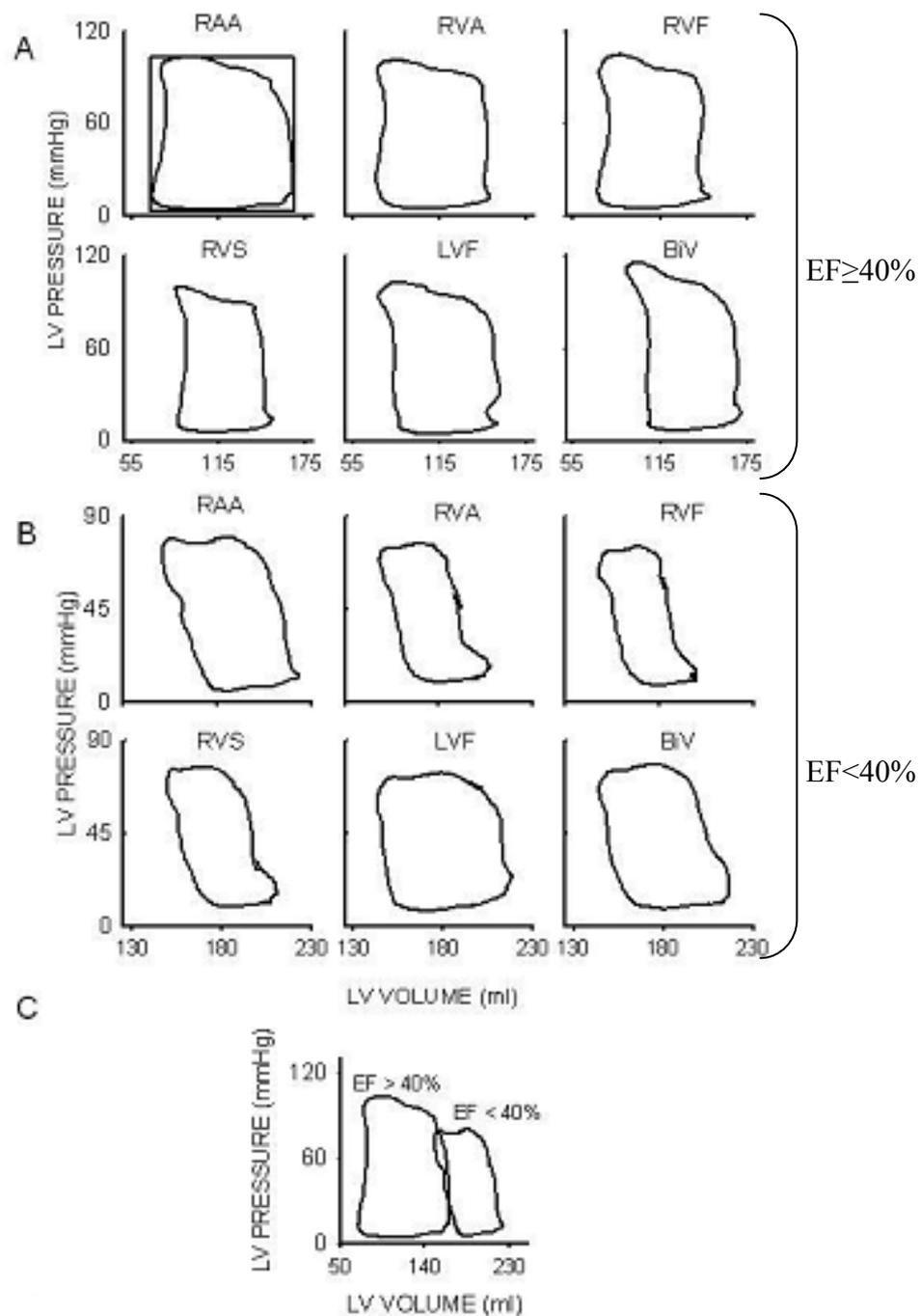
Figure 14. Representative steady-state pressure-volume diagrams from one patient with EF≥40% (A) and EF<40%. (B) during atrial overdrive pacing (AAI) and during dual chamber pacing and dual chamber bi-ventricular (BiV) pacing. (C) Comparison of basal AAI data from A and B. Rectangle in part A illustrates calculation of global cycle efficiency. CE is equal to the percentage of area occupied by the actual pressure volume loop within a rectangle determined by LV pulse pressure and LV pulse volume. LVF = left ventricular free wall; RAA = right atrial; RVA = right ventricular apex; RVF = right ventricular outflow tract free wall; RVS = right ventricular outflow tract septum.

Table 8. Hemodynamics in Patients with EF≥40%.

| Index	AAI	RVA	RVS	RVF	LVF	BiV
QRS (ms)	90±14	158±31[b]	145±27[b]	176±26[bd]	167±31[b]	134±16[bef]
CO (l/min)	5.3 ± 2.0	4.8 ± 1.8	4.3 ± 1.9[b]	4.2 ± 1.5[b]	5.1 ± 1.9[e]	5.3 ± 1.7
EF (%)	51 ± 12	48 ± 14	43 ± 14[ab]	44 ± 12[b]	47 ± 10[de]	49 ± 10
LVEDP (mmHg)	10.1 ± 3.2	14.1 ± 7.0[b]	15.9 ± 7.2[b]	14.9 ± 7.4[b]	15.4 ± 8.0[b]	13.5 ± 6.7[b]
τ (ms)	34 ± 10	39 ± 10[b]	41 ± 15[b]	39 ± 9[b]	39 ± 8	37 ± 5
-dP/dt$_{MIN}$ (mmHg/s)	-1,431 ± 407	-1,319 ± 396[b]	-1,281 ± 350[b]	-1,288 ± 357[b]	-1,235 ± 333[b]	-1,251 ± 248[b]
MAP (mmHg)	84 ± 21	88 ± 15	94 ± 13	86 ± 12	93 ± 18	87 ± 12
PP (mmHg)	60 ± 23	64 ± 19	70 ± 23	62 ± 19	64 ± 22	66 ± 21
PAP (mmHg)	26±7	26±7	27±8	27±8	26±7	24±6
E$_A$ (mmHg/ml)	2.09 ± 1.24	2.21 ± 1.17	2.59 ± 1.54	2.57 ± 1.32	2.17 ± 1.19	1.91 ± 0.78
DYS$_S$%	20.3 ± 7.7	21.7 ± 6.5	21.5 ± 7.7	21.7 ± 7.1	21.7 ± 6.9	22.4 ± 8.7
DYS$_D$%	22.5 ± 6.5	24.9 ± 5.9[b]	25.1 ± 5.9[b]	23.8 ± 6.3	24.8 ± 5.2	25.4 ± 3.2

n=17 for all except QRS, MAP, PP and PAP (n=7); QRS=QRS duration, CO=cardiac output, EF=ejection fraction, LVEDP=left ventricular end diastolic pressure, τ=time constant of LV relaxation, MAP=mean arterial pressure, PP=pulse pressure; PAP=mean pulmonary arterial pressure, DYS$_S$=Systolic dysynchrony index, DTS$_D$=Diastolic Synchrony index, [b]p<0.05 vs. AAI (RM ANOVA, Dunnet's), [c]p<0.05 vs. RVA, [d]p<0.05 vs. RVS, [e]p<0.05 vs. RVF, [f]p<0.05 vs. LVF (2 way-RM ANOVA, Student-Neuman-Keuls)

Table 9. Hemodynamics in Patients with EF<40%.

Index	AAI	RVA	RVS	RVF	LVF	BiV
QRS (ms)	102±21	161±43[b]	172±18[ab]	188±24[bc]	172±31[b]	146±19[bcdef]
CO (l/min)	4.2 ± 1.4	4.0 ± 1.8	4.2 ± 1.4	3.8 ± 1.4	5.1 ± 2.1[cde]	5.5 ± 2.7[bcde]
EF (%)	28 ± 7[a]	26 ± 10[a]	28 ± 9[a]	24 ± 7[a]	31 ± 12[ace]	31 ± 12[ace]
LVEDP (mmHg)	11.9 ± 7.4	10.4 ± 6.5	10.0 ± 4.9[a]	11.3 ± 6.6	11.7 ± 7.2	7.5 ± 8.2[abf]
τ (ms)	45 ± 14[a]	49 ± 14[a]	44 ± 11	47 ± 14	44 ± 10	41 ± 11
-dP/dt$_{MIN}$(mmHg/s)	-951 ± 253[a]	-772 ± 212[ab]	-858 ± 209[a]	-816 ± 191[ab]	-870 ± 279[a]	-849 ± 184[a]
MAP (mmHg)	81 ± 14	75 ± 15[b]	77 ± 15	80 ± 16	80 ± 17	76 ± 16
PP (mmHg)	54 ± 12	46 ± 10[ab]	50 ± 14[a]	49 ± 13	53 ± 16	46 ± 9
PAP (mmHg)	30±12	27±12	29±12	28±11	28±13	26±9
E$_A$ (mmHg/ml)	1.81 ± 0.60	1.81 ± 0.78	1.74 ± 0.45[a]	2.02 ± 0.89	1.56 ± 0.62	1.48 ± 0.90
DYS$_S$%	24.5 ± 6.7	24.4 ± 6.7[a]	24.9 ± 7.7[a]	24.7 ± 7.1[a]	23.8 ± 7.2[a]	24.3 ± 8.0[a]
DYS$_D$%	29.0 ± 5.0[a]	28.5 ± 3.5	29.5 ± 3.5	29.2 ± 3.6[a]	29.5 ± 3.4[a]	28.5 ± 3.7

n=14 for all except QRS, MAP, PP and PAP (n=7); Abbreviations as Table 2. [a]p<0.05 vs. EF≥40% (Table 2), [b]p<0.05 vs. AAI (RM ANOVA, Dunnet's), [c]p<0.05 vs. RVA, [d]p<0.05 vs. RVS, [e]p<0.05 vs. RVFW, [f]p<0.05 vs. LVF. (2-way RM ANOVA, Student-Neuman-Keuls)

LV and BiV pacing increased stroke work, cardiac output, stroke volume, EF and +dP/dtMAX in patients with EF<40% compared to RV pacing (Table 9). Furthermore, LVF and BiV pacing also enhanced CE compared to RV pacing and AAI pacing in patients with depressed EF (Figure 16). Diastolic dyssynchrony index (DYSD) also decreased with RV pacing (Table 9). Preload (LVEDV), afterload (EA) and mean pulmonary wedge pressure were unchanged in both groups. Figure 17 shows an example of the six segmental pressure-volume diagrams ranging from apex (segment 1) to base (segment 6) during atrial overdrive and dual chamber pacing from different ventricular sites in one patient with LV dysfunction. These data are summarized over the population in Figure 18 (A&B) using regional cycle efficiency (RCE) of the most apical and basal volume segment. RCE depended on pacing site and varied between the apex and base within pacing site in patients with EF<40%, but not the group with EF≥40%. In general, RVA pacing attenuated the apical RCE, and RVF and RVS pacing attenuated the basal RCE in the EF<40% group. RV minimum stroke work and dP/dtMAX were significantly lower compared to AAI, while the RV maximum values were similar to AAI (Figure 19).
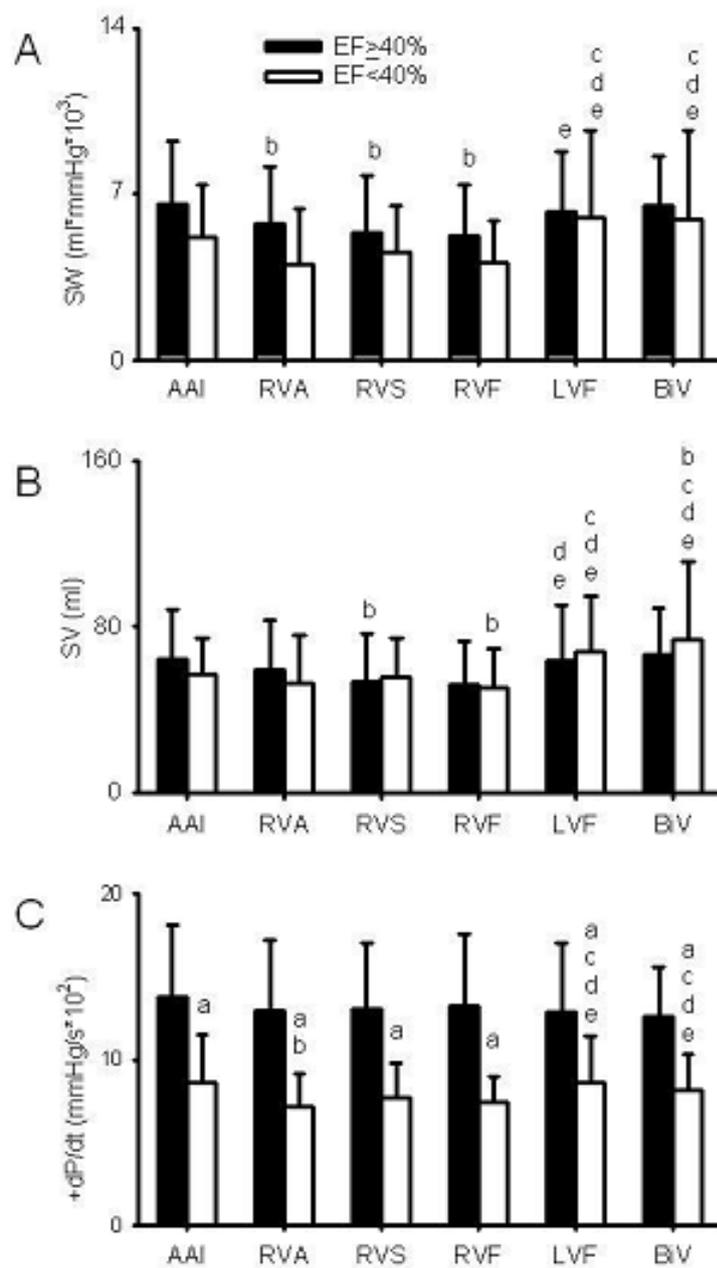
Figure 15. Alterations in LV stroke work (SW, panel A), stroke volume (SV, panel B), and +dP/dtMAX (panel C) during atrial overdrive (AAI) and alternate site ventricular pacing. a $p < 0.05$ vs. EF≥40%, b $p < 0.05$ vs. AAI (RM ANOVA, Dunnet's comparison), c $p < 0.05$ vs. RVA, d $p < 0.05$ vs. RVS, e $p < 0.05$ vs. RVF (2-way RM ANOVA, Student-Neuman-Keuls comparison).
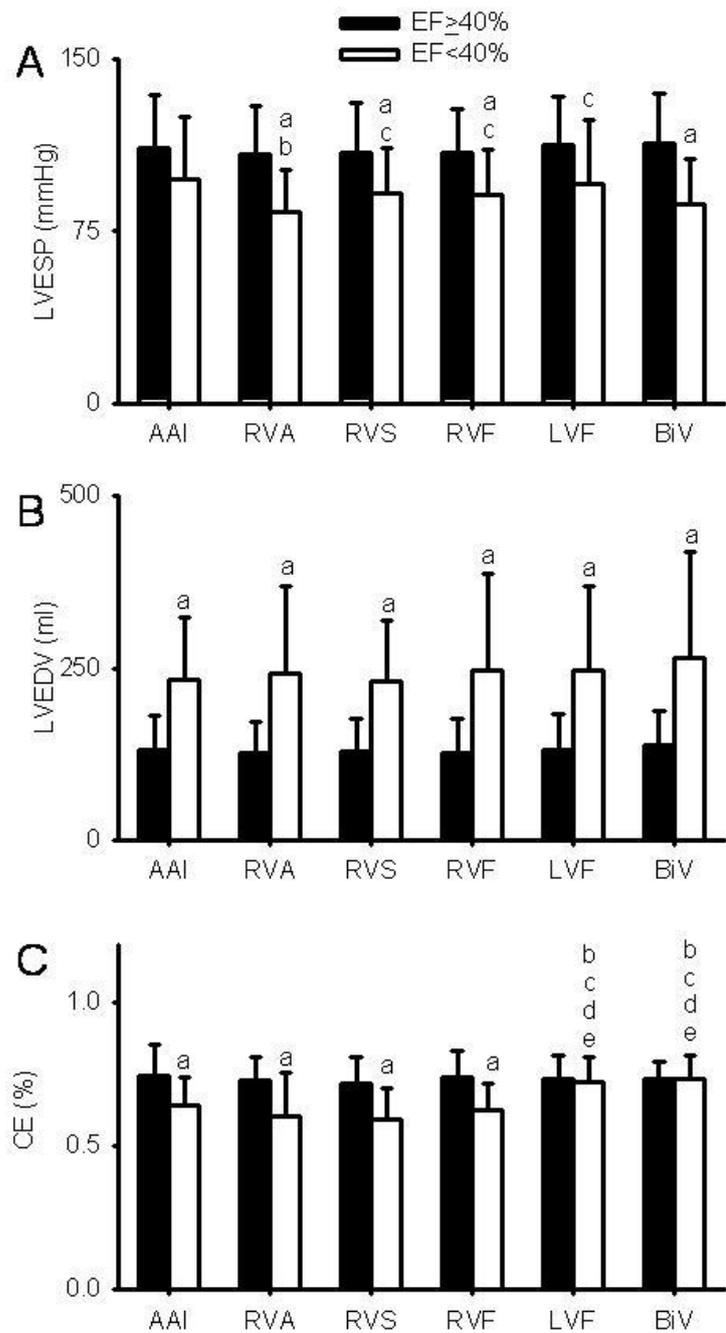
Figure 16. Alterations in LV end systolic pressure (LVESP, panel A), LV end diastolic volume (LVEDV; panel B), and cycle efficiency (CE), an index of LV synchrony (panel C) during atrial overdrive (AAI) and alternate site ventricular pacing. a $p<0.05$ vs. EF≥40%, b $p<0.05$ vs. AAI, c $p<0.05$ vs. RVA (RM ANOVA, Dunnet's comparison), d $p<0.05$ vs. RVS, e $p<0.05$ vs. RVF (2-way RM ANOVA, Student-Neuman-Keuls comparison).
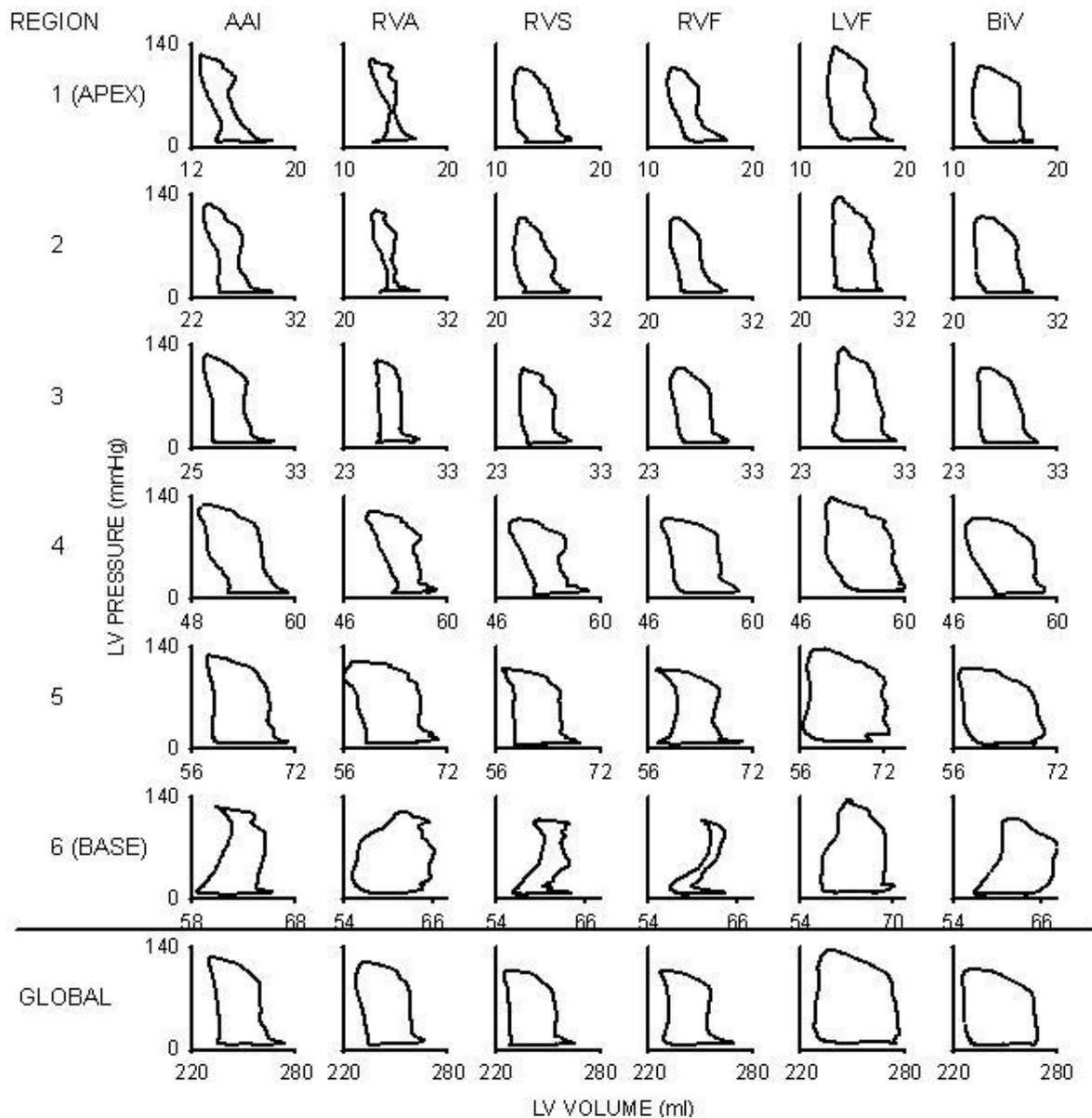
**Figure 17.** Regional and global LV pressure volume loops during atrial overdrive and dual chamber pacing from different ventricular sites in a representative patient with EF<40%. Regions are numbered from apex (1) to base (6) corresponding to the sequential volume channels along the axis of the conductance catheter. These individual signals form the global pressure-volume loop when summed. Note that RV pacing from different sites changes the regional contributions to the global pressure volume loop. RVA pacing has a greater impact on the apical segments. Conversely, RVS and RVF pacing primarily distort the basal segment. LV and BiV pacing result in more homogenous distribution of regional work.
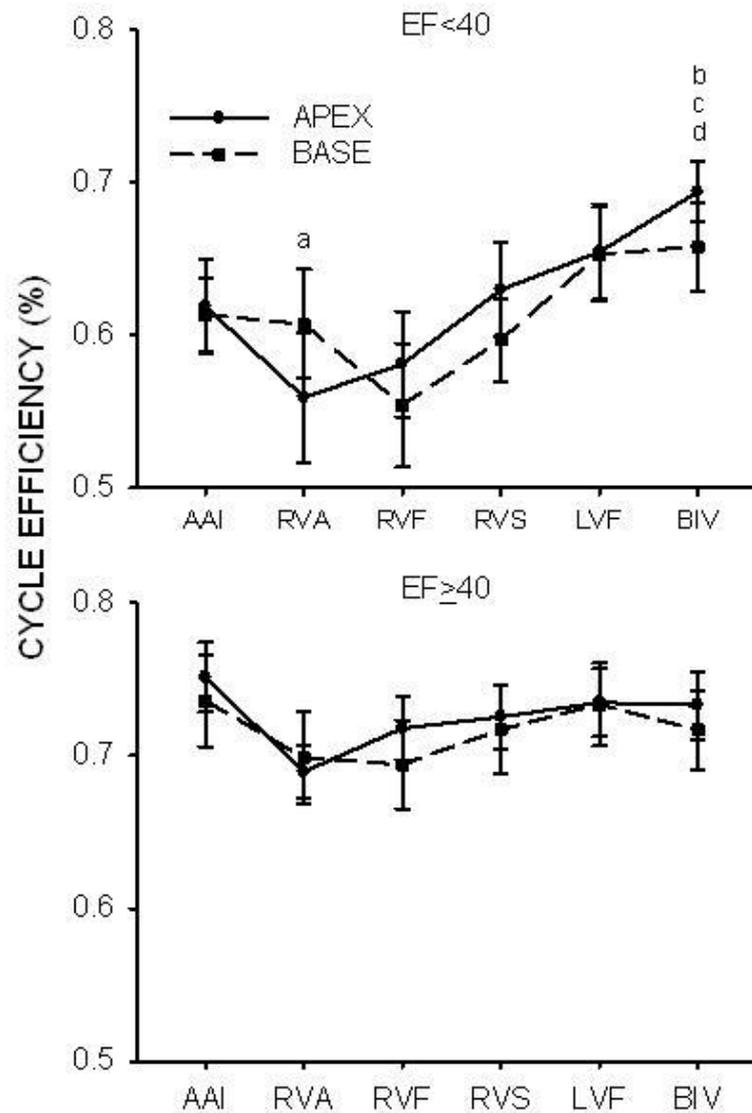
Figure 18. Distribution of regional cycle efficiency within the LV: Regional cycle efficiency was higher for the most apical and basal volume segment at each pacing site in patients with EF<40% (A) and EF≥40% (B). Regional cycle efficiency depended on pacing site and varied by region within pacing site in the group with EF<40% (A), but not the group with EF≥40%. In general, RVA pacing attenuated the apical segmental synchrony, and RVFW and RVS pacing attenuated the basal segmental synchrony in the with EF≥40% group. Data are mean±SE; (2-way RM ANOVA Student-Neuman-Keuls comparison).
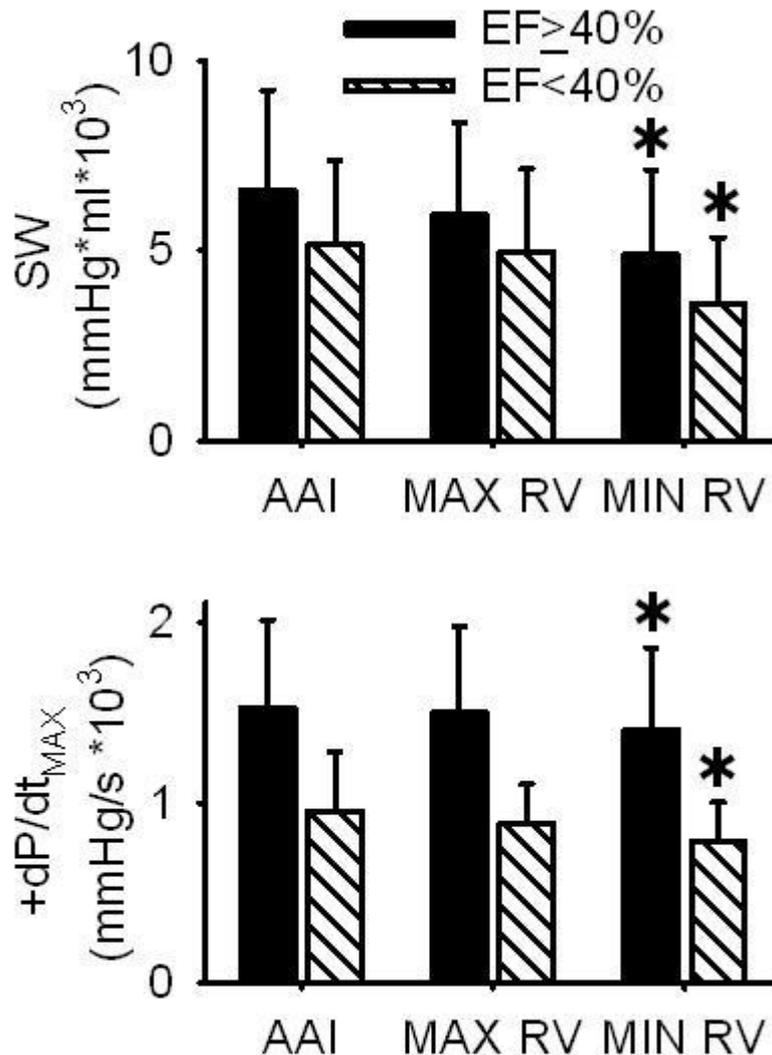
Figure 19. Stroke work (SW; top) and dP/dtMAX (Bottom) at the RV pacing site (RVA, RVS, or RVF) resulting in maximum (MAX RV) and minimum (MIN RV) stroke work or dP/dtMAX compared with stroke work measured during control (AAI): The site of maximal stroke work or dP/dtMAX was not different from AAI. Thus, RV pacing does not necessitate attenuated hemodynamics. However, the optimal RV site varied between patients. *$p < 0.05$ vs. AAI, (RM ANOVA with Student-Neuman-Keuls post hoc comparison).

Discussion

General

The majority of patients indicated for ventricular pacing do not meet current clinical indications for cardiac resynchronization therapy pacing. Furthermore, the optimal ventricular pacing site for patients with conventional indications for ventricular pacing remains controversial. The present results comparing the impact of several ventricular pacing sites on indices of LV systolic and diastolic function using pressure-volume analysis demonstrate that ventricular pacing lead location has a significant impact on LV function. In particular, acute RV pacing caused potentially deleterious reductions in cardiac output and stroke work concomitant with impaired diastolic relaxation and increased

LV end-diastolic pressure in patients with and without impaired LV function. The results further indicate that LV and BiV pacing significantly improved hemodynamics and function compared to RV pacing at 3 different sites in patients with preexisting LV dysfunction.

Patient Population

Few previously conducted clinical investigations have compared ventricular pacing sites in patients that do not meet current clinical requirements for resynchronization therapy. Simantirakis and colleagues recently observed improved LV function using both echocardiographic (173) and pressure-volume analyses (174) during acute LV and BiV pacing as compared to RVA pacing in patients with permanent atrial fibrillation and narrow-QRS duration that required rate control. Turner and colleagues demonstrated improved contractile synchrony during LV pacing in patients with congestive heart failure in the presence of either a narrow or prolonged QRS duration (38). The current results confirm and extend these previous observations by quantifying the direct cardiovascular consequences of alternate site RV vs. LV vs. BiV pacing in normal and dysfunctional myocardium and by suggesting that the benefit of alternate site ventricular pacing may vary between populations as well as between patients within those populations.

Role and Indexes of Dyssynchrony

The present results support previous studies indicating that reduced EF is associated with basal LV contractile dyssynchrony, despite narrow QRS duration (71,177,178). For example, we observed lower basal global and regional cycle efficiency as well as generally increased dyssynchrony (DYSS, DYSD table 8,9) in patients with EF<40%.

This finding completes the results of previous analysis, performed on patients with cardiac dysfunction and long QRS duration, and confirms that indexes of mechanical dyssynchrony (in this case CE and DYS) allow a more accurate identification of ventricular impairment than the QRS duration.

In particular, the DYS index played an important role. In fact, it permitted to distinguish the phases of the cardiac cycle and to describe the diastolic dysfunction. It should be considered that the majority of parameters describing the ventricular dyssynchrony with echocardiographic techniques permits to detect only the inhomogenities of the systolic phase.

Furthermore, QRS duration was greater during LV compared to BiV pacing, even though LV performance was similar during pacing with these configurations. These data confirm previous reports that QRS duration alone is a reliable indicator of neither mechanical synchrony nor LV function (71,177,178). RV pacing also produced increased LVEDP with no change in LVEDV in patients with EF > 40%, perhaps indicating the influence of ventricular interaction (179).

The shape of the LV pressure diagram, as quantified by global cycle efficiency, improved during LV and BiV pacing in patients with EF<40%. In contrast, RV pacing had minimal impact on global cycle efficiency. However, the similarities in global cycle efficiency observed during RV pacing may have resulted from dissimilar changes in regional cycle efficiency and synchrony that depended on pacing site. This caveat is illustrated in Figures 17 and 18 in which segmental pressure-volume loops are plotted during atrial overdrive

and dual chamber pacing from different ventricular sites in one patient with LV dysfunction. Note that RV pacing from different sites produced important alterations in the regional contributions to the global pressure-volume loop.

RVA pacing had a greater impact on apical segment loop morphology, whereas RVS and RVF pacing distorted the shape of the LV regional pressure-volume diagram in the basal segments. In contrast, LV and BiV pacing caused a more homogenous distribution of segmental work in the EF<40% group. These observations suggest that pacing site may influence overall global LV function depending on its relative effects on regional function and synchrony. The observations further suggest that avoiding the imposition of regional contractile dysfunction may be as important as the restoration of synchrony in order to improve long-term outcome.

Moreover, it is essential to emphasize the importance of using indexes that allow the description of regional dyssynchrony, such as CE, for the study and the optimization of the pacing therapy.

In conclusion, the conductance catheter demonstrated to be an essential tool for the assessment of the cardiac function and the dyssynchrony, allowing the automatic and operator-independent estimation of indexes that characterize the temporal and spatial distribution of ventricular inhomogenities.

RVA vs. RVOT

Several clinical trials have previously compared RVOT and RVA pacing (169-172,180), but many of these studies were limited by small sample size or brief trial duration. The current results suggest that LV systolic and diastolic function may vary acutely with RV pacing sites in patients with normal and depressed EF, respectively. No RV pacing site was superior and RV pacing did not compromise stroke work or dP/dtMAX when the optimal RV pacing site was compared to AAI (Figure 19). Thus, acute hemodynamic optimization during lead placement may be desired to attenuate the detrimental effects of long term remodeling associated with RV pacing (167). Interestingly, hemodynamic optimization of ventricular pacing lead location has been demonstrated to improve cardiac performance during placement of temporary ventricular pacing leads during cardiac surgery (181). Such optimization may also be possible in patients in the catheterization laboratory using minimally or non-invasive techniques such as arterial pulse pressure, pulse oximetry or trans thoracic echocardiography.

RV vs. LV and BiV

Previous animal (182) and clinical (180,25,28) trials have shown that both BiV and LV pacing resulted in superior LV systolic function than RV pacing. The current findings confirm and extend these previous results in patients without preexisting LV dysfunction and with a narrow QRS duration. Hay (180) as well as Bordachar et al. (183) demonstrated that BiV pacing appeared to improve LV isovolumic relaxation in comparison to LV pacing in patients with congestive heart failure and a prolonged QRS duration. In contrast, our results indicated that -dP/dt MAX and τ were similar between BiV and LVF pacing sites in both patient groups (Table 8). The explanation for the difference in our results compared to the previous studies is not clear, but may have been related to differences in the baseline characteristics of the study populations. However, when considered together, the current and

previous results suggest that single site LV pacing may represent a useful alternative to BiV pacing in some patients, despite potential subtle effects on diastolic function.

Limitations

The role of LV lead location in patients indicated for cardiac resynchronization therapy has been studied recently using dP/dtMAX (62) or conductance catheter (63). Both trials reported that the optimal LV pacing lead location varied substantially between patients.

We did not attempt to identify the best LV free wall lead location in the current investigation (63). Nevertheless, our results support the general hypothesis that the ideal site for RV or LV pacing should be tailored to the individual hemodynamic response of each patient. We quantified LV dyssynchrony using regional cycle efficiency (CE). This index is sensitive to volume shifts during isovolumic contraction and relaxation (151). The index may also be sensitive to afterload changes that can alter the trajectory of the PV loop during ejection. However, we observed no changes in EA, an index of LV afterload with pacing sites (Figures 15-16). Recent studies have emphasized the potential influence of heart rate on optimal lead position (180). Heart rate was held constant in the present trial by atrial pacing. Thus, paired analyses within patients should not have been affected by heart rate. Finally, BiV pacing interventions were performed with LVF and RVS. It is unknown if other RV sites would have produced similar results during BiV pacing.

Conclusions

Ventricular pacing lead location has an important impact on LV function in patients with narrow QRS duration in the presence or absence of preexisting LV dysfunction. LVF and BiV pacing preserved and improved systemic hemodynamics, LV function and LV cycle efficiency compared to RV sites in patients with normal and depressed EF, respectively. The data emphasize that optimizing hemodynamics during pacemaker implantation may be important in the selection of alternate ventricular pacing sites in patients with normal and depressed LV function.

6.d. Pressure-Volume Analysis of Right Ventricular Pacing Lead Location for Bi-Ventricular Pacing: Global and Regional Left Ventricular Function and Dyssynchrony

Introduction

Cardiac resynchronization therapy (CRT) has been shown to improve ejection fraction and quality of life in patients with congestive heart failure (CHF) and prolonged QRS complex duration (51,54,60). Based on these encouraging results, other investigators have examined the clinical benefits of bi-ventricular pacing in populations with normal QRS duration (38,178,184,185). Most studies conducted to date were performed with the right ventricular lead positioned in the apical location (RVA). However, standard single site RVA pacing may be associated with atrial fibrillation or exacerbation of CHF (161-163,168). Furthermore, the optimal right ventricular lead location for bi-ventricular pacing has not been extensively examined (180). Many patients with clinical indications for RV pacing, including pacemakers and implantable defibrillators also do not present indications for CRT. Thus, alternate site or bi-ventricular pacing may represent an important alternative in these patients when pacing is required. We tested the hypothesis that patients with narrow QRS may benefit from bi-ventricular pacing compared to RV apical pacing and that left ventricular (LV) function may be further improved by optimizing the position of the RV pacing lead.

Methods

We studied patients with indications for electrophysiologic study or device implantation. Subjects with a previously implanted device, valvular insufficiency or stenosis, or measured QRS duration > 125 ms were excluded from analysis.

For LV pressure and volume measurements see Chapter 5.a. and (114). Temporary pacing electrodes were positioned in the right atrial appendage (RAA), RVA, RV outflow tract free wall (RVF), RV outflow tract septum (RVS) and LV free wall (LVF) (160). Lead location was confirmed from fluoroscopic inspection and ECG morphometry (175).

For more details on the applied pacing protocol see Chapter 5.b.. In particular, constant atrial overdrive pacing (AAI) was maintained from the RAA throughout the protocol at a rate of 10 bpm greater than the sinus rate. AV delay was programmed to the measured p-wave to His interval duration minus 10 ms in order to avoid fusion pacing. Each patient received dual chamber bi-ventricular pacing from the LVF and each randomly assigned RV site.

Data Analysis
The data analysis is described in Chapter 5.c.. In particular, the hemodynamic variables analyzed were: LV systolic (LVSP) and end-diastolic (LVEDP)

pressure, +dP/dtMAX and –dP/dtMIN, LV stroke volume (SV), stroke work (SW), cardiac output (CO), EF, and the time constant of isovolumic relaxation (τ).

Similarly to the previous analysis, following parameters were considered to quantify mechanical dyssynchrony: global (CE) and regional cycle efficiency (RCE) (Chapter 4.b. and (151)).

Statistical Analysis

All hemodynamic data obtained during dual chamber bi-ventricular pacing with different RV ventricular pacing sites and were compared using 1-way ANOVA for repeated measures. Regional cycle efficiency was compared between the LV apex and base during pacing interventions was compared using 2-way repeated measure ANOVA. A Student-Neuman-Keuls test was used for post hoc comparisons. A probability (p) value less than 0.05 was considered significant. Data are presented a mean ± SD.

Results

Demographic data for the 13 patients included in the analysis are summarized in Table 10.

The average overdrive-pacing rate was 73±13 bpm. The average programmed AV delay was 103±13 ms. Representative LV pressure-volume data from a patient during AAI pacing, dual chamber pacing from the RVA and bi-ventricular pacing from the LV and the RVS, RVF or RVA, respectively are depicted in Figure 20. Bi-ventricular pacing from the LV lead and any RV site significantly (p<0.05) increased stroke volume, cardiac output and LV +dP/dt$_{MAX}$ (Figure 21, Table 11 compared to RVA pacing.

Table 10. Patient Demographics (n=13).

Age (yrs)	61 ± 10
Sex (M)	7 (54%)
EF (%)	40 ± 17
Cardiovascular History [n(%)]	
Cardiomyopathy	6(46)
CHF	7(54)
CAD	7(54)
Hypertension	11(85)
MI	6(46)
CABG	6(46)
Atrial Tachyarrhythmias	2(15)
Ventricular Tachyarrhythmias	5(38)
Bradycardia	2(15)
Syncope	3(23)

**Table 11.** Changes in LV Function during Bi-Ventricular and Right Ventricular Pacing.

	AAI	LV-RVA	LV-RVF	LV-RVS	RVA
QRS Duration (ms)	96 ± 17	146 ± 18*†	156 ± 23*	141 ± 18*†	167 ±28*
τ (ms)	37± 10	39 ± 10	39 ± 11	39 ± 11	42 ± 12
-dP/dt$_{MAX}$ (mmHg/s)	-1065 ± 360	-965 ± 293*	-952 ± 300*	-963 ± 268*	-929 ± 350*
LVESP (mmHg)	95 ± 27	91 ± 22	89 ± 26	91 ± 23	88 ± 24
LVEDP (mmHg)	11 ± 7	11 ± 8	9 ± 8	9± 9	11 ± 7
CO (l/min)	4.4 ± 1.4	4.6 ±2.0	4.8 ± 1.7†	4.7 ± 2.1†	4.0 ± 1.6
EF (%)	38 ± 18	36 ± 17	38 ± 17	36 ± 17	34 ± 17

n=13; data are mean±SD; * p<0.05 vs. AAI; † p<0.05 vs. RVA

Global LV cycle efficiency was also enhanced during bi-ventricular pacing as compared to RVA pacing alone. No significant differences with bi-ventricular pacing between different RV pacing sites were observed. However, choosing the optimal RV pacing site for bi-ventricular pacing for each patient increased stroke work, stroke volume, LV +dP/dtMAX and global CE (Figure 22). The RV site that produced optimal LV function varied among patients.
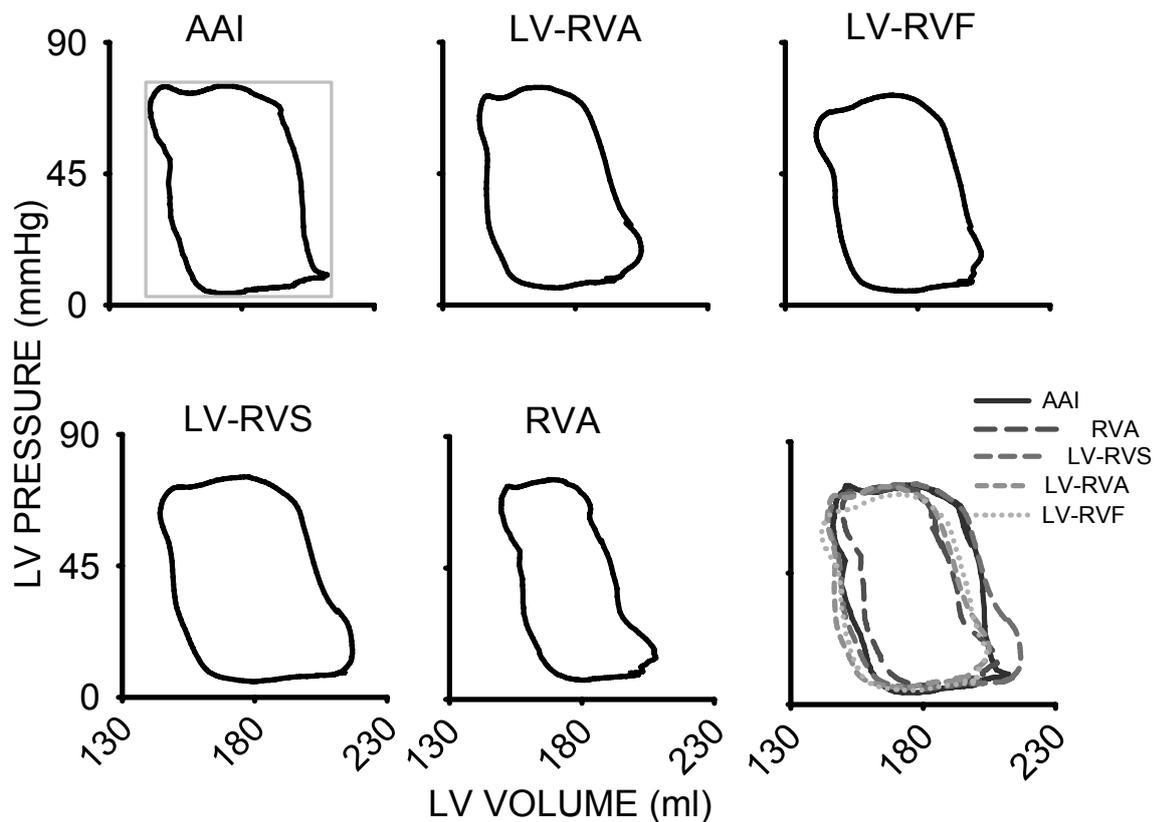
Figure 20. Representative pressure-volume diagrams for one patient during atrial overdrive pacing (AAI) from the right atrial appendage (RAA), and during biventricular pacing from the LV free wall (LV) and right ventricular apex (RVA), right ventricular free wall (RVF) or right ventricular septal outflow tract (RVS).
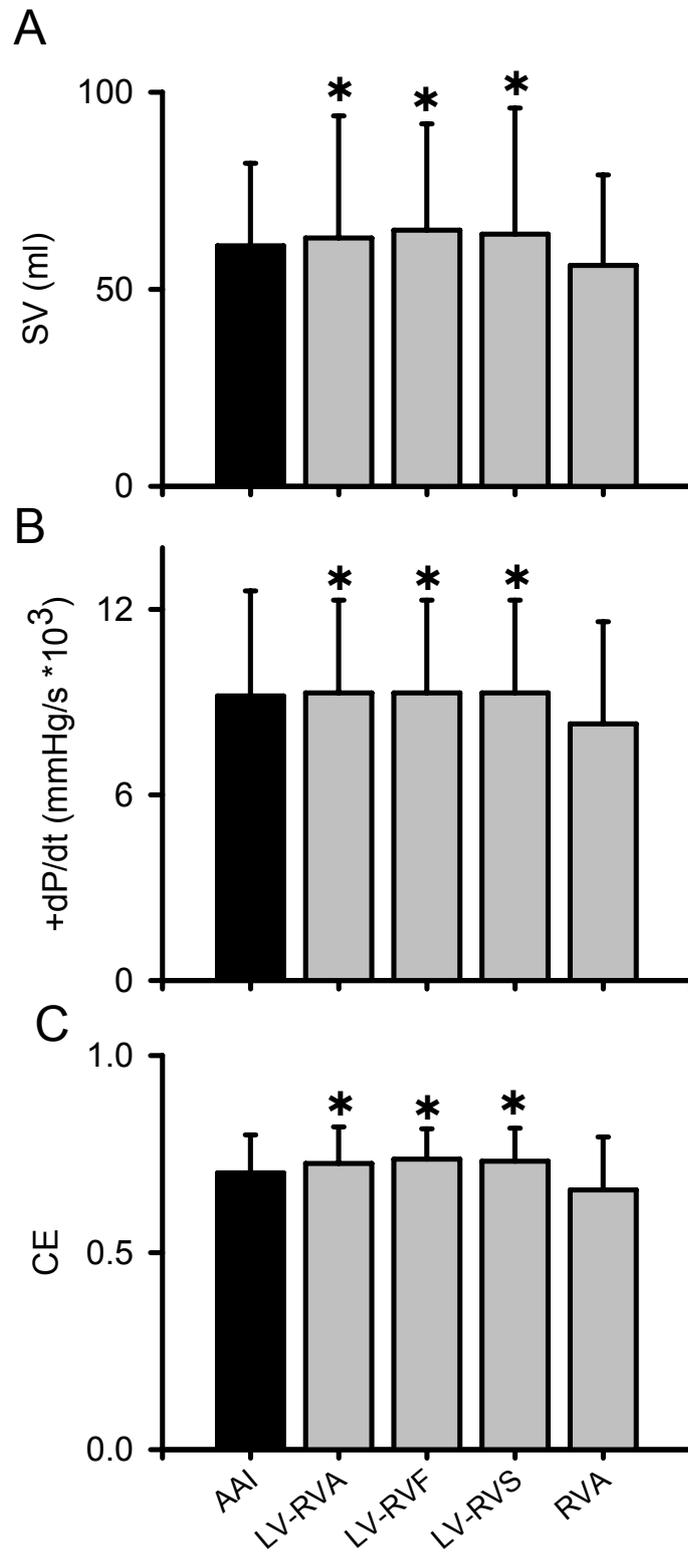
Figure 21. Histograms illustrating alterations in stroke volume (SV, panel A), LV +dP/dt$_{MAX}$ (panel B), and global cycle efficiency (CE, panel C) during bi-ventricular pacing from various RV sites. *$p < 0.05$ vs. RVA.
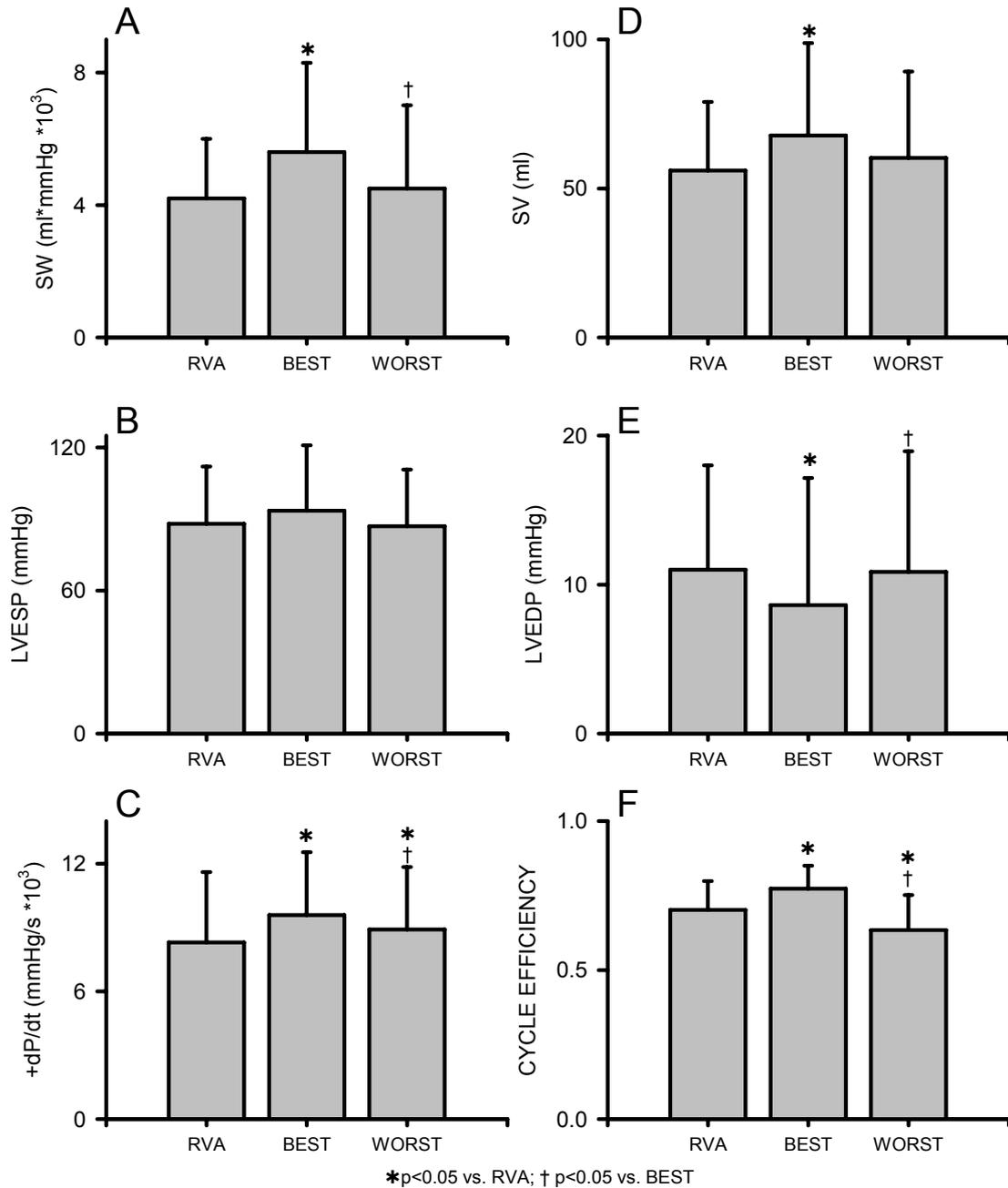
Figure 22. Histogram depicting the impact of RV pacing site optimization during bi-ventricular pacing on hemodynamics and indices of LV function: Choosing the optimal RV pacing site during bi-ventricular pacing resulted in significant improvements over both RVA and sub-optimal alternate RV sites. *p<0.05 vs. RVA; †p<0.05 vs. Best.
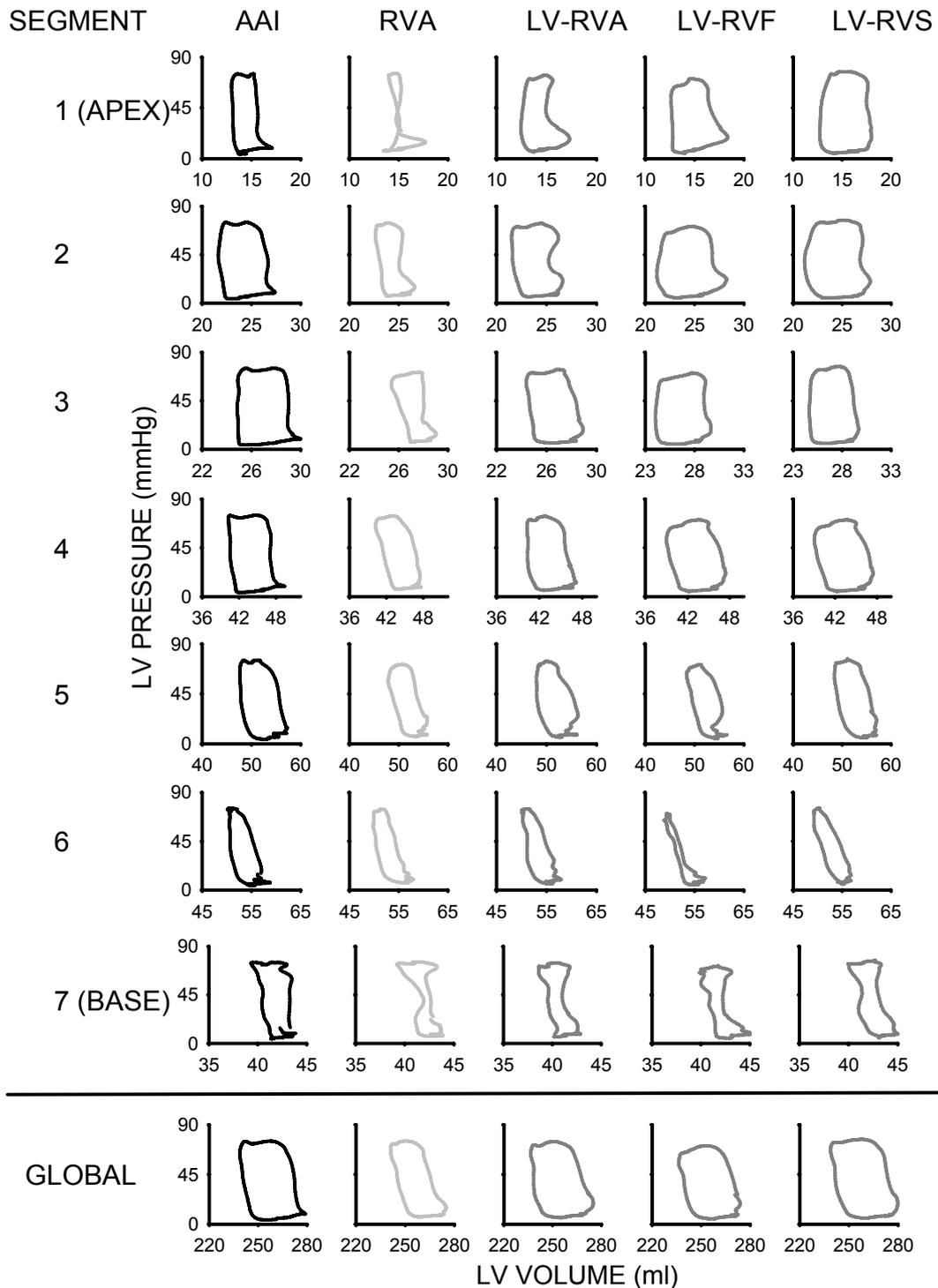
Figure 23. Representative LV pressure-regional volume diagrams obtained for different pacing sites in a patient. LV pressure is plotted as a function of each individual volume segment along the axis of the catheter ranging from the LV apex (segment 1) to the LV base (segment 7). In this illustration, regional differences in the phase of volume shift are apparent. Note that decreased global function during RVA pacing appeared to result from compromised regional function primarily near the apex. Regional LV function also varies during BIV pacing with different RV pacing sites (abbreviations as Figure 20).
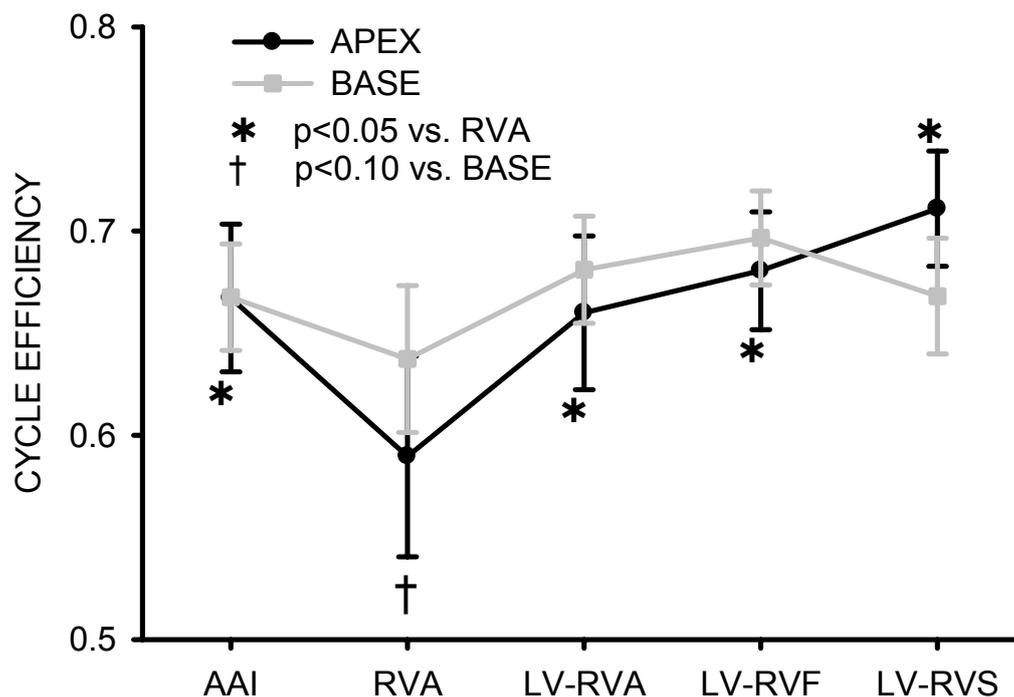
Figure 24. Changes in regional cycle efficiency during ventricular pacing: Apical segmental cycle efficiency was lower than basal segmental cycle efficiency during RVA pacing alone. Apical, but not basal segmental cycle efficiency was significantly (*p<0.05) greater during bi-ventricular pacing from any RV site than during RVA pacing.

Figure 23 shows regional pressure-volume loops constructed with individual segmental volume signals for one patient during atrial, dual chamber and bi-ventricular pacing. The changes in regional cycle efficiency between the basal and apical volume segments are shown in figure 24. Regional cycle efficiency was lower in the apex as compared to the base during dual chamber RVA pacing. Regional cycle efficiency in the LV apex was greater during bi-ventricular pacing from any RV site, but basal RCE was unaffected by pacing site.

Discussion

The results demonstrate that bi-ventricular pacing with alternate RV pacing sites produces acute improvement of LV systolic function and improves mechanical synchrony when compared to standard RVA pacing in the absence of a direct clinical indication for bi-ventricular pacing. Although no specific RV location was shown to be superior during bi-ventricular pacing, the RV pacing site that produced the optimal acute hemodynamic response varied between patients. Furthermore, optimization of RV lead location substantially enhanced acute LV performance during bi-ventricular pacing. We have previously shown that acute LV function was partially determined by right ventricular pacing site and that the RV outflow tract pacing did not always result in superior LV function compared to RVA (160). In our previous study, LV and bi-ventricular pacing preserved LV performance in patients with

normal LV function and improved LV function in patients with preexisting LV dysfunction. The current findings confirm and extend these previous results and suggest that the acute hemodynamic effects of bi-ventricular pacing are dependent on the specific RV lead location and that the optimal location may need to be determined at the time of implant.

Hay and colleagues (180) recently reported that LV systolic and diastolic function were similar during bi-ventricular pacing from RVA as compared to the RV outflow tract in patients with congestive heart failure, prolonged QRS duration and chronic atrial fibrillation using pressure-volume analysis. The current results confirm these observations in patients without a clinical indication for CRT. The current findings further suggest that LV function may be acutely improved by carefully selecting the RV lead location during bi-ventricular pacing. Other recent investigations also reported that the optimal LV pacing lead location varied substantially between patients (62,63). We did not attempt to identify the best LV free wall lead location in the current investigation, but our results support the hypothesis that the ideal site for RV pacing should be tailored to the individual hemodynamic response of each patient.

The current results challenge established guidelines for ventricular lead placement in patients indicated for pacing but without indications for CRT. Several previous studies suggest that alternate site RV pacing, LV pacing and bi-ventricular pacing exert benefits in some patients beyond current clinical indications (38,178,184,185). For example, the recently published PAVE trial evaluated bi-ventricular pacing after AV nodal ablation in patients with permanent AF (186). The results showed that bi-ventricular pacing improved functional capacity as compared to RV pacing alone. Other clinical studies have suggested that QRS duration is neither a sensitive nor specific indicator of LV mechanical dyssynchrony (38,178,184,185). Achilli and colleagues observed benefits for CRT therapy in patients with heart failure and narrow QRS duration and echocardiographically-validated mechanical dyssynchrony. In contrast, bi-ventricular pacing consistently improved acute LV function, even in patients that did not demonstrate basal dyssynchrony (as indicated by global cycle efficiency in the current study). Our data suggest that selective site biventricular pacing may represent a therapeutic option, but further prospective randomized clinical studies are required to confirm this hypothesis.

Part of the difficulty in quantifying the relative benefit of alternate site RV pacing as compared to RVA pacing has been the precise validation of lead placement. Previous attempts to identify specific RV septal or outflow tract sites using fluoroscopic or ECG data have been described (175), but these methods are often not consistently reproducible. Indeed, even the terminology used to describe specific RV septal or outflow sites has not been rigorously applied (172).

Indexes of Dyssynchrony
As an alternative to anatomic localization, some investigators have instead used QRS width as a surrogate for contractile synchrony (170,187). However,

QRS duration during RV pacing may not always be related to the synchrony of LV contraction or reflect the influence of pacing on hemodynamics. In the current investigation we based the choice of the optimal RV pacing on acute improvement of LV systolic function and CE (Figure 22). We believe that this strategy provides a useful early indication of LV functional response to pacing and therefore provides an advantage over previously described methods.

In fact, CE demonstrated to identify the ventricular dyssynchrony with high sensitivity and specificity, allowing the estimation of regional efficiency, when estimated from segmental signals.

To our knowledge, the current results are the first to suggest that global changes in cycle efficiency and LV performance may result primarily from alterations in LV apical function during pacing (Figures 23 and 24). Thus, global similarities in LV function during bi-ventricular pacing may result from dissimilar regional function depending on RV pacing site.

These data also suggest a potential mechanism for the observed variability between patients in response to RV pacing site. The data are consistent with the hypothesis that an individual patient response to RV pacing site depends on the complex interaction between precise lead location, ventricular anatomy and conduction status and the presence of pre-existing myocardial dysfunction. Prospective identification of the optimal RV pacing site for conventional or bi-ventricular pacing may be difficult unless a simultaneous hemodynamic assessment is performed.

In this analysis, the conductance catheter was demonstrated to permit the automatic and operator-independent assessment of the cardiac function and the dyssynchrony, using indexes that characterize the temporal and spatial distribution of ventricular inhomogenities.

The results should be interpreted within the constraints of several potential limitations. The current investigation included patients with and without symptomatic CHF. Alternative site RV pacing had similar effects in patients with heart failure as compared to those that did not (data not shown). A single programmed AV delay may have allowed varying degrees of intrinsic conduction and fusion to occur during alternate site RV pacing. However, we attempted to control intrinsic AV conduction by programming very short AV delays. Furthermore, the potential effects of alternate inter-ventricular timing delays were not investigated. Heart rate was held constant in the present trial by atrial pacing. Thus, paired analyses within patients should not have been affected by heart rate.

In summary, bi-ventricular pacing improves acute LV function compared to RVA pacing in patients with normal QRS duration. Global LV function did not vary significantly during bi-ventricular pacing from different RV sites but optimized RV lead position resulted in improved LV function in individual patients. These results may have important implications for tools and techniques for patients requiring ventricular pacing.

6.e. Beat-to-Beat Changes in Left Ventricular Dyssynchrony and Performance During Right Ventricular Pacing: a Conductance Catheter Analysis

Introduction

Animal and clinical studies comparing atrial and ventricular pacing indicate that right ventricular apex (RVA) pacing may be detrimental to left ventricular (LV) function since bypass of the His-Purkinje system produces LV dyssynchronous contraction (161-163). Brutsaert postulated that LV mechanical dyssynchrony may be regarded as modulator of cardiac performance together with heart rate, contractile state, preload and afterload (23). Recently it has been demonstrated that pacing site influences global LV function depending on its relative effects on regional function and synchrony (160). RV animal pacing studies showed decreased contractile function in early activated ventricular regions and hyper-functioning in late activated zones as well as decreased LV contractile state (28,101). An inverse relationship between changes in contractile state and intra-ventricular dyssynchrony was demonstrated in patients undergoing LV restoration surgery (143).

Although LV mechanical dyssynchrony has been demonstrated as key predictor for cardiac resynchronization therapy (CRT) efficacy, direct beat-to-beat relationship between LV mechanical dyssynchrony and cardiac performance during cardiac pacing remains unknown (27,40,82,188). Accordingly the aim of the present study was to evaluate beat-to-beat effects of RV pacing on LV dyssynchrony and performance from the pressure-volume plane in patients with normal ejection fraction (EF) using the pressure-volume-dyssynchrony catheter technique (27,114,140-142,145,147,188,189).

Methods

Patients
Inclusion criteria were patients with normal EF with indications to undergo electrophysiological testing. Patients with a previously implanted device, valvular insufficiency or stenosis or QRS duration > 120 ms were excluded from participation.

For LV pressure and volume measurements see Chapter 5.a..

Temporary pacing catheters were positioned in the RV apex (RVA), RV outflow tract free wall (RVF), and RV outflow tract septum (RVS). Tip location was confirmed using standard criteria.

For more details on the applied pacing protocol see Chapter 5.b.. Specifically, constant atrial overdrive pacing (AAI) was maintained throughout the protocol at a rate of 10 bpm greater than the sinus rate to avoid rhythm fluctuations. Baseline data were recorded during atrial pacing, followed by dual chamber pacing for 60 seconds from RVA, RVS, and RVF applied in random order

alternated by AAI pacing. The transitions from atrial pacing to dual chamber pacing and back to atrial pacing were recorded continuously.

Mechanical Ventricular Dyssynchrony
In order to quantify ventricular dyssynchrony for specific time-frames of the cardiac cycle and to track beat-to-beat changes of the parameters, following indexes were considered to quantify mechanical dyssynchrony: late systolic dyssynchrony (SysDysB) calculated from +dP/dtmax to end-systolic volume (ESV), early diastolic dyssynchrony from -dP/dtmax to peak filling rate (PFR) (DiaDysA) and total diastolic dyssynchrony (DiaDysT) from -dP/dtmax to R-wave (see Chapter 4.a.).
End-systolic elastance (Ees) was estimated by ESP divided by ESV. Effective arterial elastance (Ea) was calculated as ESP divided by SV. Ventricular arterial coupling was quantified as Ees/Ea (188).

Data Analysis
Multiple indices of LV systolic and diastolic function such as ESP, end-diastolic pressure (EDP) pressure, $+dP/dt_{max}$, $-dP/dt_{max}$, the time constant of isovolumic relaxation (Tau), ESV, end-diastolic volume (EDV), SV, PFR, EF and dyssynchrony values were extracted with off-line analysis. Values obtained during at least 3 heart cycles are expressed as mean±SD.
Statistical analysis was performed with paired Student's t-test for comparisons between no pacing and different pacing modes, and also by repeated-measures analysis of variance (ANOVA). Statistical correlations between variables were tested by least-squares linear regression. Multiple variate regression analysis was used to detect best predictor of SV change. Statistical significance was assumed at p<0.05. Results are presented as mean±SD.

Results

Nine patients (5 males) were enrolled, mean age 66±14 years, mean EF 57±9 % and mean QRS duration 88±21 ms. Table 12 shows hemodynamic characteristics obtained during sinus rhythm (SR), AAI pacing, and the 3 different RV pacing sites. Values of SR and atrial pacing were based on 12 beats after a stabilization of 5 min. RV pacing values were measured within 10s after RV pacing onset, excluding the first 3 paced beats. Atrial pacing at 10 beats above sinus rhythm increased cardiac output by 8% (p<.002), $+dP/dt_{max}$ by 7% (p<.002) and $-dP/dt_{max}$ by 3% (p<.03) at lower EDV (p<.02) and lower EDP (p<.01) compared with SR. No significant changes in all other measured variables, including intra-ventricular dyssynchrony measurements, were observed.
RV pacing settings compared to AAI pacing showed within 10 s decreased SV (p<.01), EF (p<.05), and $+dP/dt_{max}$ (p<.05) and increased EDP (p<.01). The diastolic relaxation indices $-dP/dt_{max}$ (<.01) and Tau (p<.01) deteriorated. LV total dyssynchrony was only significantly increased during RVA, late systolic dyssynchrony was not changed, while early diastolic dyssynchrony was increased in all RV paced modes (p<.01). EDV was only slightly decreased (p<.05) during RVF pacing whereas ESV was not changed at any RV pacing site.

Fig. 25 and 26 show LV pressure and (segmental-) volume tracings and P-V loops of transitions from AAI to atrio-RV pacing within a 10s time-span. RVF pacing (Fig. 25) induced immediate decreases in LV basal segmental volume amplitudes and increases in apical amplitudes. Initially systolic dyssynchrony increases sharply followed by a decrease around the third RV paced beat, whereas diastolic dyssynchrony remains increased during the 10s episode. P-V loops show initially distorted loops during iso-volemic contraction and relaxation (Fig. 25A), followed by improvement in cycle efficiency within the 10s time-span (Fig. 25B). Fig. 26A shows the transition from AAI to RVA pacing affecting LV apical volume segments, decreasing EDV, and increasing dyssynchrony. Immediate ejection phase compensation can be observed in the basal segment. The P-V loops show signs of post-systolic contraction starting at the second RV paced beat (Fig. 26A), followed by some SV restoration and decrease in post-systolic contraction (Fig. 26B).

Table 12. Baseline hemodynamic comparison at various pacing settings.

	SR a	AAI b	RVA c	RVF d	RVS e
HR (bpm)	77±15	88±14^a	88±14^a	88±14^a	88±14^a
CO (l/min)	5.4±1.5	5.84±1.5^a	5.13±1.2^b	4.25±1^{bb}	4.85±1.2^b
SV (ml)	72±21	70±19	59±18^b	48±15^{bb}	57±22^b
EF (%)	58±14	57±14	52±12	43±13^{bb}	50±16^b
EDV (ml)	133±51	127±49^a	122±48	121±55^b	124±50
ESV (ml)	55±37	56±39	63±39	64±39	62±39
EDP (mmHg)	9.8±2	7.6±3^a	12.7±4^b	11.6±4^b	13.4±5^{bb}
ESP (mmHg)	123±15	125±15	115±17^b	115±19	116±21
+dP/dt$_{max}$ (mmHg/s)	1538±257	1647±255^a	1494±307^b	1496±353^b	1535±281^b
-dP/dt$_{max}$ (mmHg/s)	1661±298	1712±297^a	1414±370^{bb}	1415±337^{bb}	1409±29^{bb}
Tau (ms)	32±7	31±6	40±9^{bb}	38±7^{bb}	39±8^{bb}
DysT (%)	19.3±6	19.3±6	21.9±6^b	21±7	21.5±7
SysDysB (%)	13±8	13±8	14.4±8	16±10	13.7±9
DiaDysA (%)	21±7	21±7	24±6^{bb}	24±7^{bb}	24±7^{bb}

CO, cardiac output; DiaDysA, early diastolic dyssynchrony; DysT, total dyssynchony; EDP, end-diastolic pressure; EDV, end-diastolic volume; ESP, end-systolic pressure; ESV, end-systolic volume; EF, ejection fraction; HR, heart rate; SV, stroke volume; SysDysB, late systolic dyssynchrony. ^{a}p<0.05 vs SR;^{aa}p<0.01 vs SR; ^{b}p<0.05 vs AAI;^{bb}p<0.01 vs AAI; Data is mean±sd, n=9.

Beat-to-Beat Hemodynamic Responses at Worst RV Pacing Site
The results of worst RV pacing sites for each patient (RVA 1pt, RVS 4pts, RVF 4pts), as indicated by greatest initial SV decrease, were analyzed beat-to-beat from AAI to various periods, of 2s, 9s and 60 s of RV pacing and back to AAI (table 13). Values are mean of 12 consecutive heart cycles during atrial pacing and at 60s RV pacing, and mean of 3 beats at 2s and 9s after RV pacing onset. Marked significant decreases in SV and EF by 37% and 23% respectively were observed at 2s after RV pacing onset, followed by significant relative increases of 20% and 10% at 9s. No further changes in SV and EF were observed up to 60s. Acutely after transition to atrial pacing, SV and EF recovered to initial baseline values. ESP showed an acute significant

diminution at 2s and subsequent full recovery at 9s. Initially ESV and EDV did not change significantly, however at 60s after RV pacing onset EDV was significantly (p<.05) decreased. End-systolic elastance was significantly (p<.05) decreased at 2s after RV pacing onset, followed by recovery during the remaining RV stimulation episode. Ventricular-arterial coupling showed a marked decrease (p<.004) from 2s after RV pacing onset, followed by full recovery at AAI pacing.

Peak +dP/dt was significantly (p<.05) decreased at 2s after onset of RV pacing, followed by a significant increase at 9s. The relaxation indices -dP/dt$_{max}$ and Tau showed significant (p<.01) impairment, at 2s after RV pacing onset with a mean decrease of 30% and mean prolongation of 32% respectively. At 9s and at 60s, both variables showed significant (p<.01) improvements compared to values at 2s, while both variables were remained decreased compared to baseline throughout RV pacing, followed by full recovery immediately during AAI.

Mean total LV dyssynchrony, as calculated from the whole cardiac cycle, was increased significantly throughout the RV pacing episode. Late systolic dyssynchrony, measured during the ejection phase, was markedly increased relatively by 30% at 2s after RV pacing onset, followed by a fast recovery, with no significant differences from 9s and beyond with AAI pacing. Early diastolic dyssynchrony was significantly (p<.01) increased at 2s relatively by 25%, and remained significantly (p<.05) higher throughout the 60s RV pacing episode, followed by full recovery at control atrial pacing.

**Table 13.** Beat-to-beat Hemodynamic responses at Worst right ventricular pacing site.

	AAI a	RV-2s b	RV-9s c	RV-60s d	AAI-10s e
SV (ml)	62±19	39±9^{aa}	47±14^{aabb}	46±13^{aa}	64±18^{dd}
EF (%)	52±13	40±12^{aa}	44±14^{aab}	44±14^{aa}	53±12^{dd}
EDV (ml)	126±54	118±56	120±54	118±50^{a}	125±49^{d}
ESV (ml)	61±40	65±43	63±41	61±38	62.6±38
EDP (mmHg)	9±4	10±3	12±3	11±3	9±4
ESP (mmHg)	124±13	111±20^{a}	121±18^{bb}	121±18	125±19
Ees (ml/mmHg)	2.7±1.5	2.1±1.1^{a}	2.4±1.1	2.5±1.2	2.6±1.4
Ees/Ea	1.3±.7	.7±.4^{aa}	.9±.4^{a}	.9±.5^{aa}	1.2±.7^{d}
+dP/dt$_{max}$ (mmHg/s)	1662±321	1509±238^{a}	1603±243^{bb}	1564±278	1648±313
-dP/dt$_{max}$ (mmHg/s)	1738±300	1217±284^{aa}	1411±307^{aabb}	1516±344^{aabb}	1690±333^{dd}
Tau (ms)	31±6	41±8^{aa}	38±7^{aabb}	35.6±6.6^{aabb}	33±6
PFR (ml/s)	706±186	594±275^{a}	626±25^{a}	618±216^{a}	732±180^{d}
DysT (%)	18.8±6.4	23.6±6^{aa}	20.5±7^{abb}	21±6.5^{ab}	19±6
SysDysB (%)	13±9	17±7^{aa}	14±10^{b}	14.4±9	14±8
DiaDysT (%)	19±7	24.6±4^{aa}	21.3±7^{b}	21.8±6.3^{a}	19.6±7.2

DiaDysT, total diastolic dyssynchrony; DysT, total dyssynchony; EDP, end-diastolic pressure; EDV, end-diastolic volume; Ees, end-systolic elastance; Ees/Ea; ventricular arterial coupling; EF, ejection fraction; ESP, end-systolic pressure; ESV, end-systolic volume; HR, heart rate; SV, stroke volume; EDP, end-diastolic pressure; EDV, end-diastolic volume; PFR, peak filling rate; SysDysB, late systolic dyssynchrony. ^{a}p<0.05 vs AAI;^{aa}p<0.01 vs AAI; ^{b}p<0.05 vs RV-2;^{bb}p<0.01 vs RV-2;etc. Data is mean±sd, n=9.
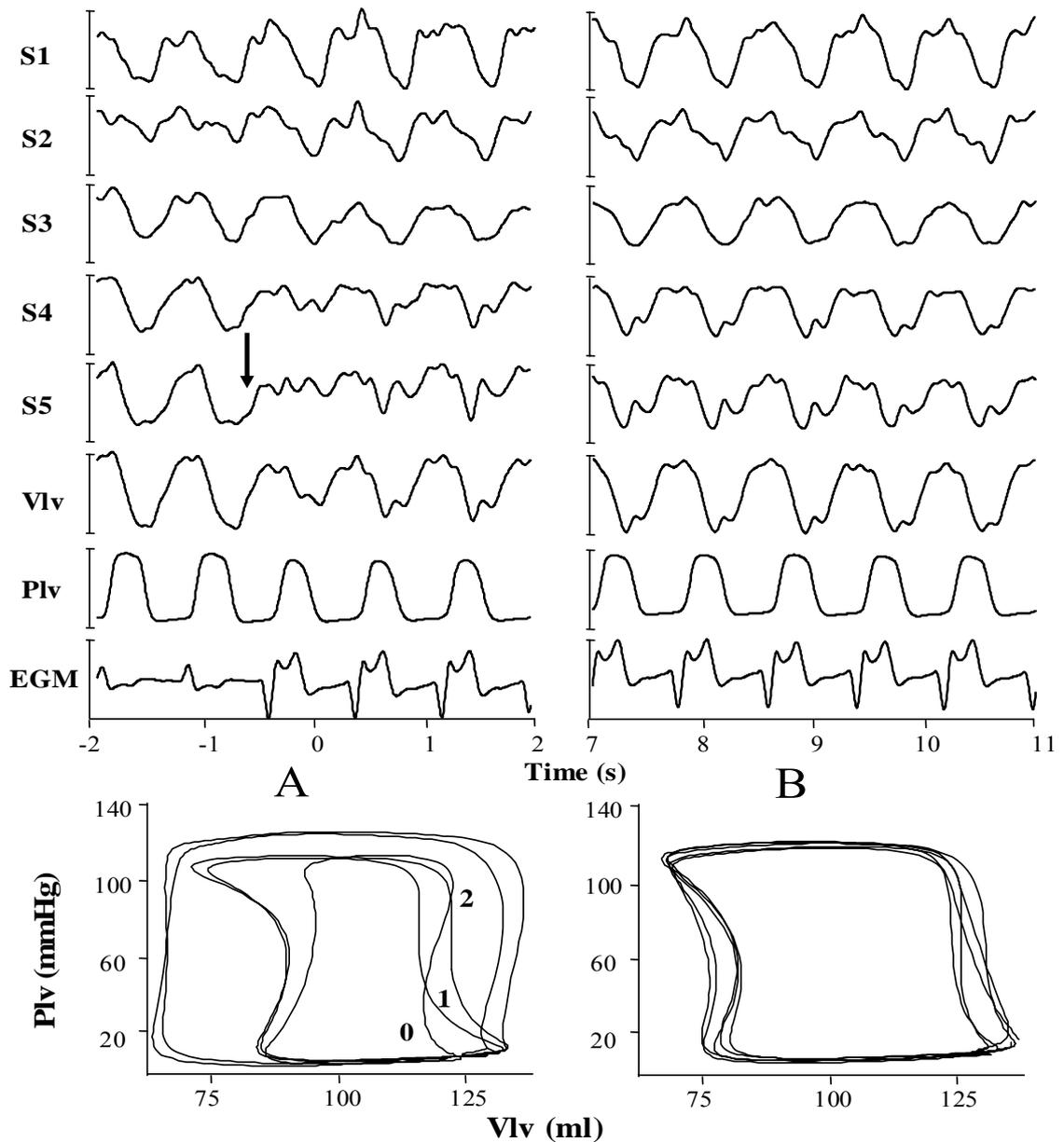
Figure 25. Left ventricular pressure (P) and volume (V) tracings and P-V loops showing transition from atrial to right ventricular free wall (RVF) pacing within a 10s time-span. RVF pacing induces immediate decreases in basal segmental volume amplitudes (see arrow at S 4) and increases in apical amplitudes (S1). The third beat after pacing onset shows a decrease of initially increased systolic dyssynchrony during the ejection phase. The P-V loops of the first paced beats show distorted loops during the iso-volemic contraction and relaxation phases. Figure 25B shows 5 recorded beats just before 10s after onset of RV pacing with less systolic dyssynchrony, but with marked early diastolic dyssynchrony. The P-V loops show improved iso-volemic contraction and less distortion during iso-volemic relaxation. EMG, intra-cardiac derived electromyogram; Plv, left ventricular pressure; S, is ventricular volume segment, S1 apical, S5, basal; Vlv, left ventricular volume. Numbers in the P-V loops indicate sequential beat numbers.
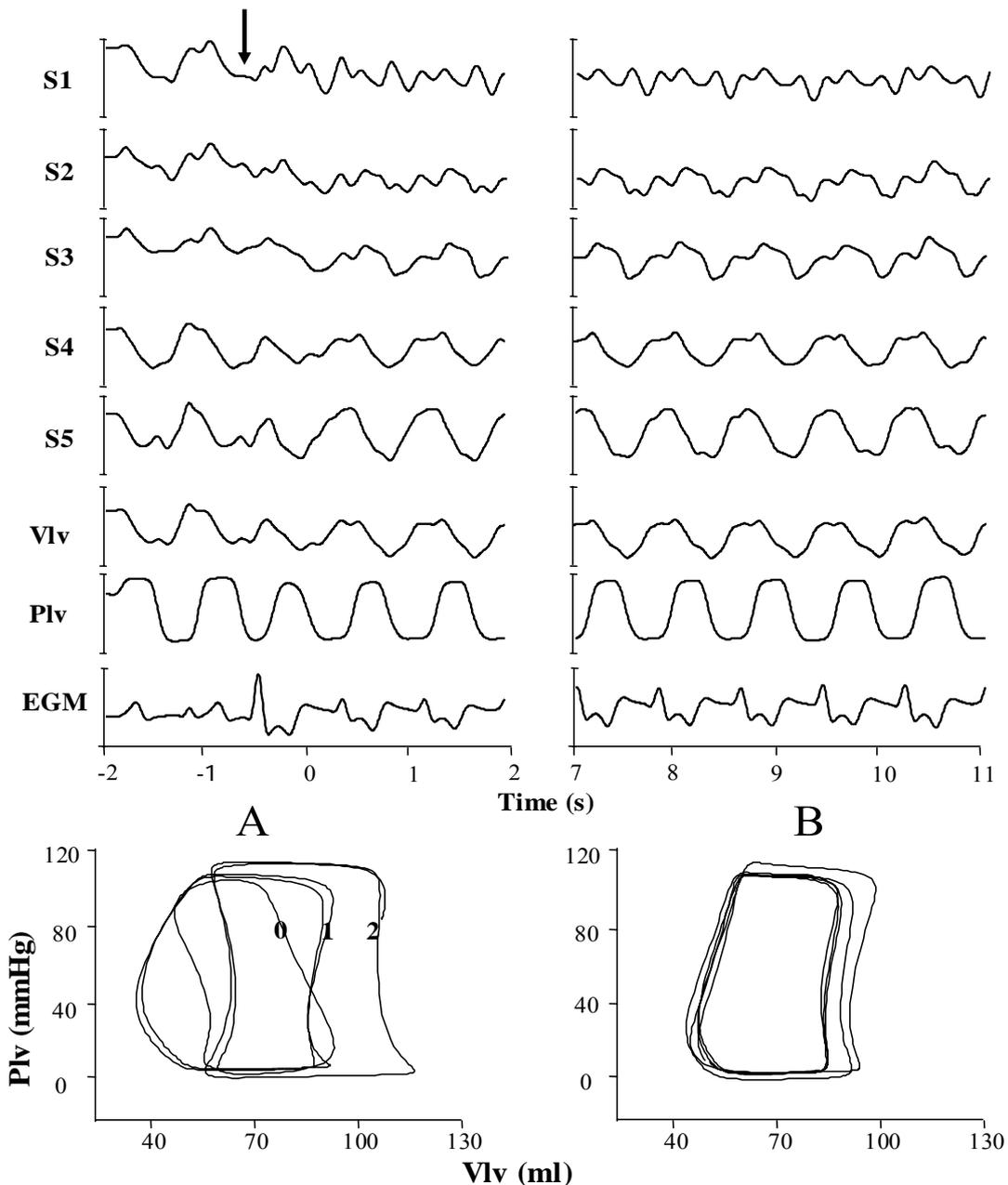
Figure 26. Left ventricular (LV) Pressure (P) and volume (V) tracings and P-V loops showing transition from atrial to right ventricular apical (RVA) pacing within a 10s time-span. RVA pacing affects apical volume segments (see arrow, S1), decreases LV end-diastolic volume and increases dyssynchrony. Compensation during the ejection phase can be observed in the basal segment (S 5). The P-V loops show signs of post-systolic contraction starting at the second RV paced beat. The P-V loops of figure 26B show some SV restoration and decrease in post-systolic contraction. EMG, intra-cardiac derived electromyogram; Plv, left ventricular pressure; S, is ventricular volume segment, S1 apical, S5, basal; Vlv, left ventricular volume. Numbers in the P-V loops indicate sequential beat numbers.

Regression Analysis
Regression analysis comparing changes of different LV function variables during the first 10s after onset of the worst RV pacing sites is shown in figure 27. SV changes inversely correlated with LV late systolic dyssynchrony changes and with changes in -dP/dt$_{max}$ (Fig 27A,D). Total diastolic

dyssynchrony inversely correlated with changes in PFR (Fig 27B) and EDV (Fig 27C). Changes in Ees correlated with changes in diastolic dyssynchrony (r=-.730, p<.001), late systolic dyssynchrony (r=-.766, p<.0001), PFR (r=.777, p<.0001) and +dP/dt$_{max}$ (r=.751, p<.001). Changes in ventricular-arterial coupling best correlated with changes in late systolic dyssynchrony (r=-.825, p<.0001) and diastolic dyssynchrony (r=-.803, p<.0001).

Multiple variate regression analysis demonstrated that SV changes within 10s were best predicted (p<.012) by changes in systolic dyssynchrony with changes in +dP/dt$_{max}$, -dP/dt$_{max}$, Tau, PFR, EDV, EF, ESP, systolic dyssynchrony, and diastolic dyssynchrony as tested variables.
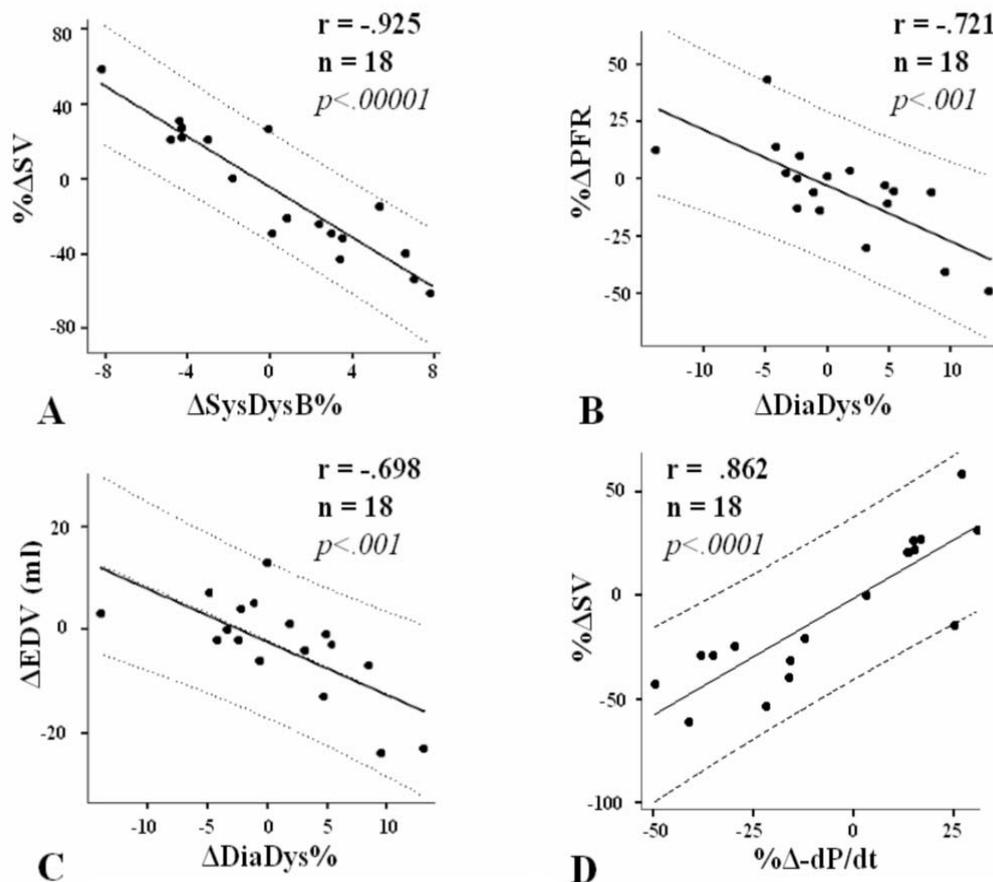
Figure 27. Regression diagrams showing changes in performance and dyssynchrony as observed within a 10s time-span from atrial to right ventricular pacing at worst pacing sites. Diagram A shows percent change in stroke volume (%ΔSV) versus left ventricular (LV) systolic dyssynchrony as measured from the ejection phase (ΔSysDysB); diagram B shows percent changes in LV peak filling rate (%ΔPFR) versus in change in LV diastolic dyssynchrony (ΔDiaDys); diagram C depicts changes in LV end-diastolic volume (ΔEDV) versus ΔDiaDys; diagram D shows %ΔSV versus percent change in –dP/dt$_{max}$. Dotted lines represent 95% prediction limits.

Discussion

This study shows beat-to-beat effects of RV pacing induced LV mechanical dyssynchrony on LV performance in patients with normal EF. At worst RV pacing site, the change in conduction pattern acutely increased systolic dyssynchrony during the ejection phase effecting subsequent decreases in SV, Ees and -dP/dtmax, and increased diastolic dyssynchrony and Tau, and

decreased PFR. These changes were effective within 3s and were followed by recovery of late systolic dyssynchrony and Ees within a 10s time-span and partial recovery of SV, EF, ESP, -dP/dtmax, and diastolic dyssynchrony. From 10s up to 60s no major changes in all measured variables occurred, except for improvement of the relaxation indices -dP/dtmax and Tau. These beat-to-beat results indicate dyssynchrony related cardiac dysfunction and suggest intrinsic dyssynchrony compensatory mechanisms, occurring within a 10s time-span.

Hemodynamic Evaluation and Stabilization
Acute hemodynamic effects of cardiac pacing are conventionally evaluated after stabilization episodes. The applied duration of stabilization periods in most cardiac pacing studies varied considerably, 30s by Hay et al, 1-2 min by Lieberman et al, 2 min by Kass et al (180,190,160). However, Aurricchio and colleagues observed that the LV paced-beat order had a significant effect on LV pressures and derivatives and pulse pressure responses, after an initial immediate increase in +dP/dtmax and pulse pressure both variables significantly decreased again after 2-3 paced beats (191). The present study shows similar reciprocal acute events for RV pacing in patients with normal EF and QRS duration. A profound decrease in cardiac performance and concomitant increase in mechanical dyssynchrony were observed immediately within 3s of RV pacing onset. Subsequently, compensatory mechanisms effected a total recovery of systolic dyssynchrony and Ees and partial recovery of SV, EF, ESP, -dP/dtmax, and diastolic dyssynchrony within 10s. Whereas no significant changes in systolic dyssynchrony could be detected from the averaged data of the first 10s (table 12), they were significantly present in the beat-to-beat analysis (table 13). Usage of any stabilization period prior to cardiovascular analysis may therefore mask acute positive or negative effects of cardiac pacing by compensatory mechanisms.

LV Mechanical Dyssynchrony
In this study we adopted indexes to quantify mechanical dyssynchrony derived by conductance catheter technique. In fact, it represents a unique tool to perform beat-to-beat evaluations, on the contrary techniques like echocardiography require beat averaging to derive indexes of dyssynchrony. For the same reason, among the indexes studied in this work we used DYS for this analysis. In fact, in addition to the good performances demonstrated in detecting dyssynchrony, it offers the highest temporal resolution. It quantifies the dyssynchrony beat-by-beat when estimated with the classical approach, and, within the beat, it allows the analysis of multiple phases of the cardiac cycle.
These considerations seem to emphasize the value of those indexes estimated over single beats, when immediate and transient effects have to be observed, that can be masked by the adoption of averaging techniques for the extraction of cardiac cycle templates.
RV pacing is known to induce LV mechanical dyssynchrony by altered activation sequence by temporal inhomogeneity inducing dyssynchrony based on impaired relaxation independent of preload and or afterload changes (28,192). Dyssynchrony of wall motion reduces mechanical efficiency of ventricular ejection by inducing premature onset and impaired relaxation (23). In patients with dilated cardiomyopathy (DCM), impairment of cardiac

performance is associated with impaired LV relaxation and diastolic and systolic ventricular mechanical dyssynchrony (82,140,145,189,190). LV mechanical dyssynchrony, as demonstrated in patients with DCM and left bundle branch block was shown to be a key predictor for multi-site pacing efficacy (104,40,82).

Patients with DCM and marked LV dyssynchrony showed decreases in LV mechanical dyssynchrony by wall stress reduction following vasodilator administration, cardiomyoplasty, intra-aortic balloon pump (IABP) or LV reduction surgery, emphasizing the relationship between load, wall stress and mechanical dyssynchrony (23,140,142,143,193). In heart failure patients undergoing premature intra-aortic balloon inflation during IABP, it was shown that systolic dyssynchony increase, evoked by late systolic increase of load, induced a premature onset and impaired relaxation (193). The present study demonstrated a marked increase in LV systolic dyssynchrony after onset of RV pacing followed by normalization within 10s, whereas diastolic dyssynchrony partially decreased after 3s, and remained stable at an increased level after10s throughout the 60s RV pacing sequence.

The markedly significant inverse correlation of systolic dyssynchrony versus SV (Fig 27A) from data measured during the first 10s of RV pacing indicates that systolic dyssynchrony, as measured from the ejection phase, is initially the most important determinant of SV as confirmed by multiple variate regression analysis.

The present study in normal hearts and the IABP study for failing hearts indicate that late systolic dyssynchrony changes not only may modulate instantly changes in SV, but also may have the capability to recover on a beat-to-beat basis (193). Moreover systolic dyssynchrony increase in a specific segment may be compensated by dyssynchrony decrease in another segment (Fig 25B, 26B). Changes in total diastolic dyssynchrony during the first 10s RV pacing inversely correlated with changes in PFR and EDV. This indicates that diastolic dyssynchrony is related to LV filling. Diastolic dyssynchrony also showed compensation as demonstrated by partial recovery at 10s after onset of RV pacing.

Simantrikis et al demonstrated by LV pressure-volume analysis an increased contractile state as measured by Ees during LV or biventricular pacing compared to RV pacing in atrial fibrillation patients with normal EF (174). In a previous study we demonstrated that contractile state as measured by Ees inversely correlated with changes in diastolic dyssynchrony in patients undergoing LV restoration (143). Also in the non-heart failure patients of the current study an inverse correlation between changes in diastolic dyssynchrony and Ees due to RV pacing is demonstrated. Decreased contractile state as measured by Ees has also been demonstrated in an animal RV pacing study by Burkhoff et al (28). Prinzen et al demonstrated in a RV animal study loss of contractile function in early activated ventricular regions, but also demonstrated hyperfunctioning in late activated zones (31). The current results confirm this compensation; basal RV pacing inducing immediate increased apical segmental filling and ejection, and apical stimulation showing reciprocal results (Fig. 25,26). At longer term, asynchronous activation de to RV pacing induces asymmetric hypertrophy and LV dilatation (194).

Ventricular Mechanical Dyssynchrony-Pathophysiology

According to Auricchio and Abraham, it is conceivable that ventricular mechanical dyssynchrony represents a newly appreciated pathophysiological process that directly depresses ventricular function and ultimately leads to ventricular dilation and heart failure (57). Brutsaert already demonstrated in normal animals that LV mechanical dyssynchrony may act as a physiologic modulator of cardiac performance together with heart rate, contractile state, preload and afterload (23). The present study, which shows this characteristic property of mechanical dyssynchrony in patients with normal EF, confirms results from previous studies in patients with heart failure (104,143,193). Mechanical ventricular dyssynchrony may therefore be regarded as an intrinsic cardiac property, with baseline dyssynchrony at increased level in heart failure patients.

As can be derived from the fast changes in systolic dyssynchrony, from beat-to-beat during the onset of RV pacing, the heart may control ejection duration by changes in systolic dyssynchrony. In direct relationship with changes in systolic dyssynchrony are changes in diastolic dyssynchrony, possibly with the ability to change cardiac function by adjusting filling rate and EDV.

Limitations of the Study

The current results should be interpreted within the constraints of certain potential limitations. We analyzed beat-to-beat hemodynamic effects occurring only within 60s after initiation of RV pacing in patients with normal EF and normal QRS duration and only at a single heart rate.

Conclusions

The usage of stabilization periods during evaluation of cardiac pacing may mask early changes in systolic and diastolic intra-ventricular dyssynchrony. The present study demonstrated a direct relationship between systolic and diastolic LV mechanical dyssynchrony and LV performance induced by RV pacing in patients with normal EF and normal ORS duration. The main LV dyssynchrony and performance related changes occurred within a 10s time span initiated by changes in ventricular mechanical dyssynchrony induced by aberrant conduction. Systolic ventricular dyssynchrony was best predictor of SV changes and showed total compensation between 3-10s after RV pacing onset. Diastolic dyssynchrony showed instant increases and compensation between 3-10s after RV pacing onset, and was markedly correlated with PFR and LVEDV.

7. Cardiac Output Derived From Left Ventricular Pressure During Conductance Catheter Evaluations: an Extended Modelflow Method

Introduction

In 1981, Baan et al. introduced a multi-electrode conductance catheter (113) for real-time continuous ventricular volume measurements. The electrodes divide the ventricular volume into parallel segments perpendicular to the long heart axis and measure the electric conductance of each segment. The segmental volume is proportional to the segmental conductance and total ventricular volume can be computed by summing the segmental volumes. However, conductive tissues and fluids surrounding the ventricle affect the measure introducing an offset in the conductance signal, i.e. parallel conductance. When parallel conductance is not quantified, only changes in conductance as a measure of changes in volume can be presented (113,118,120). To extend the conductance method to absolute volume measurements, some calibration methods have been introduced (114,123).

The conductance catheter technique was shown to accurately measure ventricular volume with high time resolution over single cardiac cycles (113,114,118,120,123,128). Nonetheless, as emphasized by Schreuder et al. (141), the concomitant use of an independent system for cardiac output (CO) estimation is advisable to confirm the results obtained with conductance volume method concerning the situations where the CO measure can be affected by the presence of artifacts. A possible approach is the simultaneous use of CO estimation from pressure signal analysis methods such as the Modelflow (195). According to Wesseling et al. (195), this method derives an aortic flow waveform from arterial pressure by simulation of a non-linear three-element aortic input impedance model, estimates stroke volume (SV) by integrating the flow waveform and calculates CO by multiplying SV by the heart rate. This method was demonstrated to reliably monitor CO changes in a wide range of hemodynamic states and to precisely estimate absolute values of CO after calibration (196).

The implementation of the Modelflow method requires the acquisition of the aortic pressure (Pao) signal that, during conductance measurements, can be obtained inserting a second micromanometer catheter in aorta or using a dual pressure sensor conductance catheter, which is not widely available.

In this paper, we propose to derive aortic flow waveform from the left ventricular pressure (Plv) by using a modified version of the Modelflow method, to obtain a simplified independent estimation of CO in the setting of conductance measurements.

Methods

The model

The aortic Modelflow method (MFao) computes relative CO from Pao (CO-MFao) using a nonlinear, time-varying three-element Windkessel model (195). The model includes aortic characteristic impedance (Z0), arterial compliance (Cw), and systemic vascular resistance (Rp) (Figure 28). Z0 and Cw depend on the aortic cross-sectional area, which can be estimated from mean arterial pressure, age, and sex by means of the arctangent model of Langewouters et al. (197). However, these estimations although precise are not highly accurate and the absolute value of the estimated CO remains uncertain, unless calibration against another method of measurement such as thermodilution is performed or a measurement of aortic diameter is introduced (198).

For each beat, Rp is obtained as the ratio of mean Pao and the CO estimated from the previous beat, minus the current value of Z0. With this scheme, the model can follow changes in systemic peripheral resistance that occur with a time constant which is typically about 10s.
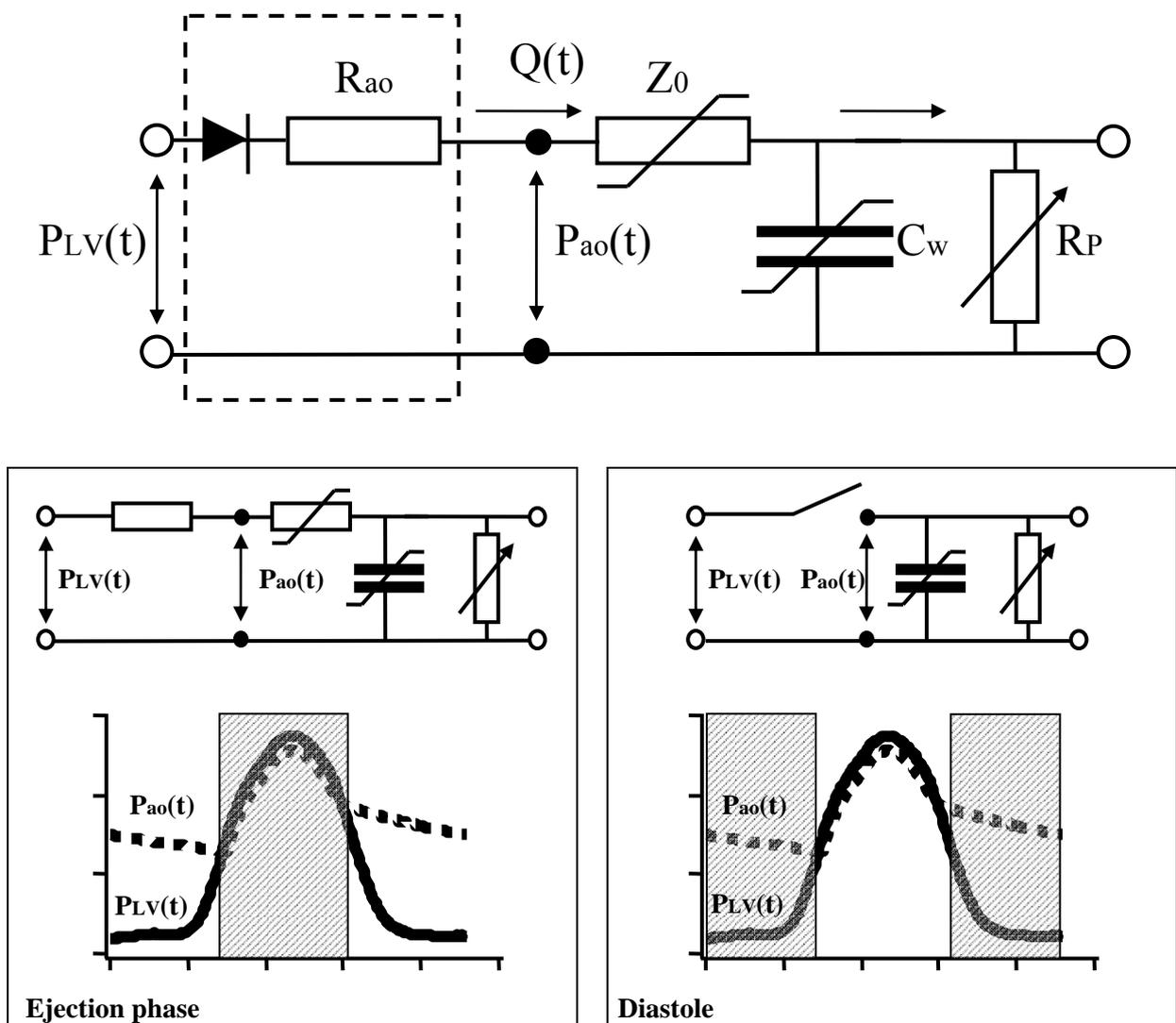
Figure 28. The standard Modelflow method uses a nonlinear, time-varying three-element Windkessel model: aortic characteristic impedance (Z0), arterial compliance (Cw), systemic vascular resistance (Rp), aortic flow (Q(t)). To describe the aortic valve the model has been extended (dashed box). In ejection phase it includes an extra linear impedance (Rao), while in

diastole Q(t) is zero: an estimated aortic pressure (Pao) is determined by the discharge of Cw over Rp, from the initial value recorded at the time of end-systole.
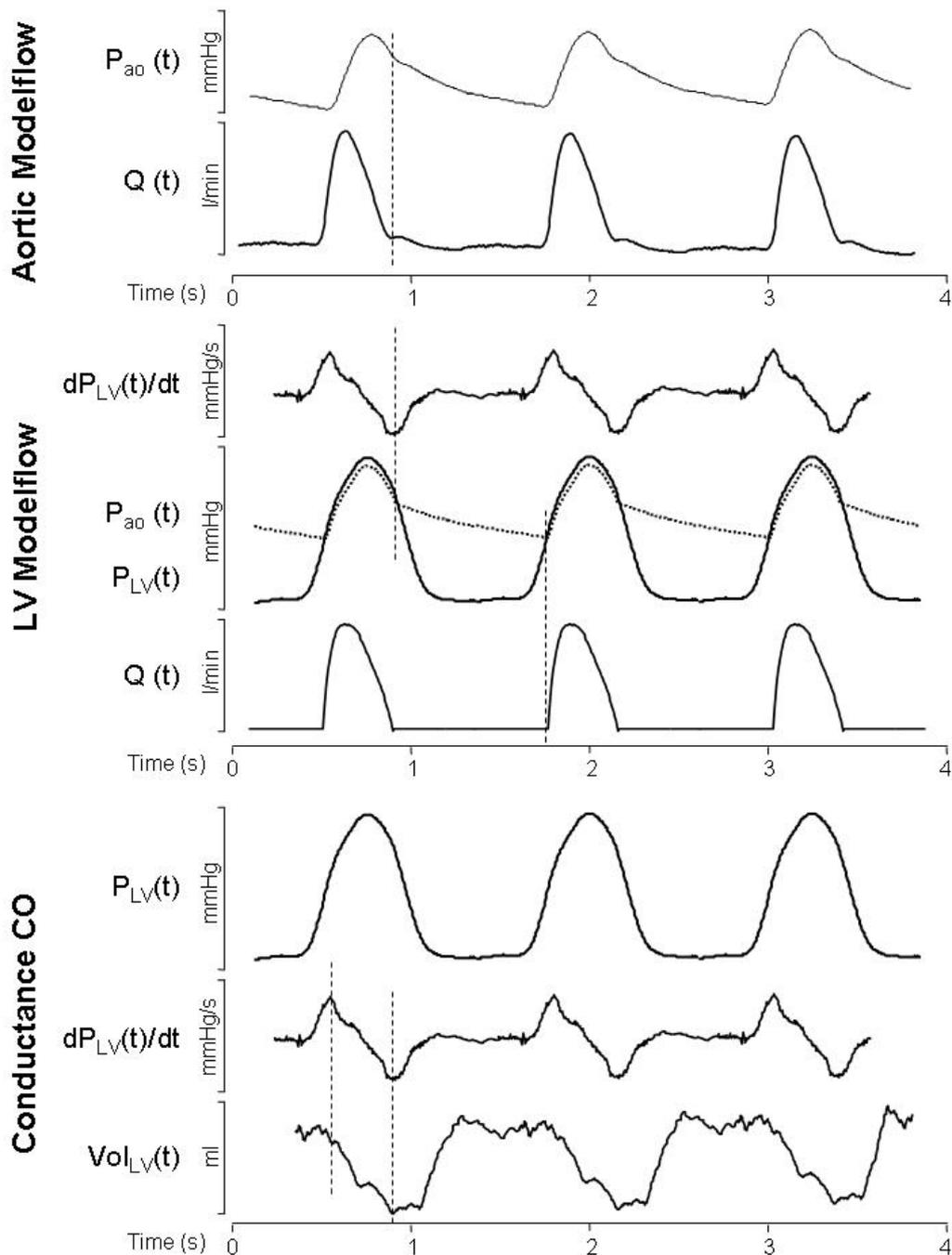
Figure 29. Acquired signals and waveforms generated with the three methods. **Aortic Modelflow:** acquired aortic pressure (Pao(t)) and estimated aortic flow signal (Q(t)). The dicrotic notch is detected by identifying the first local minimum of Q(t) after peak flow. **LV Modelflow:** acquired LV pressure (Plv(t)) and its first derivative (dPlv(t)/dt), estimated aortic pressure (Pao(t)) and aortic flow signal (Q(t)). The end-systolic time is identified considering the negative dPlv/dt maximum, while the time when the Plv signal, during its systolic increase, crosses the simulated Pao signal identifies the start of systole. **Conductance CO:** acquired LV pressure (Plv(t)), its first derivative (dPlv(t)/dt) and LV volume by conductance measurement (Vol lv(t)). In order to eliminate contribution of possible regurgitant flows, effective conductance SV is defined as the difference between conductance volumes at the times of positive dPlv/dt max and negative dPlv/dt max.

To permit the computation of CO from Plv signal (CO-MFlv), we extended the described model simulating the aortic valve (Figure 28, dashed box). The first assumption of our model is the absence of systolic mitral regurgitation as the model computes forward flow into the aorta and ignores eventual backward flow. Moreover, we assumed a fixed value resistance (Rao) for the patent aortic valve placed in series to Z0 during the ejection phase (Figure 28, left panel). In diastole (Figure 28, right panel) we considered the absence of leakage (infinite resistance): the absence of aortic flow immediately after aortic valve closure and an estimated Pao determined by the discharge of Cw over Rp, from the initial value recorded at the time of end-systole.

In our model the time of end-systole, which in MFao is detected at the first local minimum in the aortic flow signal after peak flow (199-201) in correspondence of the dicrotic notch, is selected as the time of negative dPlv/dt max. The time of the start of systole is determined by the crossing of simultaneously increasing Plv and the decreasing estimated Pao (Figure 29).

In order to characterize the Rao, instead of using an arbitrary fixed value, the following procedure is proposed. The typical approach for conductance catheter placement is the retrograde insertion via the femoral artery. Before accessing the left ventricle (LV), the Pao can be recorded using the LV catheter micromanometer. A second acquisition is then performed with the catheter in the final location and the transducer placed in LV. Thus, the Rao value can be determined as the mean difference of Plv and Pao during the systolic phase divided by the CO-MFao estimated from the Pao recording.

Once characterized Rao, its value is entered into the model and the aortic flow can be obtained simulating digitally the non-linear model. CO-MFlv is then computed by integrating the flow during systole and multiplying by heart rate.

Usually, before conductance volume acquisitions, a thermodilution CO measurement (COtd) is carried out as part of the initial calibration procedure. This result can be also applied for CO-MFlv calibration, which was shown to improve the accuracy of the method by reducing the uncertainty in the patient's aortic diameter (196) and is performed by multiplying CO-MFlv and CO-MFao by a calibration factor Klv = COtd / CO-MFlv and Kao=COtd/CO-MFao.

Patients and Materials
21 patients with heart failure, undergoing biventricular pacing device implantation for cardiac resynchronization therapy, were studied at the time of the procedure. The Ethical Committee approved the protocol and all patients gave their informed consent to participate in the study (Table 14).

Patients were mildly sedated with midazolam 5–10 mg. They all received right auricular, right ventricular and LV leads (Capsure Model 5334, Capsure Model 5534 and Attain Model 2187, respectively, Medtronic Inc, Minneapolis, USA). The LV lead was placed in a lateral or posterolateral LV coronary vein.

After permanent stimulation catheters were placed, through the femoral artery a 7-Fr combined pressure-conductance catheter with 1-cm interelectrode spacing (CD Leycom; Zoetermeer, The Netherlands) was positioned in the LV and a micromanometer catheter (Millar No. SPC-474A, Millar Instruments, Houston, TX) was advanced to the aorta. The catheters were connected to a

Cardiac Function Lab (CD Leycom) for online display and acquisition (sample frequency 250 Hz). LV volume was calibrated using thermodilution and hypertonic saline dilution, as previously described (114). Effective conductance SV was defined as the difference between conductance volumes at the times of positive dPlv/dt max and negative dPlv/dt max (Figure 29), which largely eliminates contribution of possible regurgitant flows. Conductance CO (COcond) has been then estimated by SV × heart rate.

The simulation and the data analysis were performed with a custom-made software developed in LabVIEW 5.1 (National Instruments, Houston, TX, USA).

Table 14. Demographics and baseline clinical parameters.

Patient	Age (years)	Gender	Etiology	NYHA Class	EF (%)	LVEDD (mm)	Conduction defect	QRS width (ms)
1	67	f	ISC	3	16	80	LBBB	145
2	68	f	ISC	3	30	60	LBBB	150
3	70	m	ISC	3	33	57	LBBB	160
4	64	m	DCM	4	26	63	LBBB	180
5	81	m	DCM	2	34	60	LBBB	140
6	58	m	DCM	3	25	65	LBBB	170
7	80	m	ISC	3	30	69	RBBB	160
8	68	m	DCM	3	23	65	LBBB	160
9	76	m	DCM	3	22	67	LBBB	180
10	63	f	DCM	4	27	56	RV Pace	205
11	64	m	ISC	4	15	80	RBBB	200
12	70	m	ISC	3	25	56	RV Pace	200
13	64	f	ISC	3	25	51	LBBB	120
14	70	m	DCM	3	23	48	LBBB	170
15	64	m	DCM	3	33	78	LBBB	165
16	78	m	DCM	3	40	70	RBBB	160
17	76	f	ISC	3	28	59	LBBB	160
18	68	m	ISC	3	25	65	LBBB	180
19	62	f	DCM	2	38	57	LBBB	180
20	70	m	ISC	3	25	78	LBBB	180
21	69	m	DCM	3	28	63	LBBB	170
mean (SD)	69 (6)			3.0 (0.5)	27 (6)	64 (9)		168 (21)

NYHA = New York Heart Association; EF = Ejection fraction; LVEDD = Left ventricular end-diastolic diameter; f = female; m = male; ISC = Ischemic; DCM = Dilated cardiomyopathy; LBBB = Left bundle branch block; RBBB = Right bundle branch block; RV Pace = LBBB induced by right ventricular pacing.

Measurement Protocol

Hemodynamic tests were performed during temporary stimulation both in dual chamber pacing (DDD mode - 5 bpm over spontaneous sinus rate) and, when feasible, in atrial tracking ventricular pacing (VDD mode). The interval between right atrial pacing (or sensing) and right ventricular pacing (A-V interval) and the interval between right and left ventricular pacing (V-V interval) could be programmed independently: it was previously shown that significant hemodynamic changes are obtained with sequential biventricular pacing (202) and present test was performed to study the acute response to multisite pacing by pressure-volume plane analysis

In each patient, we performed acquisitions at baseline and for each combination of different A-V (ranging from 80 ms to 160 ms, with steps of 20 ms) and V-V (from -60 ms to 40 ms, with steps of 20 ms), in DDD and VDD mode. For each step, a 30 s recording period was preceded by a stabilization period of 30 s. All measures were averaged over 10-15 cardiac cycles after extrasystolic beats were removed from analysis. During offline analysis some recordings were discarded due to excessive arrhythmic beats.

We compared CO-MFlv values with standard CO-MFao and COcond measures. In the first series, during unpaced sinus rhythm, Pao and Plv recordings were used to characterize Rao as described before. In this phase COtd, estimated during conductance calibration, was also used to calibrate CO-MFao and CO-MFlv through multiplication by a patient individual calibration factor ($Kao = COtd / CO\text{-}MFao$ and $Klv = COtd / CO\text{-}MFlv$ respectively).

Statistical Analysis

Data averages are given as mean and standard deviation (SD). Limits of agreement were computed plotting differences in data pairs against their average (Bland-Altman plots) (203). The agreement between the two models is computed as the bias (mean), with limits of agreement computed as bias $\pm$ 2SD when differences followed normal distribution. Normality was tested with the Kolmogorov-Smirnov one-sample test. The coefficient of variation was computed as $CV = (SD/mean) \times 100\%$.

Moreover, to investigate the ability of MFlv to track changes in CO, a trend score was derived. If both CO-MFao and CO-MFlv simultaneously indicate a positive trend from baseline values, the changes compare positively and a positive score is counted. If both show a negative trend, they again compare positively. When the changes in CO are in opposite directions they compare negatively and a negative score is counted. Separate scores were made for all changes regardless of size, and also for changes where CO-MFao values differed by at least 0.5 l/min, which is considered clinically relevant. The Kappa statistic and its standard error (SE) were calculated to measure the agreement between MFao and MFlv measures of CO changes.

All statistical analyses were performed using SPSS software (SPSS for Windows, version 12.0, SPSS Inc., Chicago, IL, USA).

Results

In 21 patients a total of 680 measures of acceptable quality were obtained during a median test time of 1 h 30 min. In 6 patients conductance volume

signal was not available and only pressure signals were acquired. Arrhythmias caused rejection of 143 acquisition series. Thus, excluding the 21 acquisitions used to calibrate the methods, 516 series remained for comparisons between CO-MFlv and CO-MFao. For the comparisons between CO-MFlv and COcond, 267 series were available.

In Figure 29 the acquired signals and the waveforms generated with the three methods are reported, in addition to the markers identifying the end-systolic and start systole timing points, as estimated by MFao, MFlv and conductance method. For standard MFao method, the Pao signal and the obtained aortic flow are shown. To describe MFlv method, the Plv is reported together with its first derivative that is used to identify the end-systolic point and to estimate the Pao signal. By applying the method described above, the aortic flow is then obtained. It can be noted that, the Pao waveform estimated through MFlv is similar to the real Pao also in the diastolic phase when the aortic valve is closed and the curve is completely determined by Cw and Rp. Consequently, also the aortic flow signals estimated with the two methods are similar.

Finally, with conductance method, the LV volume and the Plv are acquired and the first derivative of this latter is used to identify the end-systolic and end-diastolic volumes for COcond measurement.

Table 15 summarizes the results obtained in our patients: the ranges of CO during test, the estimated Rao, the differences between CO-MFlv and CO-MFao estimations with the errors in end-diastolic and end-systolic timing points identification and the differences between CO-MFlv and COcond estimations. The data are presented in two fashions: averaged per patient and then pooled for the group, and with all the measurements pooled.

The overall mean CO was 4.36 (1.38) l/min. Our multisite ventricular stimulation protocol produced large changes in the hemodynamic state of patients: within patients CO ranged up to 2:1 ratio during the tests, while pooling all series the range ratio for CO was 3:1.

Comparing the two Modelflow methods, the absolute error ranged from -0.27 l/min to 0.31 l/min, with a SD ranging from 0.17 l/min to 0.52 l/min. The mean absolute error for pooled data, i.e. bias (SD), was -0.04 (0.36) l/min, with limits of agreement of -0.77 and 0.70 l/min, and a coefficient of variation of 8.4%.

For the comparisons between CO-MFlv and COcond, the mean absolute error ranged from -0.52 l/min and 0.29 l/min, with a SD ranging from 0.13 l/min to 0.79 l/min. The bias was -0.10 (0.49), with limits of agreement of -1.12 and 0.90 l/min, and a coefficient of variation of 12.5%.

The Kolmogorov-Smirnov test for the difference between CO estimations (CO-MFlv Vs. CO-MFao and CO-MFlv Vs. COcond) did not indicate a significant deviation from normal distributions.

Figure 30 (panels a and b) summarizes the results obtained with pooled measures. Panel a shows scatter plot of the 516 series. Panel b shows Bland-Altman plot with the difference between CO-MFlv and CO-MFao versus their mean. The 19 largest differences, those outside the limits of agreement were recorded in 4 patients.

Table 15. Cardiac output estimation with MFlv versus standard MFao and conductance CO.

Patient	N of Series	min CO (l/min)	max CO (l/min)	Rao (mmHg*s/l)	CO-MFlv Vs CO-MFao			CO-MFlv Vs COcond CO dif (l/min)
					CO dif (l/min)	SS-point error (ms)	ES-point error (ms)	
1	12	2.65	4.33	5.0	-0.27 (0.28)	24.9 (4.1)	28.4 (15.4)	-0.09 (0.60)
2	20	2.77	3.43	6.6	-0.25 (0.20)	35.9 (2.9)	5.3 (3.9)	-0.07 (0.40)
3	37	2.82	3.52	7.1	-0.03 (0.28)	28.2 (3.8)	23.8 (6.9)	-0.01 (0.32)
4	16	2.85	3.39	4.8	0.02 (0.31)	19.2 (3.9)	25.4 (5.1)	-0.08 (0.79)
5	41	3.25	5.78	4.6	0.00 (0.42)	34.3 (3.4)	33.9 (8.4)	-0.37 (0.31)
6	20	4.12	4.85	4.5	-0.14 (0.33)	26.0 (2.6)	31.1 (4.4)	0.29 (0.46)
7	3	3.31	3.39	6.4	0.09 (0.17)	11.8 (3.7)	28.8 (1.3)	0.21 (0.28)
8	13	2.66	3.60	7.6	-0.20 (0.27)	36.1 (15.6)	19.0 (17.5)	-0.04 (0.35)
9	22	2.87	5.01	7.7	0.31 (0.26)	12.8 (8.8)	22.5 (10.0)	0.03 (0.46)
10	23	3.82	4.85	6.7	0.31 (0.22)	27.0 (3.1)	28.6 (2.6)	-0.04 (0.40)
11	47	5.33	7.30	5.7	-0.19 (0.47)	17.4 (4.7)	21.1 (2.6)	-0.52 (0.59)
12	33	2.42	2.81	7.2	0.05 (0.20)	5.0 (2.9)	26.5 (2.5)	-0.06 (0.33)
13	27	3.38	4.52	4.9	0.18 (0.20)	24.8 (2.1)	26.0 (1.8)	0.04 (0.13)
14	21	2.97	3.55	5.2	-0.16 (0.22)	29.3 (2.8)	29.0 (3.1)	-0.11 (0.41)
15	38	2.73	3.59	7.4	-0.21 (0.23)	26.5 (7.4)	20.9 (7.7)	0.02 (0.40)
16	12	3.87	4.50	6.3	-0.17 (0.24)	32.8 (4.5)	35.2 (8.6)	
17	36	3.83	7.33	8.1	-0.12 (0.43)	35.9 (2.6)	29.3 (10.3)	
18	35	5.09	7.59	7.8	0.00 (0.42)	33.3 (4.9)	30.6 (15.6)	
19	44	2.85	3.88	5.5	-0.09 (0.26)	28.5 (2.9)	32.3 (8.5)	
20	17	3.01	3.98	8.9	0.08 (0.25)	24.6 (10.5)	37.5 (10.6)	
21	20	3.35	7.51	8.3	0.16 (0.52)	38.9 (10.4)	26.4 (13.3)	
patient means (SD)		3.33 (0.78)	4.70 (1.52)	6.49 (1.35)	-0.03 (0.17)	26.4 (8.9)	26.7 (6.8)	-0.05 (0.20)
pooled means (SD)					-0.04 (0.36)	28.0 (12.6)	31.8 (24.5)	-0.10 (0.49)

N of Series = Number of acquisition series, including the series used to calibrate the methods; min CO = Minimum cardiac output recorded; max CO = Maximum cardiac output recorded; Rao = Estimated value of aortic valve resistance in systolic phase; CO dif = Differences between CO estimations; SS-point error = Difference in start-systolic time estimations between Modelflow methods; ES-point error = Difference in end-systolic time estimations between Modelflow methods.

In Figure 30 (panels c and d) the Bland-Altman plot analysis is reported for CO-MFlv Vs. COcond comparison, 10 differences lie outside the limits of agreement and were obtained in 3 patients.

Of the 516 changes in CO from baseline values, 388 (75%) were scored in the same direction by both methods. Of 112 changes greater than 0.5 l/min, 110 (98%) were indicated correctly in direction by MFlv. In both cases, the Kappa statistical analysis confirmed the presence of agreement between CO-MFlv and CO-MFao: k=0.509 with SE=0.037 (p<0.001) and k=0.964 with SE=0.025 (p<0.001), respectively.
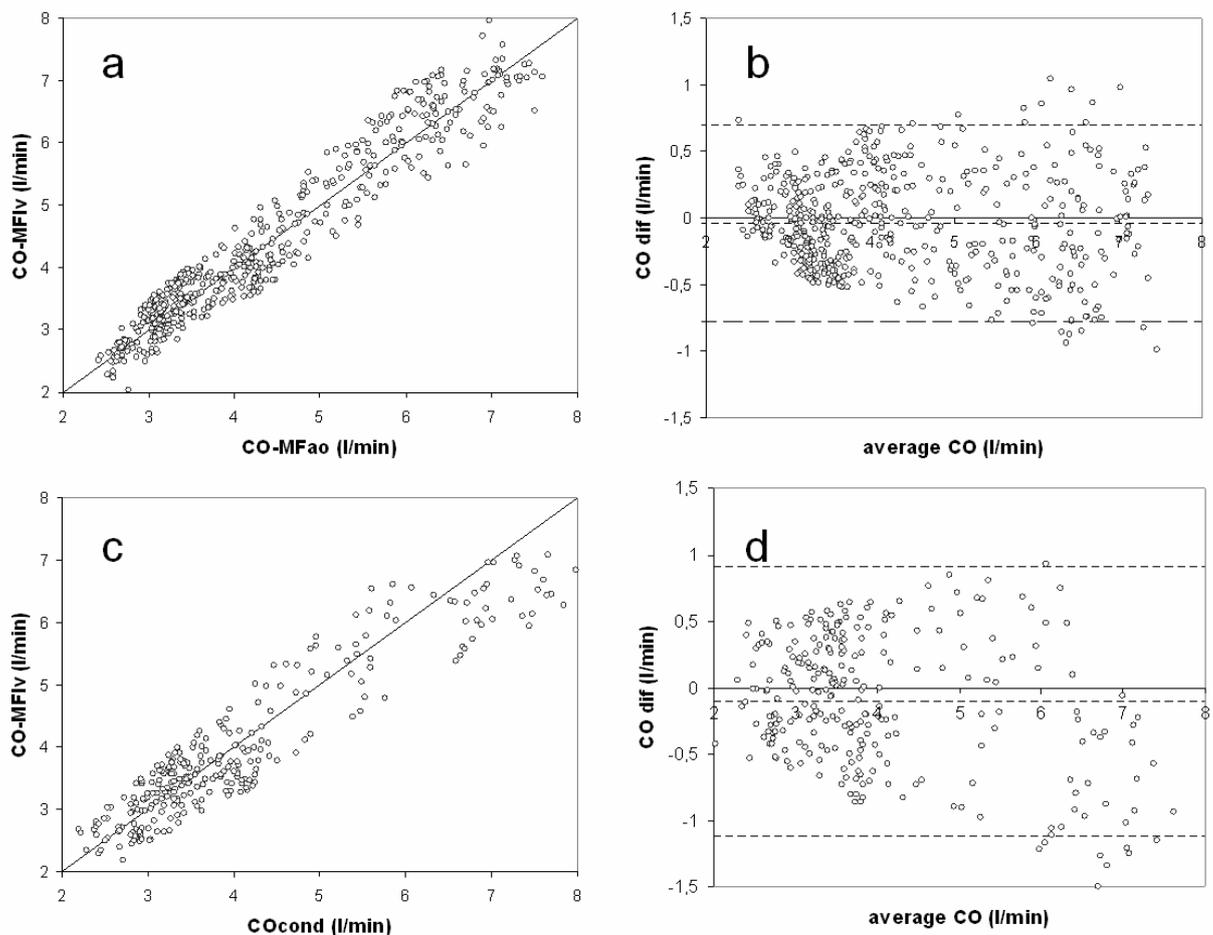
Figure 30. Diagrams showing the data pairs in all 21 patients (n=516) [**Panel a**] and in the 15 patients with conductance measurements (n=267) [**Panel c**]. In the Bland-Altman plots: COdif = CO-MFlv – CO-MFao [**Panel b**] and CO-MFlv - COcond [**Panel d**], average CO is their mean. The dashed lines indicate the bias and limits of agreement between methods.

In MFlv method, as well as in conductance estimation, the end-systolic point is identified by the time of negative dPlv/dt max and in our tests occurred at a mean of 31.8 (24.5) ms from the dicrotic notch, as predicted by MFao (Table 15).

With respect to the onset of the aortic flow obtained with MFao, the start systolic point occurred at 28.0 (12.6) ms in MFlv, and at 36.4 (8.3) ms in conductance estimation (time of positive dPlv/dt max) (p=0.045). The duration of the ejection phase as estimated by MFlv was 12.8 (27.7) ms shorter than with MFao.

Discussion

Modelflow method, with Pao signal analysis, demonstrated to provide continuous precise estimations of CO after calibration (196). The measurement of CO from the Plv signal can be extremely useful as an independent method during conductance catheter evaluations (141), or to

permit CO estimation whenever a single pressure transducer is positioned in LV for quantifying the contractile state by measuring the dPlv/dt.

In this study we presented a method for Modelflow computation from the Plv signal. CO estimation is of clinical importance for patients with heart failure. In addition, recently, many studies described the effects of cardiac pacing for the treatment of heart failure patients using conductance volume catheter technique (63,188,189). For these reasons we performed the study in patients undergoing biventricular pacing device implant for cardiac resynchronization therapy.

Thermodilution is the reference CO method in almost all studies. A single thermodilution estimate of CO has a coefficient of variation (error) of 15–20%, while a triplicate, phase-spreading injection technique has an error of 6% as the result of averaging. Thus, as stated by Critchley and Critchley (204), it is against these levels of inherent error that any new method of CO measurement has to be judged.

Unfortunately in this study we were not able to assess directly the error between our method and COtd. Conversely, for all tested series we compared CO-MFlv estimation with the standard CO-MFao, that is the method to be replaced, and versus the COcond. CO-MFlv differed -0.04 (0.36) l/min on average from CO-MFao, with limits of agreements of -0.77 and 0.70 l/min, which are within the limits of acceptability for clinical use.

The error of the comparison C of two estimations A and B can be computed as Variance (C) = Variance (A) + Variance (B) (204).

The error that we measured comparing the two Modelflow methods is around 8.4%, while the error of the standard MFao has been demonstrated to be 7% (196). However, considering the similarity of the two methods, we cannot assume their errors statistically independent, thus a covariant component needs to be added to the formula (i.e. Variance (C) = Variance (A) + Variance (B) - 2 Covariance (A,B)) (204).

The equation can be solved considering that Covariance (A,B) $\leq \sqrt{}$ Variance (A) $\times \sqrt{}$ Variance (B) and from this relation we can just conclude that the error of CO-MFlv Vs. COtd is between 7% and 16%.

On the contrary, due to the different mechanisms behind the two methods, when CO-MFlv and COcond are compared their measurement errors can be considered statistically independent.

From the data available in (133), where the accuracy of the conductance method to determine SV was tested by comparison with thermodilution, we can assume an error of around 11% for COcond measurement. Approximately, the error we found between the CO-MFlv and COcond is 13%. Thus we can conclude that CO-MFlv presents an error of $\sqrt{169-121}=7\%$, which is comparable to the probable error estimated for standard CO-MFao (196), and may therefore replace it.

Moreover, apart from quantitative estimation of CO, we found a good agreement between MFao and MFlv measures of directional CO changes, demonstrating that the MFlv can reliably track trends in CO.

A correct identification of beat-to-beat start and end systolic times is crucial for the accuracy of the proposed method. Many techniques were proposed in literature to identify the aortic valve closure by detecting the dicrotic notch from Pao signal (205). In particular, Modelflow method was used to detect and predict the dicrotic notch, by calculation of the aortic flow and identification of

its first local minimum after peak flow (Figure 29). This method demonstrated to be accurate in animal and man, during both regular rhythm and arrhythmic episodes (199-201), providing adequate results as system for real time intra aortic balloon pump inflation timing control.

In MFlv the end-systolic time is identified considering the negative dPlv/dt maximum, i.e. the point generally used in conductance CO measurements in order to eliminate contribution of possible regurgitant flows (Figure 29).

For the detection of start systolic time, we considered the time when the Plv signal, during its systolic increase, crosses the simulated Pao signal, that is determined by the discharge of the capacitor Cw (Figure 29). Other options could be the use of the ECG signal for R-waves identification or the use of the time of positive dPlv/dt max (as used in conductance CO) or the zero-crossing point of the dPlv/dt signal, as recently proposed (157). Our approach, with respect to the use of positive dPlv/dt max, resulted in significantly shorter delays, while other methods were not directly tested in this work. In our method both start and end systolic times were detected around 30 ms in advance with respect to the timing points identified by MFao, due to the phase shift of the two pressure curves. Whereas considering the ejection phase duration, the two estimations differed only 12.8 (27.7) ms.

The proposed calibration procedure permits to determine the appropriate Rao value, instead of using an arbitrary fixed value. The conductance catheter is usually placed in LV with retrograde insertion via the femoral artery. Thus, the Pao acquisition, performed before accessing LV to estimate the Rao value, does not increase the complexity of the procedure. Nonetheless, in this work we did not study specifically the sensitivity of the results to the changes in Rao.

Limitations

In this study, measurements were only used whenever heart rhythm was regular. Because many heart failure patients show frequently arrhythmia, the new method should be tested also in this condition, by comparison with a method insensitive to irregularities in heart rhythm.

A potential limitation of the method is the patient selection. Similarly to the standard aortic Modelflow method, it is required that patients have patent aortic valves and no aortic aneurysms. An aneurysm affects a patient's aortic compliance. A patent aortic valve is required for proper model CO computation as the model computes forward flow into the aorta and in regurgitation ignores backward flow. For similar reasons, as mentioned above, a second assumption for the CO-MFlv analysis is the absence of systolic mitral regurgitation.

The patients selected for our study were candidates to resynchronization therapy, these patients typically present intraventricular conduction delays that induce most frequently pre-systolic mitral regurgitation due to a lengthening of the pre-ejection time: this kind of regurgitation should not affect the precision of the method.

Conclusions

In patients without mitral valve and aortic abnormalities, undergoing conductance catheter evaluations, the continuous monitoring of CO using the

intra-ventricular pressure signal seems reliable. CO can be monitored quantitatively and continuously with a simple and low-cost method.

After an initial calibration that can be executed simultaneously and automatically during conductance calibration, this method presents near zero bias and an acceptable precision sufficient to replace conventional aortic Modelflow estimations.

Conclusions and Future Works

Dyssynchrony exacerbates heart failure in a variety of ways, generating cardiac inefficiency as well as pathobiologic changes at the tissue, cellular, and molecular levels.

CRT reduces symptoms in heart failure patients, improves cardiac structure and function, and decreases all-cause as well as heart failure morbidity and mortality. However, the individual response to the therapy varies considerably among patients fulfilling current CRT indications, and numerous works suggested that the positive response to CRT may be predicted by the presence of extensive dyssynchrony.

Dyssynchrony is commonly identified by a prolonged QRS duration with left bundle-branch block morphology on surface electrocardiogram. Moreover, various indexes based on magnetic resonance imaging or echocardiographic measurements are being used to quantify ventricular dyssynchrony. However, these methods are laborious and require substantial operator interaction and expertise.

Recently, novel indexes were introduced to quantify dyssynchrony based on volume signals acquired with the conductance catheter during cardiac catheterization. This method is invasive but offers several advantages. The results are obtained immediately, and precise geometric assumptions regarding the ventricle or labor-intensive analyses are not required.

Moreover, volumetry by conductance catheter permits to acquire real-time signals with high temporal resolution. It does not present the limitations of techniques like MRI or echocardiography that require beat averaging to derive indexes of dyssynchrony, masking all possible components associated with beat-to-beat hemodynamic variations.

In this study, the extraction of the new indexes permitted to identify two components of ventricular dyssynchrony. The first component is represented by the inhomogeneities of cardiac contraction and relaxation that occur repetitively and that can be described and quantified by coherent averaging-based indexes.

The second component corresponds to the non-recurrent mechanical inhomogeneities that are in part quantified by the classical time-domain indexes estimated from each beat or, more specifically, by the indexes extracted by the residual signal and the parameters in the frequency domain.

These non-recurrent mechanical ventricular non-uniformities are probably the expression of the substantial beat-to-beat hemodynamic variations, often associated with heart failure and due to cardiopulmonary interaction and conduction disturbances.

In present work, the complete set of conductance catheter-based indexes of dyssynchrony was used to describe the acute effects of pacing therapies. The analysis of the changes of hemodynamic variables, in agreement with the literature, demonstrated a marked improvement of the cardiac function following CRT, in patients with ventricular dysfunction.

The analysis of the indexes of dyssynchrony demonstrated that these indexes are able to detect the reduction of internal ineffective flows, the inhomogeneity during isovolumic contraction and relaxation as well as the decrease of the

beat-to-beat variations that seem associated to the spontaneous activation, in presence of ventricular dysfunction and left bundle branch block.

Moreover, we observed a significant correlation between the acute changes in stroke volume induced by the pacing and the changes of dyssynchrony, as estimated by the indexes under study.

This result may have practical implications for pacing therapy delivery. In fact, some authors advocated the need to perform a patient tailoring of pacing site, due to the considerable inter-patient variation in the hemodynamic response to pacing. The identification of parameters associated to the hemodynamic improvement may help in guiding the implant optimization.

Moreover, using our new indexes of dyssynchrony we observed that right ventricular pacing worsens cardiac function unless the pacing site is optimized, and that pacing site may influence overall global ventricular function depending on its relative effects on regional function and synchrony.

Similarly, we demonstrated that in CRT the right ventricular pacing site that produces the optimal acute hemodynamic response varies between patients.

Using conductance catheter method we also showed that the stabilization periods that are usually applied to study the acute hemodynamic effects of cardiac pacing and that in most studies varied considerably, significantly affect the results of the analysis and thus have to be standardized to permit the comparison of results.

The results obtained with this work should represent the background for the development of an automated system for optimal pacing lead delivery.

In fact, recently systems have been designed to enable physicians to complete more complex interventional procedures by providing image guided delivery of catheters through the blood vessels and chambers of the heart to treatment sites. This is achieved using computer-controlled, externally applied magnetic fields that govern the motion of the working tip of the catheter, resulting in improved navigation, shorter procedure time and reduced x-ray exposure.

This tool, together with a reliable and operator-independent system for hemodynamic evaluations, a set of indexes exhaustively describing the cardiac function and the effects of the intervention, and an efficient measurement protocol, constitute the required components of an automated closed-loop system for lead delivery.

Obviously, it will become mandatory to verify the role of automated and optimized ventricular lead placement for cardiac pacing with a prospective, randomized outcomes-based clinical study. The study should compare this optimized lead implant with conventional lead implant techniques to determine the difference in chronic response to the therapy.

References

1. Hunt SA, Abraham WT, Chin MH, et al. ACC/AHA 2005 guideline update for the diagnosis and management of chronic heart failure in the adult: summary article: a report of the American College of Cardiology/American Heart Association Task Force on Practice Guidelines (Writing Committee to Update the 2001 Guidelines for the Evaluation and Management of Heart Failure). Circulation 2005;112: 1116-1143.

2. Francis GS, Pierpont GL. Pathophysiology of congestive heart failure secondary to congestive and ischemic cardiomyopathy. In: Shaver JA, ed. Cardiomyopathies: Clinical Presentation, Differential Diagnosis, and Management. Philadelphia, Pa: FA Davis; 1988:57-74.

3. Packer M, Cohn JN, Abraham WT, et al. Consensus recommendations for the management of chronic heart failure. Am J Cardiol 1999;83:1A–38A.

4. Knight BP, Goyal R, Pelosi F, et al. Outcome of patients with nonischemic dilated cardiomyopathy and unexplained syncope treated with an implantable defibrillator. J Am Coll Cardiol 1999;33:1964-70.

5. Klein HU, Reek S. The MUSTT study: evaluating testing and treatment. J Interv Card Electrophysiol 2000;4(suppl 1):45-50.

6. Moss AJ, Zareba W, Hall WJ, et al. Prophylactic implantation of a defibrillator in patients with myocardial infarction and reduced ejection fraction. N Engl J Med 2002;346:877-83.

7. Bardy GH, Lee KL, Mark DB, et al. Amiodarone or an implantable cardioverter-defibrillator for congestive heart failure. N Engl J Med 2005;352:225-37.

8. Berry C, Murdoch DR, McMurray JJ. Economics of chronic heart failure. Eur J Heart Fail 2001;3:283–91.

9. American Heart Association. Heart Disease and Stroke Statistics: 2005 Update. Dallas, Tex; American Heart Association; 2005.

10. O'Connell JB, Bristow MR. Economic impact of heart failure in the United States: time for a different approach. J Heart Lung Transplant 1994;13:S107-12.

11. Koelling TM, Chen RS, Lubwama RN, L'Italien GJ, Eagle KA. The expanding national burden of heart failure in the United States: the influence of heart failure in women. Am Heart J 2004;147:74-8.

12. Kannel WB, Belanger AJ. Epidemiology of heart failure. Am Heart J 1991; 121:951-7.

13. Masoudi FA, Havranek EP, Krumholz HM. The burden of chronic congestive heart failure in older persons: magnitude and implications for policy and research. Heart Fail Rev 2002;7:9-16.

14. The Study Group of Diagnosis of the Working Group on Heart Failure of the European Society of Cardiology. The EuroHeart Failure Survey programme – a survey on the quality of care among patients with heart failure in Europe. Part 1: Patient characteristics and diagnosis. Eur Heart J 2003;24:442–63.

15. Bennett SJ, Huster GA, Baker SL et al. Characterization of the precipitants of hospitalisation for heart failure decompensation. Am J Crit Care 1998;7:168–74.

16. Iuliano S, Fisher SG, Karasik PE, et al: QRS duration and mortality in patients with congestive heart failure. Am Heart J 143:1085- 1091, 2002.

17. Baldasseroni S, Opasich C, Gorini M, et al: Left bundle-branch block is associated with increased 1-year sudden and total mortality rate in 5517 outpatients with congestive heart failure: A report from the Italian Network on Congestive Heart Failure. Am Heart J 143:398-405, 2002.

18. Xiao HB, Roy C, Fujimoto S, et al: Natural history of abnormal conduction and its relation to prognosis in patients with dilated cardiomyopathy. Int J Cardiol 53:163- 170, 1996.

19. Uhley H: Peripheral distribution of the canine A-V conduction system; observations on gross morphology. Am J Cardiol 5:688- 691, 1960.

20. Spach MS, Barr RC: Ventricular intramural and epicardial potential distributions during ventricular activation and repolarization in the intact dog. Circ Res 37:243-257, 1975.

21. Durrer D, van Dam RT, Freud GE, et al: Total excitation of the isolated human heart. Circulation 41:899- 912, 1970.

22. Akar FG, Spragg DD, Tunin RS, et al: Mechanisms underlying conduction slowing and arrhythmogenesis in nonischemic dilated cardiomyopathy. Circ Res 95:717- 725, 2004.

23. Brutsaert DL. Nonuniformity: a physiologic modulator of contraction and relaxation of the normal heart. J Am Coll Cardiol 9: 341–348, 1987.

24. Villari B, Vassalli G, Betocchi S, Briguori C, Chiariello M, and Hess OM. Normalization of left ventricular nonuniformity late after valve replacement for aortic stenosis. Am J Cardiol 78: 66–71, 1996.

25. Heyndrickx GR and Paulus WJ. Effect of asynchrony on left ventricular relaxation. Circulation 81: 41–47, 1990.

26. Gepstein L, Goldin A, Lessick J, Hayam G, Shpun S, Schwartz Y, Hakim G, Shofty R, Turgeman A, Kirshenbaum D, and Ben-Haim S. A Electromechanical characterization of chronic myocardial infarction in the canine coronary occlusion model. Circulation 98: 2055–2064, 1998.

27. Nelson GS, Curry CW, Wyman BT, Kramer A, Declerck J, Talbot M, Douglas MR, Berger RD, McVeigh ER, and Kass DA. Predictors of systolic augmentation from left ventricular preexcitation in patients with dilated cardiomyopathy and intraventricular conduction delay. Circulation 101: 2703–2709, 2000.

28. Burkhoff D, Oikawa RY, Sagawa K: Influence of pacing site on canine left ventricular contraction. Am J Physiol 251:H428-H435, 1986.

29. Park RC, Little WC, O'Rourke RA: Effect of alteration of left ventricular activation sequence on the left ventricular end-systolic pressure-volume relation in closed-chest dogs. Circ Res 57:706- 717, 1985.

30. Liu L, Tockman B, Girouard S, et al: Left ventricular resynchronization therapy in a canine model of left bundle branch block. Am J Physiol Heart Circ Physiol 282:H2238-H2244, 2002.

31. Prinzen FW, Hunter WC, Wyman BT, et al: Mapping of regional myocardial strain and work during ventricular pacing: Experimental study using magnetic resonance imaging tagging. J Am Coll Cardiol 33:1735- 1742, 1999

32. Baller D, Wolpers HG, Zipfel J, et al: Comparison of the effects of right atrial, right ventricular apex and atrioventricular sequential pacing on

myocardial oxygen consumption and cardiac efficiency: A laboratory investigation. Pacing Clin Electrophysiol 11:394- 403, 1988.

33. Owen CH, Esposito DJ, Davis JW, et al: The effects of ventricular pacing on left ventricular geometry, function, myocardial oxygen consumption, and efficiency of contraction in conscious dogs. Pacing Clin Electrophysiol 21:1417-1429, 1998.

34. Vernooy K, Verbeek XA, Peschar M, et al: Left bundle branch block induces ventricular remodeling and functional septal hypoperfusion. Eur Heart J 26:91- 98, 2005.

35. Silverman ME, Pressel MD, Brackett JC, Lauria SS, Gold MR, Gottlieb SS. Prognostic value of the signal-averaged electrocardiogram and a prolonged QRS in ischemic and nonischemic cardiomyopathy. Am J Cardiol 1995;75:460-4.

36. Fried AG, Parker AB, Newton GE, Parker JD. Electrical and hemodynamic correlates of the maximal rate of pressure increase in the human left ventricle. J Card Fail 1999;5:8-16.

37. Wilensky RL, Yudelman P, Cohen AI, et al. Serial electrocardiographic changes in idiopathic dilated cardiomyopathy confirmed at necropsy. Am J Cardiol 1988;62:276-83.

38. Turner MS, Bleasdale RA, Vinereanu D, et al. Electrical and mechanical components of dyssynchrony in heart failure patients with normal QRS duration and left bundle-branch block: impact of left and biventricular pacing. Circulation 2004;109:2544-9.

39. Leclercq C, Faris O, Tunin R, et al: Systolic improvement and mechanical resynchronization does not require electrical synchrony in the dilated failing heart with left bundle-branch block. Circulation 106:1760- 1763, 2002.

40. Yu CM, Chau E, Sanderson JE, et al: Tissue Doppler echocardiographic evidence of reverse remodeling and improved synchronicity by simultaneously delaying regional contraction after biventricular pacing therapy in heart failure. Circulation 105:438-445, 2002.

41. Abraham WT, Fisher WG, Smith AL, et al: Cardiac resynchronization in chronic heart failure. N Engl J Med 346:1845- 1853, 2002.

42. Saxon LA, De Marco T, Schafer J, et al: Effects of long-term biventricular stimulation for resynchronization on echocardiographic measures of remodeling. Circulation 105:1304- 1310, 2002.

43. Nelson GS, Berger RD, Fetics BJ, et al: Left ventricular or biventricular pacing improves cardiac function at diminished energy cost in patients with dilated cardiomyopathy and left bundle-branch block. Circulation 102:3053-3059, 2000.

44. Fish JM, Di Diego JM, Nesterenko V, et al: Epicardial activation of left ventricular wall prolongs QT interval and transmural dispersion of repolarization—implications for biventricular pacing. Circulation 109:2136- 2142, 2004.

45. McSwain RL, Schwartz RA, Delurgio DB, et al: The impact of cardiac resynchronization therapy on ventricular tachycardia/fibrillation: An analysis from the combined Contak-CD and InSync-ICD studies. J Cardiovasc Electrophysiol 16:1168- 1171, 2005.

46. Voigt A, Barrington W, Ngwu O, et al: Biventricular pacing reduces ventricular arrhythmic burden and defibrillator therapies in patients with heart failure. Clin Cardiol 29:74-77, 2006.

47. Ermis C, Seutter R, Zhu AX, et al: Impact of upgrade to cardiac resynchronization therapy on ventricular arrhythmia frequency in patients with implantable cardioverter-defibrillators. J Am Coll Cardiol 46:2258-2263, 2005.

48. Arya A, Haghjoo M, Dehghani MR, et al: Effect of cardiac resynchronization therapy on the incidence of ventricular arrhythmias in patients with an implantable cardioverter-defibrillator. Heart Rhythm 2:1094-1098, 2005.

49. Cleland JGF, Daubert J-C, Erdmann E, et al. The effect of cardiac resynchronization on morbidity and mortality in heart failure. N Engl J Med 2005;352:1539-49.

50. D'Ascia C, Cittadini A, Monti MG, et al: Effects of biventricular pacing on interstitial remodelling, tumor necrosis factor–alpha expression, and apoptotic death in failing human myocardium. Eur Heart J 27:201-206, 2006.

51. Cazeau S, Leclercq C, Lavergne T, et al. Effects of multisite biventricular pacing in patients with heart failure and intraventricular conduction delay. N Engl J Med 2001;344:873-80.

52. Auricchio A, Stellbrink C, Sack S, et al. Long-term clinical effect of hemodynamically optimized cardiac resynchronization therapy in patients with heart failure and ventricular conduction delay. J Am Coll Cardiol 2002;39:2026-33.

53. Higgins SL, Hummel JD, Niazi IK, et al. Cardiac resynchronization therapy for the treatment of heart failure in patients with intraventricular conduction delay and malignant ventricular tachyarrhythmias. J Am Coll Cardiol 2003;42:1454-9.

54. Abraham WT, Fisher WG, Smith AL, et al. Cardiac resynchronization in chronic heart failure. N Engl J Med 2002;346:1845-53.

55. Young JB, Abraham WT, Smith AL, et al. Combined cardiac resynchronization and implantable cardioversion defibrillation in advanced chronic heart failure: the MIRACLE ICD Trial. JAMA 2003;289:2685-94.

56. Bristow MR, Saxon LA, Boehmer J, et al. Cardiac-resynchronization therapy with or without an implantable defibrillator in advanced chronic heart failure. N Engl J Med 2004;350:2140-50.

57. Auricchio A, Abraham WT. Cardiac resynchronization therapy: current state of the art: cost versus benefit. Circulation 2004;109:300-7.

58. Saxon LA, Ellenbogen KA. Resynchronization therapy for the treatment of heart failure. Circulation 2003;108:1044-8.

59. Navia JL, Atik FA, Grimm RA, et al. Minimally invasive left ventricular epicardial lead placement: surgical techniques for heart failure resynchronization therapy. Ann Thorac Surg 2005;79:1536-44.

60. Abraham WT, Young JB, Leon AR, et al. Effects of cardiac resynchronization on disease progression in patients with left ventricular systolic dysfunction, an indication for an implantable cardioverter-defibrillator, and mildly symptomatic chronic heart failure. Circulation 2004;110:2864-8.

61. Butter C, Auricchio A, Stellbrink C, et al. Effect of resynchronization therapy stimulation site on the systolic function of heart failure patients. Circulation 2001;104:3026–3029.

62. Gold MR, Auricchio A, Hummel JD, et al. Comparison of stimulation sites within left ventricular veins on the acute hemodynamic effects of cardiac resynchronization therapy. Heart Rhythm 2005;2:376–381.

63. Dekker AL, Phelps B, Dijkman B, et al. Epicardial left ventricular lead placement for cardiac resynchronization therapy: optimal pace site selection with pressure-volume loops. J Thorac Cardiovasc Surg 2004;127:1641–1647.

64. Rossillo A, Verma A, Saad EB, et al. Impact of coronary sinus lead position on biventricular pacing: mortality and echocardiographic evaluation during longterm follow-up. J Cardiovasc Electrophysiol 2004;15:1120–1125.

65. Gasparini M, Mantica M, Galimberti P, et al. Is the left ventricular lateral wall the best lead implantation site for cardiac resynchronization therapy? Pacing Clin Electrophysiol 2003;26:162–168.

66. Ansalone G, Giannantoni P, Ricci R, et al. Doppler myocardial imaging to evaluate the effectiveness of pacing sites in patients receiving biventricular pacing. J Am Coll Cardiol 2002;39:489–499.

67. Bax JJ, Ansalone G, Breithardt OA, et al. Echocardiographic evaluation of cardiac resynchronization therapy: ready for routine clinical use? A critical appraisal. J Am Coll Cardiol 2004;44:1-9.

68. Rouleau F, Merheb M, Geffroy S, et al. Echocardiographic assessment of the interventricular delay of activation and correlation to the QRS width in dilated cardiomyopathy. Pacing Clin Electrophysiol 2001;24:1500–6.

69. Auricchio A, Stellbrink C, Butter C, et al. Clinical efficacy of cardiac resynchronization therapy using left ventricular pacing in heart failure patients stratified by severity of ventricular conduction delay. J Am Coll Cardiol 2003;42:2109 –16.

70. Molhoek SG, Bax JJ, Van Erven L, et al. QRS duration and shortening to predict clinical response to cardiac resynchronization therapy in patients with end-stage heart failure. Pacing Clin Electrophysiol 2004;27:308 –13.

71. Bleeker GA, Schalij MJ, Molhoek SG, et al. Relationship between QRS duration and left ventricular dyssynchrony in patients with end-stage heart failure. J Cardiovasc Electrophysiol 2004;15:544 –9.

72. Ghio S, Constantin C, Klersy C, et al. Interventricular and intraventricular dyssynchrony are common in heart failure patients, regardless of QRS duration. Eur Heart J 2004;25:571– 8.

73. Pitzalis MV, Iacoviello M, Romito R, et al. Cardiac resynchronization therapy tailored by echocardiographic evaluation of ventricular asynchrony. J Am Coll Cardiol 2002;40:1615–22.

74. Pitzalis MV, Iacoviello M, Romito R, et al. Ventricular asynchrony predicts a better outcome in patients with chronic heart failure receiving cardiac resynchronization therapy. J Am Coll Cardiol 2005;45:65–9.

75. Marcus G, Rose E, Viloria EM, et al. Septal to posterior wall motion delay fails to predict reverse remodeling or clinical improvement in

patients undergoing cardiac resynchronization therapy. J Am Coll Cardiol 2005;46:2208 –14.

76. Breithardt OA, Stellbrink C, Kramer AP, et al. Echocardiographic quantification of left ventricular asynchrony predicts an acute hemodynamic benefit of cardiac resynchronization therapy. J Am Coll Cardiol 2002;40:536–45.

77. Kawaguchi M, Murabayashi T, Fetics BJ, et al. Quantitation of basal dyssynchrony and acute resynchronization from left or biventricular pacing by novel echo-contrast variability imaging. J Am Coll Cardiol 2002;19:2052– 8.

78. Ansalone G, Giannantoni P, Ricci R, et al. Doppler myocardial imaging in patients with heart failure receiving biventricular pacing treatment. Am Heart J 2001;142:881–96.

79. Garrigue S, Reuter S, Labeque JN, et al. Usefulness of biventricular pacing in patients with congestive heart failure and right bundle branch block. Am J Cardiol 2001;88:1436–41.

80. Yu CM, Chau E, Sanderson JE, et al. Tissue Doppler echocardiographic evidence of reverse remodeling and improved synchronicity by simultaneously delaying regional contraction after biventricular pacing therapy in heart failure. Circulation 2002;105:438–45.

81. Bax JJ, Marwick TH, Molhoek SG, et al. Left ventricular dyssynchrony predicts benefit of cardiac resynchronization therapy in patients with end-stage heart failure before pacemaker implantation. Am J Cardiol 2003;92:1238–40.

82. Yu CM, Fung WH, Lin H, Zhang Q, Sanderson JE, Lau CP. Predictors of left ventricular reverse remodeling after cardiac resynchronization therapy for heart failure secondary to idiopathic dilated or ischemic cardiomyopathy. Am J Cardiol 2003;91:684–8.

83. Notabartolo D, Merlino JD, Smith AL, et al. Usefulness of the peak velocity difference by tissue Doppler imaging technique as an effective predictor of response to cardiac resynchronization therapy. Am J Cardiol 2004;94:817–20.

84. Sogaard P, Egeblad H, Kim WY, et al. Tissue Doppler imaging predicts improved systolic performance and reversed left ventricular remodeling during long-term cardiac resynchronization therapy. J Am Coll Cardiol 2002;40:723–30.

85. Sogaard P, Egeblad H, Pedersen AK, et al. Sequential versus simultaneous biventricular resynchronization for severe heart failure: evaluation by tissue Doppler imaging. Circulation 2002;106:2078–84.

86. Bax JJ, Bleeker GB, Marwick TH, et al. Left ventricular dyssynchrony predicts response and prognosis after cardiac resynchronization therapy. J Am Coll Cardiol 2004;44:1834–40.

87. Yu CM, Fung JW, Zhang Q, et al. Tissue Doppler imaging is superior to strain rate imaging and postsystolic shortening on the prediction of reverse remodeling in both ischemic and nonischemic heart failure after cardiac resynchronization therapy. Circulation 2004;110:66 –73.

88. Breithardt OA, Stellbrink C, Herbots L, et al. Cardiac resynchronization therapy can reverse abnormal myocardial strain distribution in patients

with heart failure and left bundle branch block. J Am Coll Cardiol 2003;42:486 –94.

89. Sun JP, Chinchoy E, Donal E, et al. Evaluation of ventricular synchrony using novel Doppler echocardiographic indices in patients with heart failure receiving cardiac resynchronization therapy. J Am Soc Echocardiogr 2004;17:845–50.

90. Popovic ZB, Grimm RA, Perlic G, et al. Noninvasive assessment of cardiac resynchronization therapy for congestive heart failure using myocardial strain and left ventricular peak power as parameters of myocardial synchrony and function. J Cardiovasc Electrophysiol 2002;13:1203–8.

91. Dohi K, Suffoletto MS, Schwartzman D, Ganz L, Pinsky MR, Gorcsan J, III. Utility of echocardiographic radial strain imaging to quantify left ventricular dyssynchrony and predict acute response to cardiac resynchronization therapy. Am J Cardiol 2005;96:112– 6.

92. Gorcsan J, III, Kanzaki H, Bazaz R, Dohi K, Schwartzman D. Usefulness of echocardiographic tissue synchronization imaging to predict acute response to cardiac resynchronization therapy. Am J Cardiol 2004;93:1178–81.

93. Yu CM, Zhang Q, Fung JW, et al. A novel tool to assess systolic asynchrony and identify responders of cardiac resynchronization therapy by tissue synchronization imaging. J Am Coll Cardiol 2005;45: 677–84.

94. Kühl HP, Schreckenberg M, Rulands D, et al. High-resolution transthoracic real-time three-dimensional echocardiography: quantitation of cardiac volumes and function using semi-automatic border detection and comparison with cardiac magnetic resonance imaging. J Am Coll Cardiol 2004;43:2083–90.

95. Kapetenakis S, Siva A, Corrigan N, Cooklin M, Kearney MT, Monaghan MJ. Real-time three-dimensional echocardiography: a novel technique to quantify global left ventricular mechanical dyssynchrony. Circulation 2005;112:992–1000.

96. Zhang Q, Yu CM, Fung JW, et al. Assessment of the effect of cardiac resynchronization therapy on intraventricular mechanical synchronicity by regional volumetric changes. Am J Cardiol 2005; 95:126 –9.

97. Bogaert JG, Bosmans HT, Rademakers FE, et al. Left ventricular quantification with breath-hold MR imaging: comparison with echocardiography. Magma 1995;3:5–12.

98. Axel L, Dougherty L. MR imaging of motion with spatial modulation of magnetization. Radiology 1989;171:841–5.

99. Zerhouni EA, Parish DM, Rogers WJ, Yang A, Shapiro EP. Human heart: tagging with MR imaging—a method for noninvasive assessment of myocardial motion. Radiology 1988;169:59–63.

100. O'Dell WG, Moore CC, Hunter WC, Zerhouni EA, McVeigh ER. Three-dimensional myocardial deformations: calculation with displacement field fitting to tagged MR images. Radiology 1995;195:829–35.

101. Prinzen FW, Hunter WC, Wyman BT, McVeigh ER. Mapping of regional myocardial strain and work during ventricular pacing:

experimental study using magnetic resonance imaging tagging. J Am Coll Cardiol 1999;33:1735– 42.

102. Leclercq C, Faris O, Tunin R, et al. Systolic improvement and mechanical resynchronization does not require electrical synchrony in the dilated failing heart with left bundle-branch block. Circulation 2002;106:1760–3.

103. Curry CW, Nelson GS, Wyman BT, et al. Mechanical dyssynchrony in dilated cardiomyopathy with intraventricular conduction delay as depicted by 3D tagged magnetic resonance imaging. Circulation 2000;101:E2.

104. Nelson GS, Curry CW, Wyman BT, et al. Predictors of systolic augmentation from left ventricular preexcitation in patients with dilated cardiomyopathy and intraventricular conduction delay. Circulation 2000;101:2703–9.

105. Osman NF, Kerwin WS, McVeigh ER, Prince JL. Cardiac motion tracking using CINE harmonic phase (HARP) magnetic resonance imaging. Magn Reson Med 1999;42:1048–60.

106. Osman NF, Prince JL. Visualizing myocardial function using HARP MRI. Phys Med Biol 2000;45:1665– 82.

107. Osman NF, McVeigh ER, Prince JL. Imaging heart motion using harmonic phase MRI. IEEE Trans Med Imaging 2000;19:186 –202.

108. Osman NF, Sampath S, Atalar E, Prince JL. Imaging longitudinal cardiac strain on short-axis images using strain-encoded MRI. Magn Reson Med 2001;46:324 –34.

109. Wyman BT, Hunter WC, Prinzen FW, Faris OP, McVeigh ER. Effects of single- and biventricular pacing on temporal and spatial dynamics of ventricular contraction. Am J Physiol Heart Circ Physiol 2002;282:H372–9.

110. Helm RH, Leclercq C, Faris OP, et al. Circumferential versus longitudinal motion-based analysis of cardiac dyssynchrony implications for assessing cardiac resynchronization. Circulation 2005;111:2760–7.

111. Vine DL, Dodge HT, Frimer M, et al. Quantitative measurement of left ventricular volumes in man from radiopaque epicardial markers. Circulation 1976;54:391-398.

112. Rankin JS, McHale PA, Arentzen CE, et al. The three dimensional dynamic geometry of the left ventricle in the conscious dog. Circulation Res 1976;39:304-313.

113. Baan J, Jong TTA, Kerkhof PLM, et al. Continuous stroke volume and cardiac output from intraventricular dimensions obtained with impedance catheter. Cardiovascular Research 1981;15:328-334.

114. Baan J, van der Velde ET, de Bruin HG, et al. Continuous measurement of left ventricular volume in animals and humans by conductance catheter. Circulation 1984;70:812-823.

115. Steendijk P, van der Velde ET, Baan J. Single and dual excitation of the conductance-volume catheter analysed in a spheroidal mathematical model of the canine left ventricle. Eur Heart J 1992;13(Supplement E): 28-34.

116. Steendijk P, van der Velde ET, Baan J. Left ventricular stroke volume by single and dual excitation of conductance catheter in dogs. Am J Physiol 1993;264(Heart Circ Physiol 33):H2198-H2207.

117. Wu CC, Skalak TC, Schwenk TR, et al. Accuracy of the conductance catheter for measurement of ventricular volumes seen clinically: effects of electric field homogeneity and parallel conductance. IEEE Trans Biomed Eng 1997; 44:266-277.

118. Clavin OE, Spinelli JC, Alonso H et al. Left intraventricular pressure–impedance diagrams (DPZ) to assess cardiac function. Part 1: morphology and potential sources of artifacts. Med Progn Technol 1986;11:17–24.

119. McKay RG, Spears JR, Aroesty JM et al. Instantaneous measurement of left and right ventricular stroke volume and pressure–volume relationships with an impedance catheter. Circulation 1984;69:703–710.

120. Spinelli JC, Clavin OE, Cabrera EI et al. Left intraventricular pressure–impedance diagrams (DPZ) to assess cardiac function. Part II: determination of end-systolic loci. Med Progn Technol 1986;11:25–32.

121. Gawne TJ, Gray KS, Goldstein RE. Esimating left ventricular offset volume using dual-frequency conductance catheters. J Appl Physiol 1987;63:872-876.

122. White PA, Brookes CIO, Ravn HB, et al. The effect of changing excitation frequency on parallel conductance in different sized hearts. Cardiovascular Research 1998; 38:668-675.

123. Kornet L, Schreuder JJ, van der Velde ET, et al. A new approach to determine parallel conductance for left ventricular volume measurements. Cardiovasc Res 2000;48:455-463.

124. Tachibana H, Takaki M, Lee S, et al. New mechanoenergetic evaluation of left ventricular contractility in in situ rat hearts. Am J Physiol 1997;272:H2671-H2678.

125. White PA, Brookes CIO, Ravn H, et al. Validation and utility of novel volume reduction technique for determination of parallel conductance. Am J Physiol 2001;280:H475-H482.

126. Herrera MC, Olivera JM, Valentinuzzi ME. Parallel conductance estimation by hypertonic dilution method with conductance catheter: effects of the bolus concentration and temperature. IEEE Trans Biomed Eng 1999;46:830-837.

127. Szwarc RS, Mickleborough LL, Mizuno S, et al. Conductance catheter measurements of left ventricular volume in the intact dog: parallel conductance is independent of left ventricular size. Cardiovasc Res 1994;28:252-258.

128. Applegate RJ, Cheng CP, Little WC. Simultaneous Conductance Catheter and Dimension Assessment of Left Ventricle Volume in the intact Animal. Circulation 1990; 81:638-648.

129. Boltwood CM, Appleyard RF, Glantz SA. Left ventricular volume measurement by conductance catheter in intact dogs. Parallel conductance volume depends on left ventricular size. Circulation 1989;80:1360-1377.

130. Szwarc RS, Ball HA. Simultaneous LV and RV volumes by conductance catheter: effects of lung insufflation on parallel conductance. Am J Physiol 1998; 275:H653-H661.

131. Lankford EB, Kass DA, Maughan WL, et al. Does volume catheter parallel conductance vary during a cardiac cycle? Am J Physiol 1990;258:H1933-H1942.

132. Szwarc RS, Laurent D, Allegrini PR, et al. Conductance catheter measurement of left ventricular volume: evidence for nonlinearity within cardiac cycle. Am J Physiol 1995;268:H1490-H1498.

133. Kornet L, Schreuder JJ, van der Velde ET, et al. The volume-dependency of parallel conductance throughout the cardiac cycle and its consequence for volume estimation of the left ventricle in patients. Cardiovasc Res 2001;51:729-735.

134. Baan J, Aouw Jong TT, Kerkho PLM, et al. Continuous registration of relative left ventricular volume in man. Circulation 1982;66(suppl II):277(abst).

135. Kass DA, Midei M, Graves W, et al. Use of a conductance (volume) catheter and transient inferior vena cava occlusion for rapid determination of pressure-volume relationships in man. Catheterization and Cardiovascular Diagnosis 1988;15:192-202.

136. Hayward CS, Kalnins WV, and Kelly RP. Gender-related differences in left ventricular chamber function. Cardiovasc Res 49: 340–350, 2001.

137. Kass DA, Grayson R, and Marino P. Pressure-volume analysis as a method for quantifying simultaneous drug (amrinone) effects on arterial load and contractile state in vivo. J Am Coll Cardiol 16: 726–732, 1990.

138. Kass DA, Midei M, Graves W, et al. Use of a conductance (volume) catheter and transient inferior vena caval occlusion for rapid determination of pressure-volume relationships in man. Cathet Cardiovasc Diagn 15: 192–202, 1988.

139. MacGowan GA, Haber HL, Cowart TD, et al. Direct myocardial effects of OPC-18790 in human heart failure: beneficial effects on contractile and diastolic function demonstrated by intracoronary infusion with pressure-volume analysis. J Am Coll Cardiol 31: 1344–1351, 1998.

140. Schreuder JJ, Steendijk P, Van der Veen FH, et al. Acute and short-term effects of partial left ventriculectomy in dilated cardiomyopathy: assessment by pressure-volume loops. J Am Coll Cardiol 2000;36:2104-2114.

141. Schreuder JJ, Van der Veen FH, Van der Velde ET, et al. Beat-to-beat analysis of left ventricular volume and stroke volume by conductance catheter and aortic pulse contour in cardiomyoplasty patients. Circulation 1995;91:2010-2017.

142. Schreuder JJ, van der Veen FH, van der Velde ET, et al. Left ventricular pressure-volume relationships before and after cardiomyoplasty in patients with heart failure. Circulation. 1997;96:2978-2986.

143. Schreuder JJ, Castiglioni A, Maisano F, et al. Acute decrease of left ventricular mechanical dyssynchrony and improvement of

contractile state and energy efficiency after left ventricular restoration. J Thorac Cardiovasc Surg 2005;129:138-145.

144.   Dekker A, Phelps B, Dijkman B, et al. Epicardial left ventricular lead placement for cardiac resynchronization therapy: Optimal pace site selection with pressure-volume loops. J Thorac Cardiovasc Surg 2004;127:1641-1647.

145.   Steendijk P, Tulner SAF, Schreuder JJ, et al. Quantification of left ventricular mechanical dyssynchrony by conductance catheter in heart failure patients. Am J Physiol 2004;286:H723-H730.

146.   Strum DP, Pinsky MR. Modeling of asynchronous myocardial contraction by effective stroke volume analysis. Anesth Analg 2000;90:243–51.

147.   Van Der Velde ET, Van Dijk AD, Steendijk P, et al. Left ventricular segmental volume by conductance catheter and cine-CT. Eur Heart J 1992;13(Suppl E):15–21.

148.   Steendijk P, Van Der Velde ET, and Baan J. Single and dual excitation of the conductance-volume catheter analysed in a spheroidal mathematical model of the canine left ventricle. Eur Heart J 1992;13(Suppl E):28–34.

149.   Steendijk P, Van Der Velde ET, and Baan J. Left ventricular stroke volume by single and dual excitation of conductance catheter in dogs. Am J Physiol 1993;264:H2198–H2207.

150.   Wu CC, Skalak TC, Schwenk TR, et al. Accuracy of the conductance catheter for measurement of ventricular volumes seen clinically: effects of electric field homogeneity and parallel conductance. IEEE Trans Biomed Eng 1997;44:266-277.

151.   Varma C, O'Callaghan P, Mahon NG, et al. Effect of multisite pacing on ventricular coordination. Heart 2002;87:322–328.

152.   Porciani MC, Lilli A, Macioce R, et al. Utility of a new left ventricular asynchrony index as a predictor of reverse remodelling after cardiac resynchronization therapy. Eur Heart J. 2006;27:1818-1823.

153.   Rompelman O, Ros HH. Coherent averaging technique: a tutorial review. Part 1: Noise reduction and the equivalent filter. J Biomed Eng. 1986;8:24-9.

154.   Rompelman O, Ros HH. Coherent averaging technique: a tutorial review. Part 2: Trigger jitter, overlapping responses and non-periodic stimulation. J Biomed Eng. 1986;8:30-5.

155.   Ropella KM, Sahakian AV, Baerman JM, Swiryn S. The coherence spectrum. A quantitative discriminator of fibrillatory and nonfibrillatory cardiac rhythms. Circulation 1989;80:112-9.

156.   Carter C, Knapp CH, Nuttall B. Estimation of the magnitudesquared coherence function via overlapped fast Fourier Transform processing. IEEE Trans Audio Electroacoustics. 1973;21:337-44.

157.   Al-Khalidi AH, Lewis ME, Townened JN, et al. A novel and simple technique to allow detection of the position of the R-waves from intraventricular pressure waveforms: application to the conductance catheter method. IEEE Trans Biomed Eng. 2001;48:606-610.

158.	Leclercq C, Kass DA. Retiming the failing heart: principles and current clinical status of cardiac resynchronization. J Am Coll Cardiol 39: 194–201, 2002.

159.	Saxon LA, De Marco T. Cardiac resynchronization: a cornerstone in the foundation of device therapy for heart failure. J Am Coll Cardiol 38: 1971–1973, 2001.

160.	Lieberman R, Padeletti L, Schreuder J et al. Ventricular Pacing Lead Location Alters Systemic Hemodynamics and Left Ventricular Function in Patients With and Without Reduced Ejection Fraction. J Am Coll Cardiol 2006;48:1634-41.

161.	Andersen HR, Nielsen JC, Thomsen PE, et al. Long-term follow-up of patients from a randomized trial of atrial versus ventricular pacing for sick-sinus syndrome. Lancet. 1997;350:1210-16.

162.	Connolly SJ, Kerr CR, Gent M, et al. Effects of physiologic pacing versus ventricular pacing on the risk of stroke and death due to cardiovascular causes. Canadian Trial of Physiologic Pacing Investigators. N Engl J Med. 2000;342:1385-91.

163.	Lamas GA, Lee KL, Sweeney MO, et al.Ventricular pacing or dual-chamber pacing for sinus-node dysfunction. N Engl J Med 2002;346:1854-62.

164.	Tse HF, Lau CP. Long-term effect of right ventricular pacing on myocardial perfusion and function. J Am Coll Cardiol. 1997;29:744-9.

165.	Tantengco MV, Thomas RL, Karpawich PP. Left ventricular dysfunction after long-term right ventricular apical pacing in the young. J Am Coll Cardiol. 2001;37:2093-100.

166.	Karpawich PP, Rabah R, Haas JE. Altered cardiac histology following apical right ventricular pacing in patients with congenital atrioventricular block. Pacing Clin Electrophysiol. 1999;22:1372-7.

167.	Thambo JP, Bordacher P, Garrigue S. Detrimental ventricular remodeling in patients with congenital complete heart block and chronic right ventricular apical pacing Circulation 2004;110:3766-3772.

168.	Wilkoff B et al. Dual-chamber pacing or ventricular backup pacing in patients with an implantable defibrillator; The dual chamber and VVI implantable defibrillator (DAVID) trial. JAMA 2002;288:3115-3123.

169.	Gold MR, Brockman R, Peters RW, et al. Acute hemodynamic effects of right ventricular pacing site and pacing mode in patients with congestive heart failure secondary to either ischemic or idiopathic dilated cardiomyopathy. Am J Cardiol. 2000;85:1106-9.

170.	Tse HF, Yu C, Wong KK, et al. Functional abnormalities in patients with permanent right ventricular pacing: the effect of sites of electrical stimulation. J Am Coll Cardiol. 2002;40:1451-8.

171.	Stambler BS, Ellenbogen K, Zhang X, et al. Right ventricular outflow versus apical pacing in pacemaker patients with congestive heart failure and atrial fibrillation. J Cardiovasc Electrophysiol. 2003;14:1180-6.

172.	de Cock CC, Giudici MC, Twisk JW. Comparison of the haemodynamic effects of right ventricular outflow-tract pacing with right ventricular apex pacing: a quantitative review. Europace. 2003;5:275-8.

173. Puggioni E, Brignole M, Gammage M, et al. Acute comparative effect of right and left ventricular pacing in patients with permanent atrial fibrillation. J Am Coll Cardiol. 2004;43:234-8.

174. Simantirakis EN, Vardakis KE, Kochiadakis GE, et al. Left ventricular mechanics during right ventricular apical or left ventricular-based pacing in patients with chronic atrial fibrillation after atrioventricular junction ablation. J Am Coll Cardiol. 2004;43:1013-8.

175. Lieberman R, Grenz D, Mond HG, Gammage MD. Selective site pacing: defining and reaching the selected site. Pacing and Clin Electrophysiol. 2004;27(II):883-6.

176. Kelly RP, Ting CT, Yang TM, et al. Effective arterial elastance as index of arterial vascular load in humans. Circulation. 1992;86:513-21.

177. Yu CM, Lin H, Zhang Q, Sanderson JE. High prevalence of left ventricular systolic and diastolic asynchrony in patients with congestive heart failure and normal QRS duration. Heart. 2003;89:54-60.

178. Achilli A, Sassara M, Ficili S, et al. Long-term effectiveness of cardiac resynchronization therapy in patients with refractory heart failure and "narrow" QRS. J Am Coll Cardiol. 2003;42:2117-24.

179. Bleasdale RA, Turner MS, Mumford CE, et al. Left ventricular pacing minimizes diastolic ventricular interaction, allowing improved preload-dependent systolic performance. Circulation. 2004;110:2395-400.

180. Hay I, Melenovsky V, Fetics BJ, et al. Short-term effects of right-left heart sequential cardiac resynchronization in patients with heart failure, chronic atrial fibrillation, and atrio-ventricular nodal block. Circulation. 2004;110:3404-3410.

181. Spotnitz HM. Optimizing temporary perioperative cardiac pacing. J Thorac Cardiovasc Surg. 2005;129:5-8.

182. Peschar M, de Swart H, Michels KJ, et al. Left ventricular septal and apex pacing for optimal pump function in canine hearts. J Am Coll Cardiol. 2003;41:1218-26.

183. Bordachar P, Lafitte S, Reuter S, et al. Biventricular pacing and left ventricular pacing in heart failure: similar hemodynamic improvement despite marked electromechanical differences. J Cardiovasc Electrophysiol. 2004;15:1342-7.

184. Yu CM, Fung JW, Chan CK, et al. Comparison of efficacy of reverse remodeling and clinical improvement for relatively narrow and wide QRS complexes after cardiac reynchronization therapy for heart failure. J Cardiovasc Electrophysiol. 2004;15:1058-65.

185. Turner MS, Bleasdale RA, Mumford CE, et al. Left ventricular pacing improves haemodynamic variables in patients with heart failure with a normal QRS duration. Heart. 2004;90:502-5.

186. Doshi RN, Daoud EG, Fellows C, et al. Left ventricular-based cardiac stimulation post AV nodal ablation evaluation (the PAVE study). J Cardiovasc Electrophysiol. 2005;16:1160-1165.

187. Schwaab B, Frohlig G, Alexander C, et al. Influence of right ventricular stimulation site on left ventricular function in atrial synchronous ventricular pacing. J Am Coll Cardiol. 1999;33:317-322.

188.   Steendijk P, Tulner SA, Bax JJ, et al. Hemodynamic effects of long-term cardiac resynchronization therapy. Analysis by pressure-volume loops. Circulation 113:1295-1304, 2006.

189.   Steendijk P, Tulner SAF, Wiemer M, et al. Pressure-volume measurements during cardiac resynchronization therapy. Eur Heart J 6 (suppl D);D35-D42, 2004.

190.   Kass DA, Chen C-H, Curry C, et al. Improved left ventricular mechanics from acute VDD pacing in patients with dilated cardiomyopathy and ventricular conduction delay. Circulation 99:1567-1573, 1999.

191.   Auricchio A, Stellbrink C, Block M, et al. Effect of chamber and atrioventricular delay on acute systolic function of paced patients with congestive heart failure. Circulation 99:2993-3001, 1999.

192.   Zile MR, Blaustein AS, Shimizu G, et al. Right ventricular pacing reduces the rate of left ventricular relaxation and filling. J Am Coll Cardiol 10:702-709, 1987.

193.   Schreuder JJ, Maisano F, Donelli A, et al. Beat-to-beat effects of intraaortic balloon pump timing on left ventricular performance of patients with low ejection fraction. A Thorac Surg 79:872-880, 2005.

194.   Van Oosterhout MFM, Prinzen FW, Arts T, et al. Asynchronous electrical activation induces asymmetric hypertrophy of the left ventricular wall. Circulation 98:588-595, 1998.

195.   Wesseling KH, Jansen JRC, Settels JJ, et al. Computation of aortic flow from pressure in humans using a nonlinear, three-element model. J. Appl. Physiol. 1993;74:2566-2573.

196.   Jansen JRC, Schreuder JJ, Mulier JP, et al. A comparison of cardiac output derived from the arterial pressure wave against thermodilution in cardiac surgery patients. Br J Anaesth. 2001;87:212-222.

197.   Langewouters GJ, Wesseling KH, Goedhard WJA. The static elastic properties of 45 human thoracic and 20 abdominal aortas in vitro and the parameters of a new model. J. Biomech. 1984;17:425-435.

198.   de Vaal JB, de Wilde RB, van den Berg PC, et al. Less invasive determination of cardiac output from the arterial pressure by aortic diameter-calibrated pulse contour. Br J Anaesth. 2005;95:326-331.

199.   Hoeksel SAAP, Jansen JRC, Blom JA, Schreuder JJ. Detection of dicrotic notch in arterial pressure signals. J Clin Monit. 1997;13:309–316.

200.   Donelli A, Jansen JRC, Hoeksel B, et al. Performance of a real-time dicrotic notch prediction algorithm in arrhythmic human aortic pressure signals. J Clin Monit 2002;17:181–185.

201.   Schreuder JJ, Castiglioni A, Donelli A, et al. Automatic intraaortic balloon pump timing using an intrabeat dicrotic notch prediction algorithm. Ann Thorac Surg. 2005;79:1017–1022.

202.   Perego GB, Chianca R, Facchini M, et al. Simultaneous vs. sequential biventricular pacing in dilated cardiomyopathy: an acute hemodynamic study. Eur J Heart Fail. 2003;5:305-313.

203.   Bland JM, Altman DG. Statistical methods for assessing agreement between two methods of clinical measurement. Lancet. 1986;1:307-310.

204.   Critchley LA, Critchley JA. A meta-analysis of studies using bias and precision statistics to compare cardiac output measurement techniques. J Clin Monit Comput. 1999;15:85-91.

205.   Oppenheim MI and Sittig DF. An innovative dicrotic notch detection algorithm which combines rule-based logic with digital signal processing techniques. Comput Biomed Res. 1995;28:154-170.

Appendix

Ancillary Studies and Publications

a. Physiologic Pacing: New Modalities and Pacing Sites.

Abstract

Right ventricular (RV) apical pacing impairs left ventricular function by inducing dyssynchronous contraction and relaxation. Chronic RV apical pacing is associated with an increased risk of atrial fibrillation, morbidity, and even mortality. These observations have raised questions regarding the appropriate pacing mode and site, leading to the introduction of algorithms and new pacing modes to reduce the ventricular pacing burden in dual chamber devices, and a shift of the pacing site away from the RV apex. However, further investigations are required to assess the long-term results of pacing from alternative sites in the right ventricle, because long-term results so far are equivocal. The potential benefit of prophylactic biventricular, monochamber left ventricular, and bifocal RV pacing should be explored in selected patients with a narrow QRS complex, especially those with impaired left ventricular function. His bundle pacing is a promising and evolving technique that requires improvements in lead technology.

b. Long-Term Survival in Patients Treated With Cardiac Resynchronization Therapy: A 3-Year Follow-Up Study From the InSync/InSync ICD Italian Registry

Abstract

Background
Studies reporting the long-term survival of patients treated with cardiac resynchronization therapy (CRT) outside the realm of randomized controlled trials are still lacking. The aim of this study was to quantify the survival of patients treated with CRT in clinical practice and to investigate the long-term effects of CRT on clinical status and echocardiographic parameters.

Methods
The study population consisted of 317 consecutive patients with implanted CRT devices from eight Italian University/Teaching Hospitals. The patients were enrolled in a national observational registry and had a minimum follow-up of 2 years. A visit was performed in surviving patients and mortality data were obtained by hospital file review or direct telephone contact.

Results
During the study period, 83 (26%) patients died. The rate of all-cause mortality was significantly higher in ischemic than nonischemic patients (14% vs 8%, P = 0.002). Multivariate analysis showed that ischemic etiology (HR 1.72, CI 1.06–2.79; P = 0.028) and New York Heart Association (NYHA) class IV (HR 2.87, CI 1.24–6.64; P = 0.014) were the strongest predictors of all-cause mortality. The effects of CRT persisted at long-term follow-up (for at least 2 years) in terms of NYHA class improvement, increase of left ventricular ejection fraction, decrease of QRS duration (all P = 0.0001), and reduction of left ventricular end-diastolic and end-systolic diameters (P = 0.024 and P = 0.011, respectively).

Conclusions
During long-term (3 years) follow-up after CRT, total mortality rate was 10%/year. The outcome of ischemic patients was worse mainly due to a higher rate of death from progressive heart failure. Ischemic etiology along with NYHA class IV was identified as predictors of death. Benefits of CRT in terms of clinical function and echocardiographic parameters persisted at the time of long-term follow-up.

c. Effects of Cardiac Resynchronization Therapy in Patients With Mild Symptoms of Heart Failure With Respect to Severely Symptomatic Heart Failure Patients: the InSync/InSync ICD Italian Registry.

Abstract

Background
Cardiac resynchronization therapy (CRT) is recommended for patients with NYHA class III or IV heart failure (HF) and evidence of ventricular dyssynchrony. The effects of CRT in NYHA class II patients are still controversial. Aim of this study was to evaluate the effects of CRT in NYHA II with respect to NYHA III and IV patients.

Methods
The study population consisted of 952 patients (188 were in NYHA II) consecutively implanted with biventricular devices. They were enrolled in a national observational registry and underwent baseline evaluation and periodical follow-up visits. We estimated the clinical outcome after 12-month of CRT, and we assessed the long-term survival.

Results
At a median follow-up of 16 months, significantly less major cardiovascular events were reported in the NYHA II patients compared to the NYHA III/IV patients (rate 13.0 vs. 23.0 per 100 patient-years of follow-up, $p < 0.001$).
The percentage of patients who improved the NYHA class after 12 months of CRT was lower in NYHA II than in NYHA III/IV patients (34% Vs. 69%, $p < 0.001$), while the absolute increase of ejection fraction was similar in the two groups (8 ± 9% Vs. 9 ± 11%, p=NS), as well as the reduction of end-diastolic diameter (-3 ± 8mm Vs. -3 ± 8mm, p=NS) and end-systolic diameter (-4 ± 10mm Vs. -6 ± 10mm, p=NS). The NYHA II group experienced lower all-cause mortality (log-rank test p=0.018). In both groups, the patients with major cardiovascular events during follow-up exhibited less or no reverse remodeling compared to those with better long-term clinical outcome.

Conclusions
Our results indicate that CRT induced similar improvements of ventricular function in both groups, whereas the improvement in functional status was significantly lower for NYHA II than for III/IV patients. A positive effect of CRT on cardiac dimensions was associated with long-term beneficial effect on disease progression in NYHA II patients.

d. Efficacy of Cardiac Resynchronization Therapy in Very Old Patients. The InSync/InSync ICD Italian Registry

Abstract

Background
This study aimed to assess the effects of cardiac resynchronization therapy (CRT) in $\geq$80years old patients versus patients <80years, in terms of clinical, functional and echocardiographic parameters, survival and incidence of arrhythmic events.

Methods
The study population consisted of 1181 patients (85 were $\geq$80years old) consecutively implanted with CRT devices, with and without ICD capabilities. They were enrolled in a national observational registry and underwent baseline evaluation and periodical follow-up visits. We estimated the clinical outcome after 12-month of CRT, and the mortality data.

Results
In the overall population, NYHA class and LV ejection fraction (EF) improved, and LV diameter decreased. Similar changes were observed in the two groups after CRT. In the study population, 157 patients died, 144 (13%) in <80years group and 13 (15%) in $\geq$80years group. There was higher all-cause mortality (Log-rank test, $p=0.015$) among $\geq$80years patients and a trend toward higher sudden cardiac death (SCD) ($p=0.057$), with similar non-sudden cardiac death ($p=0.293$). However, using the combined end-point of SCD or appropriate shock from a defibrillator for ventricular fibrillation, and considering the higher proportion of combined CRT-defibrillator devices implanted in younger patients, no significant differences resulted between groups ($p=0.455$). In both groups, lower EF was associated with higher mortality.

Conclusions
Our results demonstrate similar efficacy of CRT in patients aged $\geq$80years and in those under 80, in terms of clinical and functional parameters and in terms of reverse remodeling. Similarly, CRT results in comparable effects on death for worsening heart failure and on sudden cardiac death.

e. Limited Thoracotomy as a Second Choice Alternative to Transvenous Implant for Cardiac Resynchronization Therapy Delivery

Abstract

Aims
Left ventricular (LV) pacing via transvenous implantation has an overall success rate ranging from 88% to 92%. The aim of this study was to assess whether LV pacing via limited thoracotomy would be feasible and safe when used on a routine basis for those cases in which standard transvenous procedures proved to be ineffective or unsatisfactory.

Methods and results
We enrolled 33 patients (8 females, 65±10 years) who experienced a transvenous implantation failure. All patients underwent a limited thoracotomy and an epicardial lead was implanted. The procedure time was 51±28 min. No surgical or post-operative complications occurred and optimal lateral position was achieved for all patients. In the 12 months follow-up period, 5 patients died from refractory heart failure, the remaining patients did not experience complications. At implant, the mean pacing threshold was 1.3±0.7 V, bi-ventricular pacing impedance was 476±201 X and R-wave amplitude was 15.0±6.1 mV. No significant differences were found in any of the electrical parameters between baseline and follow-up. Significant improvement was observed in functional and echocardiographic parameters.

Conclusions
Our results suggest that a combined approach to cardiac resynchronisation therapy delivery, including a transvenous attempt followed by a back up thoracotomic procedure, could potentially guarantee the success.

f. Evolution and Prognostic Significance of Diastolic Filling Pattern in Cardiac Resynchronization Therapy.

Abstract

Background
Cardiac resynchronization therapy (CRT) is an emerging treatment for heart failure patients with left bundle branch block; in these patients left ventricle filling pattern (LVFP) abnormalities are recognized as cause of symptoms and predictors of outcome. We investigated the effects of CRT on diastolic function and the prognostic value of LVFP in patients on CRT.

Methods
65 patients treated with CRT were studied over a 12 months period. At baseline, according to defined echocardiographic criteria, restrictive LVFP (RFP) was present in 25 patients, whereas 40 patients showed no-RFP.

Results
After CRT, opposite changes occurred in the two groups. In no-RFP patients, early-to-atrial filling velocity ratio (E/A) increased from 0.8 ± 0.3 to 1.0 ± 0.6 (p = 0.006) and E wave deceleration time (DT) decreased from 234 ± 83 ms to 196 ± 51 ms (p = 0.028). In 13 RFP patients, E/A decreased from 2.2 ± 0.9 to 0.8 ± 0.5 and DT increased from 128 ± 43 ms to 205 ± 52 ms (both p < 0.001), leading to reversal of RFP. In both groups, clinical, functional and echographic benefits were evident, with mortality rates of 5% (2/40) and 15% (2/13) respectively. The remaining patients showed persistence of RFP (E/A and DT unchanged), no improvement and a mortality rate of 42% (5/12) (p = 0.005, versus no-RFP).

Conclusions
CRT improves diastolic function, inducing also reversal of LVFP in a consistent number of RFP patients. The persistence of RFP after CRT is associated to an extremely poor prognosis.

g. Results of the SCART Study: Selection of Candidates to Cardiac Resynchronization Therapy

Abstract

Aims
To prospectively determine whether pre-specified selection criteria of ECG, echocardiography (ECHO) and tissue Doppler imaging (TDI) may predict the response to cardiac resynchronization therapy (CRT).

Methods
In this multicenter, prospective, non-randomized study, 96 heart failure patients with NYHA class III-IV symptoms, ejection fraction ≤35% and at least one marker of ventricular dyssynchrony according to pre-specified ECG, ECHO or TDI criteria were enrolled. The primary end-point was the improvement in clinical composite score at six months.

Results
At the enrollment, 70 patients fulfilled ECG criterion (QRS duration ≥ 150ms), 77 subjects demonstrated ECHO signs of dyssynchrony, while TDI dyssynchrony criteria were present in 37 patients.
The overall responder rate was 78/96 (81%). In particular, the primary end-point was reached in 68 patients with ECHO criteria, compared to 10 patients not satisfying them (88% vs. 53%, p=0.001).
Patients satisfying ECHO selection criteria showed a significant greater reduction of LVESD (p=0.029) and a larger improvement of QoL (p=0.017) with respect to patients not fulfilling them. Neither ECG nor TDI criteria seemed to predict the response to CRT.

Conclusions
In our patient population, mechanical indexes of dyssynchrony as detected by ECHO seemed to identify responders to CRT. Although TDI is useful to evaluate the reduction of ventricular dyssynchrony after CRT, the pre-selected TDI inclusion criteria used in this analysis did not increase the number of responder to CRT.

h. Prediction of Response to Cardiac Resynchronization Therapy: the Selection of Candidates for CRT (SCART) Study.

Abstract

Background
The aim of this study was to evaluate the ability of baseline clinical and echocardiographic parameters to predict a positive response to CRT.

Methods
We analyzed 6-month data from the first 133 consecutive patients enrolled in a multicenter prospective study. These patients had symptomatic heart failure (HF) refractory to pharmacological therapy (NYHA class II–IV), left ventricular ejection fraction (LVEF) ≤35%, and prespecified electrocardiographic, echocardiographic or tissue Doppler imaging markers of left ventricular (LV) dyssynchrony.

Results
After a follow-up period of 6 months, 1 patient died and 13 were hospitalized for worsening HF. There were significant ($P < 0.01$) clinical, functional, and echocardiographic improvements that included: New York heart Association Class, Quality-of-Life Score, QRS duration, LVEF, LV end-diastolic and endsystolic diameter (LVESD), and severity of mitral regurgitation A positive response was documented in 90/133 (68%) patients who presented an improved clinical composite score associated to an increase in LVEF ≥ 5 units. A multivariate analysis identified that a smaller LVESD (OR = 0.957, 95% CI 0.920–0.996; P = 0.030) and longer interventricular mechanical delay (IVMD) (OR = 1.017, 95% CI 1.005–1.029, P = 0.007) as independent predictors of a positive response. Receiver-operating curve analysis showed that a positive response to CRT may be predicted in patients with IVMD > 44 ms (with a sensitivity of 66% and a specificity of 55%) or with LVESD < 60 mm (with a sensitivity of 66% and a specificity of 61%).

Conclusions
Our results confirm the limited value of QRS duration in the selection of patients for CRT. A less-advanced stage of disease and echocardiographic evidence of interventricular dyssynchrony demonstrated to predict response to CRT, while intraventricular dyssynchrony did not predict response.